

**THE ROLE OF POLYCOMB GROUP PROTEIN EZH2 IN CANCER
PROGRESSION**

by

Qi Cao

A dissertation submitted in partial fulfillment
of the requirements for the degree of
Doctor of Philosophy
(Pathology)
in The University of Michigan
2008

Doctoral Committee:

Professor Arul M. Chinnaiyan, Chair
Professor Eric R. Fearon
Professor Richard R. Neubig
Professor James Varani
Assistant Professor Sooryanarayana Varambally

© Qi Cao

All Rights Reserved

2008

ACKNOWLEDGEMENTS

First, I would like to thank my mentor, Dr. Arul M. Chinnaiyan, for supporting, instructing, inspiring and encourageing me to finish my doctoral research. And, I would also like to thank Dr. Sooryanarayana Varambally for discussing and helping me design experiments, and overcome difficulties and problems during my study. I also would like to thank Dr. Eric Fearon, Dr. Richard Neubig, and Dr. James Varani for serving on my Doctoral committee and giving me valuable suggestions on this dissertation.

I would like to thank Jindan Yu, Saravana Dhanasekaran, Scott A. Tomlins, Bharathi Laxman, Xuhong Cao, Jianjun Yu, Julie Kim and Rohit Mehra, who have contributed to most of the work described here. Additionally, I would like to thank all the members in the Chinnaiyan lab for their support. Without them, none of the work described here could have been completed. I would also like to thank Dr. Celina Kleer for her support on the study of EZH2 in breast cancer.

I would like to express my deepest love to my wife, Yifan and my daughter, Andrea. Thanks for giving me unconditional love and support through my Doctoral study and the writing of this work. Finally, I'd like to thank my friends and family for their support.

TABLE OF CONTENTS

ACKNOWLEDGMENTS	ii
LIST OF FIGURES	iv
LIST OF TABLES	v
CHAPTER 1 INTRODUCTION	1
CHAPTER 2. EZH2 IS A MARKER OF AGGRESSIVE BREAST CANCER AND PROMOTES NEOPLASTIC TRANSFORMATION OF BREAST EPITHELIAL CELLS	40
CHAPTER 3. REPRESSION OF E-CADHERIN BY THE POLYCOMB GROUP PROTEIN EZH2 IN CANCER	71
CHAPTER 4. A CAUSAL ROLE FOR MICRORNA-101 IN UPREGULATING EZH2 IN AGGRESSIVE TUMORS	98
CHAPTER 5. CONCLUSION	118
APPENDIX	122

LIST OF FIGURES

Figure		
1.1	Two Distinct Human Polycomb Group Complexes	33
1.2	Model for PcG regulation and function	34
2.1	EZH2 mRNA transcript and protein levels are elevated in breast cancer	65
2.2	High EZH2 levels are associated with aggressive breast cancer	66
2.3	Anchorage-independent growth mediated by EZH2	67
2.4	EZH2 orchestrates cell invasion both <i>in vitro</i> and <i>in vivo</i>	68
3.1	Over expression of EZH2 enhances invasion	86
3.2	EZH2 mediates repression of E-cadherin transcript and protein	87
3.3	E-cadherin over-expression attenuates EZH2-mediated cell invasion	89
3.4	Regulation of the E-cadherin promoter by EZH2	90
3S1	The repression of E-cadherin increases with EZH2 increases	92
3S2	E-boxes of E-cadherin are necessary for EZH2 to repress E-cadherin promoter activity	93
4.1	EZH2 is a target of hsa-miR-101	110
4.2	hsa-miR-101 regulates EZH2 transcript and protein expression.	111
4.3	hsa-miR-101 inhibits cell growth, and invasion and tumor growth	113
4.4	Genomic aberration in cancer leads to the down regulation of miR-101	115

LIST OF TABLES

Table

1.1	Main components of Polycomb group proteins and their role in cancer	31
2.1	Demographics of patients with clinical follow-up used in this study	60
2.2	Independent factors predictive of death from breast cancer	62
2.3	Association between EZH2 and clinical characteristics	63
2.4	Univariate Cox model	64

CHAPTER 1

INTRODUCTION

The multitude of cell types that constitute an adult human being contain the same genetic material. During development, a cell's fate is decided by the initial gene expression. After acquiring its fate and position, this cellular identity is maintained by keeping some genes "on" and others "off". If the maintenance mechanism fails, cells may lose their properties of proliferation, differentiation, adhesion or invasion when and where they should not(1, 2). Cancer is a result of defects in maintaining the cellular memory, causing cells to react inappropriately. The Polycomb Group (PcG) and trithorax Group (trxG) have been identified to keep the cellular memory and prevent changes in cell type specific transcription programs(1, 3). They are known to be involved in the process of histone modification, DNA methylation and chromatin transformation(4-10).

To establish and maintain the cell identity, many pathways are involved in repressing specific sets of genes. From *Drosophila* to mammals, the genes of Polycomb group and trithorax group are widely conserved and they maintain the transcription patterns which are set in the first stages of embryonic life, and in the adulthood. TrxG and

PcG respectively regulate active and repressed genes related to development and cell cycle regulation. Both groups consist of multi-protein complexes which can modify chromatin and change its structure. As known, chromatin contains the imprints underlying the cellular memory and epigenetic inheritance. In *Drosophila* and mammals, both trxG and PcG bind to a specialized DNA element, Polycomb/trithorax Response Elements [PREs/TREs] to perform their epigenetic function(11, 12).

By genetic screening, trxG and PcG were initially identified in *Drosophila* to establish and maintain homeobox (Hox) gene expression patterns(13-15). But the function of the trxG and PcG is not limited to regulate Hox gene expression(16). Further studies have shown that these proteins bind to thousands of chromosomal site in addition to the Hox genes(14, 15). In mammals, PcG genes expression exhibits a spatial and temporal pattern(15).

PcG proteins appear to perform their functions by forming complexes. Two distinct Polycomb complexes have been characterized by immunoprecipitation, yeast-two-hybrid and size-fractionation experiments in mammalian system (**Figure 1.1**). BMI-1, RING1, HPH1/2/3, and HPC1/2/3 (Psc, dRING, ph and Pc in *Drosophila*)(9, 10, 17) proteins constitute the Polycomb Repressive Complex 1 (PRC1) and EZH2, EED, SUZ12, RbAp46/48 and AEBP2 (E(z), Esc, Su(z)12, and RbAp48 in *Drosophila*)(9, 10, 15, 17) make the Polycomb Repressive Complex 2 (PRC2). The PRC2 was shown to physically associate with Yin Yang 1 (YY1, the human homolog of Pho in *Drosophila*)(18), which is the only known DNA binding protein of the Polycomb group, while all the others do

not have apparent DNA binding motifs(17). However, YY1 binding sites alone are not sufficient to alter the epigenetic pattern. It is shown that HDAC which is associated to EED(19, 20) is required for PRC2 to perform its function. EZH2/E(z) contains a conserved histone methyltransferase domain, SET domain, named after SU(var)3-9, E(z) and Trithorax which contain this enzymatic domain(17). Based on recent discoveries, a model is proposed to illustrate how Polycomb group complexes perform their function. At the beginning, the histone tails on the chromatin are acetylated and target genes are transcriptionally active. Once the cellular memory is disturbed, through the cell signaling pathway, PRC2 receives the signal from the cell signaling pathway and binds to a PRE. HDAC is then recruited to the PRE to deacetylate the histone tails, so that PRC2 can methylate the histone tails. This alters chromatin structure and enables PRC2 and HDAC to access the target gene promoters. Further, the histone tails on the gene promoters are deacetylated and then methylated. This methylation establishes a binding site for the N-terminal chromodomain of PcG proteins so that PRC1 is recruited to the promoters of target genes to repress their expression by repressing transcription initiation(7, 21, 22). Accordingly, PRC2 is also called PRCi (initiation), and PRC1 is called PRCm (maintenance).

Human *E(z)* homolog EZH2 was initially identified as a protein associated with proto-oncogene VAV in lymphoma. The gene of EZH2 maps to chromosome 7q35 and consists of 20 exons, encoding 746 amino acid residues(23). By yeast two-hybrid screen with EZH2, human Esc homolog EED was identified to interact with EZH2 *in vitro*, and

by co-IP, EZH2 and EED were confirmed to form a complex *in vivo*. Several studies demonstrated that the WD40 domains of EED are essential for this EZH2-EED complex, while the point mutants in the WD40 domain blocked the interaction between EZH2 and EED(9, 24-26).

Another polycomb protein SUZ12 is also characterized as an essential component of PRC2 for its HMTase enzymatic activity. Several interacting partners of the EZH2-EED complex include SUZ12, RbAp48 and AEBP2, which were identified by isolating and characterizing the enzymatic complex which had high HMTase activity to histone H3(9). The reconstituted complex of EZH2, EED, SUZ12, RbAp48 and AEBP2 can specifically methylate Histone H3 *in vitro*. GST pull down assays showed that EZH2 strongly binds to EED, but not to other proteins; Besides EZH2, EED can also interact with SUZ12 and AEBP2, while RbAp48 strongly binds to SUZ12 and weakly to EED and AEBP2. In this complex, EZH2, EED and SUZ12 are required for the HMTase activity, and RbAp48 helps SUZ12 interact with EZH2-EED, and AEBP2 significantly increases the EZH2-EED-SUZ12 HMTase activity(9).

In 2002, Kuzmichev *et al.* found that PRC2 exhibited HMTase activity and could specifically methylate H3K9 and H3K27(27). Furthermore they proved that the methylation of H3K27 provides a mark for PRC1 protein PC1 binding, therefore, PRC1 is recruited to the targets. Generally the PRC2 protein EZH2 preferentially methylates Lysine 27 on histone 3 (H3K27)(8-10, 27). But under certain conditions, it can also methylate other substrates, such as H3K9 and H1BK26. Because EZH2 is the only known

histone methyltransferase which can tri-methylate H3K27, the level of tri-me-H3K27 is used as the marker of EZH2 enzymatic activity. Some groups also reported that there exist Polycomb Repressive Complex 3 (PRC3) and Polycomb Repressive Complex 4 (PRC4) in cells(6, 27, 28). The human EED has four different isoforms due to alternate translation initiation sites from the same mRNA. All of these isoforms can associate to EZH2 to form different complexes and bind to their substrates. EED1 (the largest isoform) and EZH2 form PRC2 (~400-kDa complex) and methylate H3K27 in the presence of histone H1. EED3 and EED4 (the two shortest isoforms) can form PRC3 (~400-kDa complex) with EZH2, and methylate H3K27 when histone 1 is absent. EED2, SirT1, which specifically binds to EED2, and EZH2 form PRC4 (~1.5-MDa complex) and methylate K26 residue on H1B.

Recently, another Polycomb group protein polycomblike (Pcl)/PHF1 has been identified to interact with the PRC2 complex in *Drosophila* and mammals(29, 30). By tandem affinity purification (TAP) strategy, Nekrasov *et al.* characterized a distinct PRC2 complex containing Pcl from a transgenic *Drosophila* strain expressing a TAP-Pcl fusion protein. Like the regular PRC2 complex, the Pcl-PRC2 is a H3K27 specific HMTase. But the authors demonstrated that H3K27me3 levels are much lower in the Pcl^{-/-} strains than in wild-type. By contrast, H3K27me1 and H3K27me2 levels are higher in Pcl^{-/-} strains than in wild-type, suggesting that Pcl/PHD1 is required for generating high levels of tri-methylated H3K27 and maintaining the Polycomb-repressed chromatin structure.

While the PRC2 complex possesses HMTase activity, the PRC1 complex has been identified to exhibit H2AK119 ubiquitin E3 ligase activity(7, 21, 22). The mammalian PRC1 H2AK119 ubiquitin E3 ligase complex consists of several PcG proteins and the RING2/RING1B protein is the catalytic subunit. The presence of BMI1, RING1/RING1A and PC3 significantly increases the complex ubiquitin E3 ligase activity of the complex, while RING1/RING1A with reconstituted N-terminus has ubiquitin E3 ligase activity as well. Notably, BMI-1 interacts with RING1/RING1A, RING2/RING1B, PH2 and PC3, indicating that BMI-1 is important for the integrity of this complex. Although another Polycomb protein Mel-18 can replace BMI-1 and maintain the PRC1 complex, Mel-18 could not stimulate the ubiquitin E3 ligase activity. Interestingly, knockdown of BMI-1 upregulates most late Hox genes and downregulates most early Hox genes(7). And knockdown of BMI-1 results in decreasing the H2A ubiquitination level and upregulating HoxC13. However, the binding of SUZ12 or the H3K27 methylation level of the HoxC13 promoter is not affected by loss of BMI-1. Very importantly, when SUZ12 is knocked-down, the HoxC13 promoter H3K27 methylation level is decreased, and PRC1 could not bind to the promoter effectively, resulting a decrease of H2A ubiquitination. All these experiments provide a hierarchical recruitment model explaining how PRC2 and PRC1 exert their function to repress gene expression. PRC2 methylates H3K27 and provides a binding site for PRC1 recruitment through the specific recognition of the H3K27 methyl mark by the chromodomain of the Polycomb (Pc) protein. And then PRC1 can ubiquitinate H2A and turn off the gene expression.

Besides RING2/RING1B, another PRC1 protein Pc2 is reported to have SUMO E3 ligase activity(31). In 2003, Kagey *et al.* characterized that Pc2 is involved in the ubiquitination of the transcriptional repressor CtBP1 and CtBP2. Pc2 can interact with CtBP1 and CtBP2 via a PLDLS-like motif and recruit them to the PRC1. The sequence of Pc2 does not exhibit obvious similarity to any other known E3s. In 2005, the same group found that the C-terminal of Pc2 can act as a docking site for UBC9, a well known ubiquitin E2, and its substrates CtBP1 and CtBP2.

Recently, Vire *et al.* reported that EZH2 can directly control DNA methylation, so that the two processes which can repress gene expression(4), Histone methylation and DNA methylation are connected, and this finding elucidates a mechanism by which Polycomb Group and DNA methyltransferases (DNMTs) work together to repress gene expression. The authors demonstrated that the complex pulled down with GST-EZH2 possesses DNMT activity and this complex contains EZH2, DNMT1, DNMT3A and DNMT3B, and that the N-terminal H-I and H-II domains of EZH2 are required for establishing and maintaining this complex. Furthermore, reciprocal co-immunoprecipitation (co-IP) confirmed that DNMTs interact with PRC2, EZH2 and EED in vivo. Notably, similar to the effect of DNA methylation inhibitor 5'-aza-deoxycytidine treatment, knock-down of EZH2, DNMT1, DNMT3A or DNMT3B markedly increases expression of their target genes, but not of the housekeeping genes. By ChIP in EZH2 RNAi cells, the authors demonstrated that EZH2 is essential for

DNMTs recruiting to the promoters of their targets, while RNA polymerase II could interact with the promoters and turn on the expression of target genes.

Several papers reported that PcG proteins are involved in the *de novo* DNA methylation in cancers or cancer cell lines(32). By ChIP analyses, it is shown that genes with DNA methylation in cancer are marked with Polycomb proteins. Interestingly, many tumor suppressors are repressed by active *de novo* DNA methylation, and are pre-marked with H3K27 tri-methylation, indicating the mechanism by which EZH2 and PRC2 promote cancer progression. In normal tissues, some tumor suppressors are marked with H3K27 tri-methylation, but not *de novo* DNA methylation, demonstrating that EZH2 alone is not sufficient for DNA methylation, and several other components have to be recruited to methylate DNA to facilitate gene repression.

Although EZH2 is required for DNA methylation, it is not required for maintaining DNA methylation and keeping the genes off. Some evidence demonstrated that knock-down of EZH2 can de-repress genes whose promoters are methylated, such as MYT1 and WNT1; But for the genes whose promoters are hypermethylated, such as MLH1, knockdown of EZH2 could not increase their expression, even though the H3K27 trimethylation level is decreased because of the EZH2 knockdown(33).

EZH2 and PcG in development

In the *Drosophila* embryo, the segmental body plan is set in the first three and a half hours of development(34). Every segment has its own developmental fate

determined by a particular combination of homeotic gene products. Furthermore, maintenance of that decision is ensured by a particular combination set of homeotic proteins. The initial pattern of homeotic gene transcription in each segment is established by transcription factors encoded by the segmentation genes. After 5 to 7 hours of development, the transcriptional factors which control the initial development differentiation pattern decay and the relay is taken by the Polycomb (PcG) and trithorax (trxG) groups of proteins. PcG and trxG proteins have been identified in *Drosophila* to maintain the homeotic proteins and long-term gene silencing during development. However, *E(z)* and *Esc* are different from other PcG proteins because *E(z)* and *Esc* are required since early during development while the other PcG proteins appear to be required relatively late(34). Furthermore, *E(z)* and *Esc* are the most highly conserved PcG genes throughout evolution, since they are the only two PcG genes found in the *C. elegans* genome.

In mammals, two homologues of *E(z)* have been characterized and named as EZH1 and EZH2. Sequence analysis shows that EZH1/2 have four conserved domains aligning to *E(z)*(24, 26), which are homologue domain I (H1 domain), homologue domain II (H2 domain), cysteine-rich domain and C-terminal SET domain. Biochemical study demonstrates that the C-terminal SET has histone methyltransferase activity and preferentially methylates Lysine 27 on Histone H3. The N-terminal H1 and H2 domains are protein-protein interaction domains. Yeast two-hybrid studies revealed that EZH2 can bind to the WD40 domains of EED through the H1 and H2 domains of EZH2. In addition,

EZH2 can bind to VAV through the H2 domain of EZH2, indicating that EZH2 plays a role in signal-dependent T-cell activation.

In 2001, O'Carroll et al. reported that EZH2 is required for early mouse development and the homozygous EZH2 null mutations result in early lethality(34). The authors found that at day 10.5, homozygous EZH2 null mutant embryos could not grow. And at day 7.5 the EZH2 mutant embryos were significantly smaller than their littermates. Some of the EZH2 mutant embryos were extremely growth retarded and the other displayed increased amounts of extraembryonic tissue along with growth retardation. The authors also reported development arrest and gastrulation failure in embryos from EZH2 heterozygous intercrosses. The same group also reported that oocytes depleted of the maternal supply of EZH2 show severe growth retardation. And oocytes depleted of EZH2 lacked methylated H3K27 and H3K9, while the level of methylated H3K4 is same as that of wild-type oocytes(35).

PcG proteins are also reported to have a role in X chromosome inactivation (Xi) (36-39). In mammals, dose compensation is achieved by transcriptional silencing of one of the two X chromosomes in females. The process of Xi consists of multiple steps: choosing the active X chromosome, initiating the silence of Xi and maintaining the Xi throughout all the subsequent cell divisions. The non-coding RNA Xist (X inactivation specific transcript) is specifically transcribed from the Xic (X inactivation center) on the Xi, and covers the center of Xi in *cis* and triggers inactivation. Once Xist covers Xi, PRC2 is recruited and tri-methylates H3K27 on Xi, and PRC1 could be independently

recruited to Xist where it monoubiquitinates H2AK119. EED is important for protecting the inactive X-chromosome from differentiation-induced reactivation(36, 38, 40).

PcG in stem cells

Stem cells are a type of pluripotent cell with the ability to self-renew and differentiate to progenitors. To maintain the status of stem cells and control their fate, PcG proteins are employed for histone modifications, including histone methylation and ubiquitination, and DNA methylation. Studies have demonstrated that EZH2, EED, SUZ12 and RNF2 are essential for embryonic development(41, 42). EZH2, EED or RNF2 deficient mice are embryonic lethal and EZH2-null or EED-null embryonic stem (ES) cells could not be established. In hematopoietic stem cells (HSCs), both PRC1 and PRC2 are reported in regulating the self-renewal and differentiation of HSCs, consistent with the notion that PRC1 and PRC2 have to perform their functions sequentially to regulate gene expression(43).

Recently, several groups have launched a global approach to identify the target loci for binding of PcG proteins by genome-wide mapping in human fibroblasts, human ES cells, mouse ES cells or Drosophila(44-48). All of these studies demonstrated that PcG proteins directly repress a large number of regulators that are involved in early developmental steps, a wide variety of developmental processes, and cell differentiation. PcG proteins also regulate genes in a variety of signaling pathways including WNT, FGF

(Fibroblast Growth Factor), BMP (Bone Morphogenic Protein) and TGF β (Transforming Growth Factor β). These signals are required for lineage differentiation and are associated with cancer progression. These studies of PcG in ES cells give clues about how dysregulation of PcG proteins perform their function to promote tumorigenesis.

Polycomb group and Cancer

Multiple lines of evidence show that PcG proteins are dysregulated and play important roles in cancer progression (**Table 1.1**)

The PRC1 protein BMI-1 was the first reported PcG protein to be associated with cancer development. BMI-1 is the human homologue of *Drosophila* Psc and has been reported to promote the generation of B- and T-cell lymphomas by collaborating with c-MYC. One proposed mechanism suggested that BMI-1 may inhibit c-MYC induced apoptosis via INK4A/ARF and regulate cell proliferation and senescence (49, 50). INK4A and ARF play a role to restrict cellular proliferation in response to aberrant mitogenic signaling. INK4A is a cyclin-dependent kinase inhibitor and it can activate the RB pathway. ARF can inhibit MDM2 function to induce p53. In many types of tumors, the INK4A/ARF locus is found to be mutated, deleted or epigenetically silenced.

Interestingly, when neuroblastoma (NB) and other cancerous human cells were treated with siRNA against BMI-1, cells grew poorly and had elevated levels of apoptosis within three days after transfection, whereas neurons and other normal human cells did

not show this phenomenon. Furthermore, RNAi mediated suppression of BMI-1 led to significant cell death in human embryonic carcinoma stem cells, but not in normal embryonic stem cells, indicating that BMI-1 may perform as a cancer stem cell factor to regulate the growth and survival of cancer(51).

Another PRC1 protein RING1 was also shown to interact with BMI-1 and overexpression of RING1 represses engrailed and increases expression of c-JUN and c-FOS. Furthermore, RING1 induces anchorage-independent growth of Rat1a and NIH3T3 cells with overexpression of RING1 can form tumors in nude mice(52-54).

EZH2 is a biomarker of metastatic prostate cancer.

Among epithelial derived tumors, EZH2 was first observed to be significantly associated with metastatic prostate cancer. Along with MTA-1, HPN, PIM1 and several other genes, EZH2 is overexpressed in hormone-refractory, metastatic prostate cancer, and is a biomarker of prostate metastases(55). Through gene expression profiles of benign prostate, prostate cancer (PCa) and metastatic prostate cancer, EZH2 was one of the top genes upregulated in metastatic prostate cancer(56-62). Importantly, the EZH2 protein level was significantly increased in metastatic prostate cancer compared to PCA or benign prostate, while EED levels were not altered in metastatic prostate cancer(57). To determine the expression of EZH2 protein levels *in situ*, a wide spectrum of cancer tissues was evaluated in a tissue microarray format. EZH2 antibodies mainly stained the nucleus since EZH2 has a nuclear localization sequence. And the intensity of EZH2

staining increased from benign, prostatic atrophy, prostatic intraepithelial neoplasia, clinically localized prostate cancer, to metastatic prostate cancer. Furthermore, expression of EZH2 was significantly associated with clinical failure. However, EZH2 protein was not correlated to Gleason score, tumor stage or surgical margin status.

EZH2 is essential for cell proliferation. When EZH2 was knocked-down by RNA interference in the prostate cell lines PC3 and RWPE and the osteosarcoma cell line U2OS(57, 63), cell proliferation was significantly inhibited, but EZH2 RNAi did not induce apoptosis. And notably, EZH2 depleted cells showed cell-cycle arrest in the G2/M phase indicating that EZH2 plays a role in cell proliferation by mitigating G2/M transition.

Importantly, ectopic expression of EZH2 does not upregulate any other genes in prostate or breast cells and the C-terminal SET domain is essential for EZH2 to perform its histone methyltransferase activity. Notably the HDAC inhibitor trichostatin A can completely block EZH2 function, suggesting that HDAC activity is required for EZH2 and PRC2 to exert their functions(57).

To explain why EZH2 is overexpressed in prostate metastases, the genomic region of EZH2 has been analyzed by array comparatively genomic hybridization (aCGH) and fluorescence in situ hybridization (FISH) in prostate cancer cell lines and clinical prostate tumors. It is reported that the number of EZH2 copies is increased in prostate cancer cell lines DU145, PC-3, 22Rv1 and LNCaP, and also in the xenograft cell line LuCaP41. Importantly, EZH2 is amplified in 26% of hormone-naïve prostate cancer and

54% of hormone-refractory prostate cancer samples, suggesting that EZH2 gene amplification might result in overexpression of EZH2 in prostate metastases(59, 61).

Interestingly, EZH2 was observed to be highly over expressed in prostate carcinoma metastasis precursor cells with PRC1 protein BMI1(64). By quantitative immunofluorescence colocalization analysis, Berezovska *et al.* demonstrated a marked enrichment of the population of circulating human prostate carcinoma metastasis precursor cells with dual-positive high-BMI1/EZH2-expressing cells. RNA interference against BMI1 or EZH2 showed that high levels of BMI1 and EZH2 help prostate cancer cells resist apoptosis that is induced in cells of epithelial origin in response to attachment deprivation. Importantly, depletion of BMI1 or EZH2 in prostate carcinoma metastasis precursor cells diminishes their tumorigenic, metastatic and proliferation potential when injected into mice.

Recently, a Polycomb repression signature in metastatic prostate cancer has been revealed to predict cancer outcome(65). To investigate the role of PRC2 in metastatic prostate cancer, Yu et al. performed ChIP-on-chip by anti-SUZ12 and anti-H3K27me3 antibodies in late-stage, aggressive prostate cancer tissues. Genome-wide location analysis showed that there is a strong overlap between the genomic sites occupied by SUZ12 and H3K27me3 in metastatic prostate cancer and prostate cancer cell lines. Oncomine Molecular Concept Map (MCM) analysis showed that H3K27 occupied genes are consistent with genes down-regulated in prostate, breast and lung cancers, since EZH2 is upregulated in aggressive cancers and PRC2 are transcriptional repressors.

Importantly, there is a strong link between H3K27 occupied genes in prostate metastases and H3K27me₃-, SUZ12-, or EED-occupied genes in embryonic stem cells, which indicates that the function of PRC2 to control stem cell pluripotency and differentiation is essential for prostate cancer progression. In addition, the Polycomb repression signature is able to successfully predict the clinical outcome of prostate and even breast cancer patients.

Among the genes regulated by EZH2 in prostate cancers, ADRB2, a G-protein coupled receptor (GPCR) of the β -adrenergic signal pathway, has been characterized as one of the key proteins(66). By down-regulation of the key target genes, EZH2 promotes cell anchorage-independent growth, migration and invasion potential, and then induces prostate metastasis. By cDNA microarray, ADRB2 was identified as a target of EZH2. Overexpression of EZH2 can repress ADRB2 at both transcript and protein levels, and the recently discovered EZH2 inhibitor, DZNep(67), can prevent ADRB2 repression by EZH2. Notably, the promoter of ADRB2 is occupied by the PRC2 complex and H3K27me₃. However the dominant negative mutant of EZH2 (EZH2 Δ SET) does not bind to the ADRB2 promoter. Also, the HDAC inhibitor, SAHA, blocks PRC2 to access the ADRB2 promoter, consistent with the mechanism that HDAC activity is required for PRC2 to perform its transcriptional repression. Interestingly, ADRB2 expression is low in prostate cancer cell lines which have high EZH2 levels. Stable prostate cell line clones of EZH2 knock down showed a marked increase in ADRB2 expression. Importantly, co-expression of ADRB2 decreases the EZH2-mediated epithelial cell invasion, while an

antagonist of ADRB2 makes the non-invasive epithelial cells invasive. Furthermore, ADRB2 antagonist treated or stable ADRB2 knock-down non-invasive epithelial cells exhibit a mesenchymal phenotype with fibroblast-like shape, and the epithelial-mesenchymal transition (EMT) markers such as Vimentin, N-cadherin are increased while ADRB2 activity is inhibited or expression is decreased. Similar to the EZH2 stable knock-down, the agonist of ADRB2 inhibits tumor growth in a xenograft mouse model. All these clues indicate that EZH2 promotes anchorage-independent cell growth, migration, invasion and tumorigenesis through ADRB2 and other signaling pathways.

Another tumor suppressor, prostatic secretory protein 94 amino acids (PSP94), has been characterized as a target of EZH2(68). There is an inverse correlation between EZH2 and PSP94 in advanced, hormone-refractory prostate cancer. The promoter of MSMB which encodes PSP94 is occupied by PRC2 and H3K27me3. Furthermore, overexpression of EZH2 represses MSMB expression while EZH2 RNAi increases MSMB mRNA level. Importantly, both the HDAC inhibitor TSA and the DNA methyltransferase inhibitor 5'-aza-deoxycytidine de-repress MSMB from the repression of EZH2.

Another potent growth inhibitor, the human DOC-2/DAB2 interactive protein (hDAB2IP, also called ASK-interacting protein 1 (AIP1)), is reported as a target of EZH2 in prostate cancer(69). Similar to ADRB2 and PSP94, there is a negative correlation between EZH2 and hDAB2IP in normal prostate epithelium, primary prostate cancer cells and metastatic prostate cancer cell lines. Knock-down of EZH2 increases hDAB2IP

mRNA, while overexpression of EZH2 represses hDAB2IP promoter activity and protein level. Importantly, EZH2 and the PRC2 complex bind to the promoter of hDAB2IP and overexpression of EZH2 leads to H3K27 tri-methylation of hDAB2IP promoters to repress hDAB2IP expression.

EZH2 is usually located in nucleus since it has a nuclear localization signal (NLS), but it is reported that in *ex vivo* isolated thymocytes, a fraction of EZH2 is also present in cytoplasm(70, 71). Later, Bryant et al. reported that EZH2 is overexpressed in both nucleus and cytoplasm in malignant prostate tissues comparing to normal prostate tissues(72). Interestingly, EZH2 can form a functional histone methyltransferase complex with EED and SUZ12 in the cytoplasm, and this complex can methylate H3K27 when incubated with nucleosome *in vitro*. Also, the cytosolic PRC2 complex associates with VAV1 indicating this cytosolic PRC2 complex may play a role in VAV-dependent pathways, such as T cell antigen receptor (TCR) mediated actin polymerization. Similarly, knock-down of EZH2 in prostate cancer cells increases polarized actin (F-actin). This function of EZH2 may help illuminate the mechanism by which EZH2 promotes prostate cancer invasion and metastasis.

EZH2 is a biomarker of aggressive breast cancer.

Every year, over 180,000 American women are diagnosed with breast cancer. Although most of them will receive some kind of treatment such as chemotherapy and radiotherapy, mortality for those 20% of patients with recurrences and or metastases is

nearly 100%. Given the high mortality rate, the main challenge is to find some good prognostic factors regulating breast cancer development and progression that will facilitate early diagnosis of breast cancer with high specificity (73, 74).

Based on our previous work characterizing EZH2 in prostate cancer(55, 57), our group investigated the role of EZH2 in breast cancer and demonstrated that EZH2 is elevated at both the transcript and protein levels in invasive and metastatic breast cancer when compared to normal breast tissues(75). Immunohistochemical analyses performed on a spectrum of breast cancer tissues demonstrated that high EZH2 levels were strongly associated with poor clinical outcome in patients. Higher EZH2 protein levels were associated with a shorter disease-free interval after initial surgical treatment, lower overall survival, and a high probability of disease-specific death (i.e. death due to breast cancer). Also, high EZH2 expression was associated with disease-specific death in patients with lymph node-negative disease, but not in patients with positive lymph nodes. EZH2 expression was associated with disease-specific survival in patients with stage I and II disease, but not in patients with advanced stage (stages III and IV). Kaplan–Meier analysis showed that EZH2 levels were strongly associated with bad outcome in both ER-positive and -negative invasive carcinomas suggesting that EZH2 has prognostic utility independent of ER status.

Importantly, overexpression of EZH2 could increase HDAC enzymatic activity. Also overexpression of EZH2, but not the dominant negative mutant of EZH2, EZH2 Δ SET, promotes anchorage-independent growth in epithelial cells. Furthermore,

three different *in vitro* or *in vivo* invasion assays have been employed showing that EZH2 overexpression increases the invasion potential of breast epithelial cells, while EZH2 Δ SET could not. Notably, the HDAC inhibitors TSA and SAHA could attenuate invasion induced by EZH2. All of those clues indicate that both HDAC and HMTase activity are essential for the PRC complex to exert its function to regulate gene expression.

However, the expression patterns of PRC1 and PRC2 are different in various stages of tumor progression. The PRC1 complex expression is always high in normal breast tissues, preinvasive lesions and invasive breast carcinomas, which is consistent with the function of PRC1 to maintain the gene expression pattern. But in normal breast tissues, EZH2 and EED are rarely detectable except in the cycling cells. In the preinvasive lesions, EZH2 is still rarely detectable in the well-differentiated ductal carcinoma *in situ* (DCIS), while in poorly differentiated DCIS, EZH2 expression is significantly increased and detectable. EZH2 expression is highest in poorly differentiated invasive breast carcinomas but is still undetectable in well-differentiated invasive carcinomas. Interestingly, EZH2 expression is significantly higher in patients with BRCA1 heterozygous mutation who have much higher risk of developing breast cancer than in control patients. Also histologically normal breast tissues from patients who developed cancer had significant up-regulation of EZH2 when compared with tissues from patients who did not develop cancer. All of these evidences demonstrated

that EZH2 expression is associated with cancer progression and is a biomarker of the precancerous state in morphologically normal tissues.

To investigate the mechanism by which EZH2 promotes cell transformation and invasion, we did cDNA microarray analyses and ChIP-on-chip measurements in samples with EZH2 overexpression or knock-down samples. Among the list of EZH2 regulated genes, the tumor suppressor E-cadherin appears to be one of the key targets. Our previous work in prostate cancer demonstrated that there is an inverse correlation between EZH2 and E-cadherin in prostate cancer progression(76). In normal prostate and breast samples, EZH2 expression is low while E-cadherin expression is very high and there is good E-cadherin membrane staining by immunohistochemical analysis or immunofluorescence microscopy. In aggressive prostate and breast cancers, however, EZH2 expression is increased while E-cadherin expression is repressed. A similar pattern is observed in normal and cancerous cell lines prostate or breast. Importantly, When EZH2 is ectopically overexpressed in prostate and breast epithelial cells E-cadherin is repressed at both the transcript and protein levels. Also, this EZH2 mediated repression could be inhibited by the HDAC inhibitor SAHA. Furthermore, co-expression of E-cadherin can attenuate EZH2-mediated invasion in prostate and breast epithelial cells, indicating that E-cadherin is an important target of EZH2 in cancer progression. With an E-cadherin promoter activity assay, we demonstrated that the E-boxes of A and C are essential for EZH2 to repress E-cadherin. The promoter of E-cadherin is occupied by the PRC2 complex and shows H3K27 tri-methylation by PRC2 when EZH2 is overexpressed. In the

presence of the HDAC inhibitor SAHA, PRC2 could not bind to the E-cadherin promoter, H3K27 tri-methylation was absent, and the acetylation level of histone H3 was increased, indicating that E-cadherin expression is activated by SAHA. This work is consistent with the finding that in ES cells, PRC2 occupies the promoter of E-cadherin and represses its expression, indicating that the function of PRC2 to control stem cell pluripotency and differentiation is important for cancer progression.

Besides repressing tumor suppressors, EZH2 also represses genes associated with DNA repairs(77, 78). In mammals, hampered Double-strand break (DSB) repair could lead to chromosomal abnormalities resulting in cell death or cancer. To repair the DSB, the homologous recombinase RAD51 and its paralogs are required. Multiple studies demonstrate that RAD51 paralogs are important for maintaining chromosomal integrity in the early and late stage of homologous recombination (HR). Our group has reported that overexpression of EZH2 significantly downregulates the RAD51 paralogs, RAD51L1, RAD51L2, RAD51L3, XRCC2 AND XRCC3, at both the transcript and protein levels. Those RAD51 paralogs are required for the formation of DNA damage–induced RAD51 repair focus. Once any of them are mutated, RAD51 foci formation is significantly attenuated. We demonstrated that overexpression of EZH2 in breast epithelial cells markedly decreases RAD51 foci formation after induction of DSB by etoposide, indicating that HR repair is less effective in EZH2 overexpressing cell than in control cells. Furthermore, overexpression of EZH2 significantly decreases the survival, clonogenic capacity and colony-forming ability of breast epithelial or cancer cell lines.

All of this evidence suggests that EZH2 play an important role in the HR mechanism of DNA repair which may cause aneuploidy in breast epithelial cells.

As a component of a transcriptional repressive complex, EZH2 mainly performs its function to repress tumor suppressors and promote cancer progression. But studies in *Drosophila* indicate that EZH2 may have function as a transcriptional activator to increase the expression of some genes. Recently some evidence shows that in breast cancer cells, where EZH2 increases levels of the oncogene c-Myc and cyclin-D1, known estrogen receptor (ER) and WNT targets, which are important in the regulation of cell cycle and proliferation(79). In ER positive cell lines MCF7 and MDA-MB-231, overexpression of EZH2 significantly enhanced the promoter activities of c-Myc and cyclin D1. Notably, this enhancement was dependent on ER since ER antagonist ICI182780 abolished the EZH2 mediated enhancement of promoter activity. Interestingly the homolog EZH1 did not regulate c-Myc and cyclin D1 promoter activities, demonstrating the specificity of EZH2. Furthermore, GST pull-down and reciprocal co-immunoprecipitation (co-IP) assays demonstrated that ER α , EZH2 and β -catenin form a functional complex in vitro and in vivo. ChIP assay analysis confirmed that this complex is recruited to the promoters of c-Myc and cyclin D1. However, neither ER β nor AR interacted with EZH2, indicating the specificity of ER α for this complex. The study of mutants of EZH2 showed that the homolog domains 1 and 2 are essential for this ER α , EZH2 and β -catenin complex to activate c-Myc and cyclin D1 promoter activity, while

the cys-rich domain and SET domain are not required for maintaining this complex or for mediating its function.

Besides c-Myc and cyclin D1, EZH2 also activates cyclin A2(80). Unlike the mechanism of increasing c-Myc and cyclin D1, EZH2 up-regulates cyclin A2 indirectly. It was showed that EZH2 can bind to pRb2/p130 and repress its function, which in turn de-repress the expression of cyclin A2. Like the other two members of the Rb family, pRb/p105 and p107, pRb2/p130 functions as a transcriptional repressor of cell cycle promoting genes. HDAC1 is required for E2F-Rb complex to perform its function to repress the expression of its targets. As another well-known transcriptional repressor, EZH2 and its complex also interact with HDAC1 to perform their function. Some evidence showed that EZH2 may interact with HDAC1 and pRb2/p130 subsequently interfering with pRb2/p130 mediated repression. Reciprocal co-IP demonstrated that EZH2 and pRb2/p130 form a complex in vitro and in vivo. While overexpression of pRb2/P130 alone represses cyclin A2 promoter activity, co-expression of EZH2 abolishes the repression induced by pRb2/p130 by inhibiting pRb2/p130-HDAC1 binding to the promoter of cyclin A2. Furthermore the C-terminus of pRb2/p130 is important for forming the complex containing EZH2-HDAC-pRb2/p130. These two studies provide mechanisms through which EZH2 may act as a transcriptional activator rather than a repressor.

EZH2 in other cancers

The transcriptional repressor EZH2 is also involved in other types of cancer progression, such as bladder(81-85), gastric(86), lung(87), liver (88) and leukemia(58, 89) besides prostate and breast.

In 2005, Sudo *et al.* reported that EZH2 expression is significantly higher in human liver cancer cell lines and tissue specimens compared to normal sections(88). They also noted that the invasion potential to the portal vein of cancer cells is significantly higher in the group with high EZH2 expression than in the low EZH2 category. Chen *et al.* demonstrated that knock-down of EZH2 markedly inhibits the growth of hepatocellular carcinoma (HCC) cells and reduces the tumorigenicity of HCC cells in the nude xenograft mice. Importantly, growth of established HCC tumors could be significantly reduced by treatment with EZH2 shRNA or siRNA suggesting EZH2 may be a potential therapy target. The authors reported that EZH2 knock-down inhibits HCC cell growth by repressing OP-18/stathmin.

In bladder and gastric cancers(83-86), EZH2 is increased at both the transcript and protein levels in cancer cell lines and cancer tissue specimens relative to normal controls. EZH2 expression is also associated with cell invasion in bladder cancer. Importantly, Kaplan-Meier analysis indicated that patients with high level of EZH2 had a worse prognosis than those with lower levels.

The regulation of EZH2 in cancer

Elucidation of the mechanism of EZH2 dysregulation in cancer will help in understanding the biology of this protein in cancer progression. In 2003, Bracken et al. identified E2F1-3 regulation of EZH2 and PRC2 in cancer cells(63). Activation of E2F1-3 can markedly increase EZH2, EED and SUZ12 expression levels, while overexpression of pRB and p16, the upstream regulators which can repress the activity of E2Fs, decrease expression of EZH2 and EED. Mouse embryonic fibroblasts (MEFs) with a pRb^{-/-} genotype had elevated levels of EZH2 and EED. Furthermore, loss of p16 leads to overexpression of PRC2 at the transcript and protein levels, and induces the DNA hypermethylation of PRC2 targets. Also, EZH2 is reported to be down-regulated in senescent cells by p53 activation(90) and this downregulation is dependent on p21/waf1, which can inactivate E2F pathway. By ChIP and promoter activity assays, it was shown that E2F1-3 can directly bind to the promoters of EZH2 and EED and upregulate their expression. However, E2F1-3 cannot regulate the activity of the EZH2 promoter without potential E2F binding sites. Since E2F3 is amplified and overexpressed in prostate and bladder cancers, all of the evidence provides a mechanism to explain the upregulation of EZH2 during cancer progression.

Interestingly, BMI-1 is also reported as a target of E2F1-3(91), but not of E2F4 or E2F5. Promoter assays and ChIP studies indicated that E2F1-3 directly binds to and increases wild-type BMI-1 promoter activity. This does not occur with a mutated promoter in which the potential E2F binding site is mutated. This finding is consistent with the mechanism by which PRC2 and PRC1 perform their function together to bring

about gene repression. **Figure 1.2** proposes a possible pathway of how PcG proteins are regulated and exert their function in cancer.

Another possible mechanism of EZH2 overexpression in cancers could be due to gene amplification (58). Copy number variation of EZH2 (>4 copies) is known to occur in multiple cancers, including bladder (2/7), breast (9/65), colon (5/22), glioblastoma (2/14), larynx (5/11), lung (3/15), lymphoma (1/11), sarcoma (1/9), stomach (2/14), testis (3/11) and late stage of prostate cancer (33/125 of hormone native prostate cancer and 25/46 of hormone refractory prostate cancer).

EZH2 may have a cytoplasmic function when it loses its nuclear localization signal (70-72) and this mutant protein could promote cancer development. In several cell types including late stage of prostate cancer, this EZH2 mutant can form a PRC2 complex with HMTase activity in the cytosol and promote TCR/PDGF-induced actin polymerization and induce tumorigenesis.

Another report suggests protein phosphorylation as a possible mechanism to regulate the activity of EZH2. In 2005, Cha *et al.* showed that EZH2 is downstream of the PI3K-Akt signaling pathway, which is involved in cell proliferation, motility and survival(92). The authors found an inverse correlation between activated Akt and the level of H3K27 tri-methylation. An inhibitor of the PI3K-Akt pathway, LY294002, was able to block phosphorylated Akt mediated repression of H3K27 tri-methylation. By co-IP, the authors demonstrated that constitutively activated Akt interacted with EZH2 or EZH2 Δ SET and that Akt could phosphorylate the Ser21 of EZH2. Interestingly, this

phosphorylated EZH2 does not affect the formation of a PRC2 complex, but it does reduce its affinity to H3K27. Hence, this phosphorylated EZH2 has less HMTase activity. Therefore, activated Akt could repress EZH2 activity, decrease the level of H3K27 trimethylation and increase the expression of EZH2 targets. They also showed that the S21A-EZH2 mutant has much higher HMTase activity and a stronger interaction with chromatin than does wild type EZH2. This S21A-EZH2 significantly repressed EZH2 target expression. This finding provides a possible method to repress EZH2 function for cancer therapy.

Recently, a novel mechanism that may dysregulate PRC2 in cancer progression was identified. Li et al. reported that in endometrial stromal tumors there is a series of rearrangements of DNA within the genes coding for the PRC2 complex (93). The authors discovered that in three primary endometrial stromal sarcomas (ESSs) cell lines, there exists a t(7;17) translocation and the C-terminus of SUZ12 is fused to the N-terminus of JAZF1. Importantly, this fusion protein can restore EZH2 activity and help methylate H3K27. Since PRC2 expression is usually very low in normal differentiated cells, this phenomenon of a fusion protein demonstrates a novel mechanism to dysregulate PRC2 and promote cancerigenesis.

EZH2 as a target for cancer therapy

The enzymatic activity (HMTase) and its function as an epigenetic repressor along with its established role in cancer progression, makes EZH2 an attractive target for

cancer therapy. We and others have shown that knock-down of EZH2 inhibits cancer cell growth, motility, invasion and tumorigenesis. Small interfering RNA against EZH2 reduced EZH2 expression in several cancer cell lines, significantly inhibited cell proliferation and the cells were arrested at the G2/M phase (57, 63, 66). In addition, the EZH2 knock down cells did not retain their invasive potential when injected into mice. This was apparent from the lack in tumor formation(66). Interestingly, tumor size was decreased and growth inhibited in established tumors in mice when an shRNA against EZH2 was delivered. This indicates the promise that EZH2 holds as a candidate for cancer therapy(94).

Synthetic peptide fragments of EZH2 were able to stimulate peripheral blood mononuclear cells (PBMCs) and produce EZH2-specific cytotoxic T lymphocytes (CTLs). Interestingly, those EZH2-specific CTLs can generate IgG against EZH2 and are toxic to HLA-A24 positive cells(95). This finding provides an alternative approach to inhibit EZH2 function in cancer progression.

EZH2 and PRC2 mediate their function as a complex with HDAC and our group demonstrated that the HDAC inhibitors TSA and SAHA can abrogate EZH2's function in H3K27 methylation, transcriptional repression and cell invasion(57, 66, 75). However, these agents are global inhibitors and regulate EZH2 indirectly and might produce undesirable side effects from a clinical standpoint. Now many groups are working on small molecule inhibitor screening for EZH2 based on wide range of approaches. Recently, Tan et al. has discovered that S-adenosylhomocysteine hydrolase

inhibitor 3-Deazaneplanocin A (DZNep) can deplete EZH2, EED and SUZ12 protein levels, inhibiting H3K27 methylation(67). The authors showed that following depletion of PRC2 by DZNep, RNA polymerase II can occupy the promoters of PRC2 targets and transcriptionally activate them. Interestingly, DZNep can re-activate some hypermethylated genes where 5'-Aza-dC and TSA failed, suggesting that DZNep could cause DNA demethylation. However, PRC2 repression by DZNep was not dependent on this function. In addition, DZNep could induce apoptosis specifically in cancer but not in normal cells. Hence is a compound that holds high promise for further characterization.

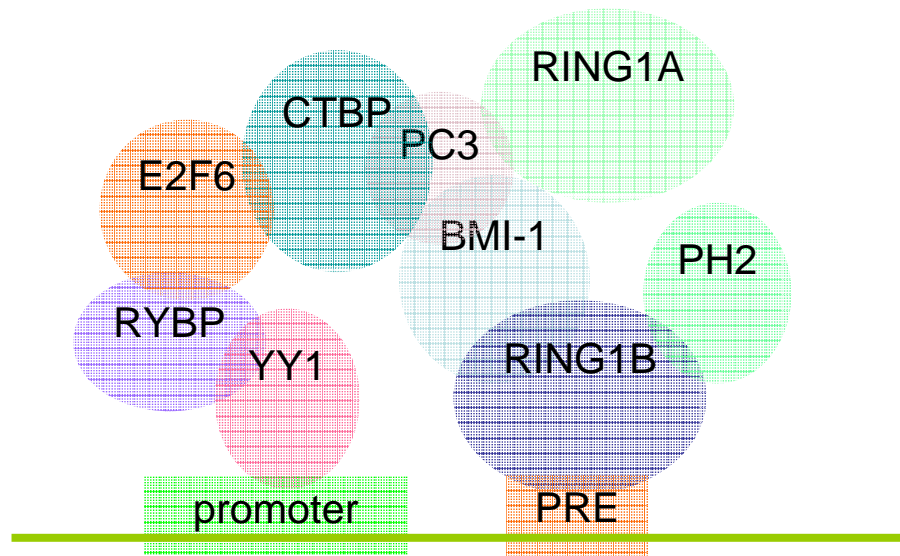
Table 1.1 Main components of Polycomb group proteins and their role in cancer

Drosophila proteins	Human homologues	Complex	Biochemical activities	Role in cancer
Pc	HPC1 HPC2 HPC3	PRC1	Recognition of methylated Histones; SUMO ligase E3 (HPC2)	
Ph	HPH1 HPH2 HPH3	PRC1	Stabilization of PRC1 complex	
Psc	BMI1 MEL18	PRC1	Integrity of PRC1 complex, increase of ubiquitination E3 ligase activity	Target of E2F1-3; Immortalize normal human oral keratinocytes; Promote the generation of B- and T-cell lymphomas with c-Myc; Overexpressed in B cell non-Hodgkin lymphoma, breast cancer, colorectal carcinoma, Hodgkin's lymphoma, liver carcinoma, medulloblastoma, non-small cell lung cancer, oral squamous cell carcinoma and prostate cancer,
Ring	RING1/RING1A RING2/RING1B	PRC1	Ubiquitin ligase E3	Overexpressed in Hodgkin's lymphoma prostate cancer; Increase c-Jun and c-Fos; Induce anchorage-independent growth and form tumor in nude mice;
Pho	YY1	PRC1 PRC2	DNA binding; Interact with E2Fs and Mdm2	Co-operate with c-myc and E2Fs; Inhibits the activation of p53; Enhances cyclooxygenase-2 gene expression in macrophages; Overexpressed in osteosarcoma and prostate

				cancer
E(z)	EZH1 EZH2	PRC2	Histone methyltransferase; Interact with DNA methyltransferases DNMT1, DNMT3A and DNMT3B, and directly control DNA methylation	Target of E2F1-3; Promote anchorage-independent growth and invasion; Essential for cell proliferation; Regulation of actin polymerization; Prognostic marker of aggressive breast cancer and prostate cancer; Impair DNA repair in breast cancer cells; Overexpressed in B cell non-Hodgkin lymphoma, bladder cancer, breast cancer, colon cancer, gastric cancer; liver cancer, lung cancer, Hodgkin's lymphoma, mantle cell lymphoma, melanoma and prostate cancer;
Esc	EED	PRC2	Interact with HDACs	Substrate preference of PRC2
Su(z)12	SUZ12	PRC2	Integrity of PRC2 complex	Overexpressed in breast cancer, colon cancer and lung cancer; Fusion protein of JAZF1-SUZ12 in breast cancer.
Pcl	PHF1	PRC2	Interact with EZH2	Enhance EZH2 Histone H3K27 tri-methylation activity.

A

PRC1



PRC2

B

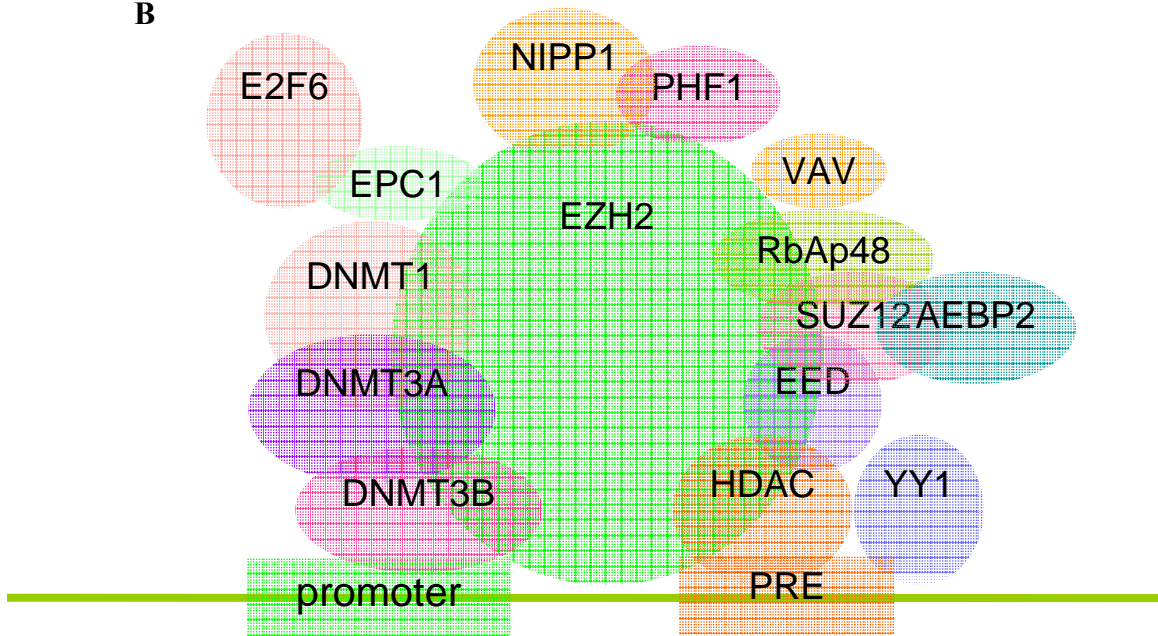


Figure 1.1 Two Distinct Human Polycomb Group Complexes. Each PcG Complex interacts with a polycomb response element (PRE) and functions to repress target genes

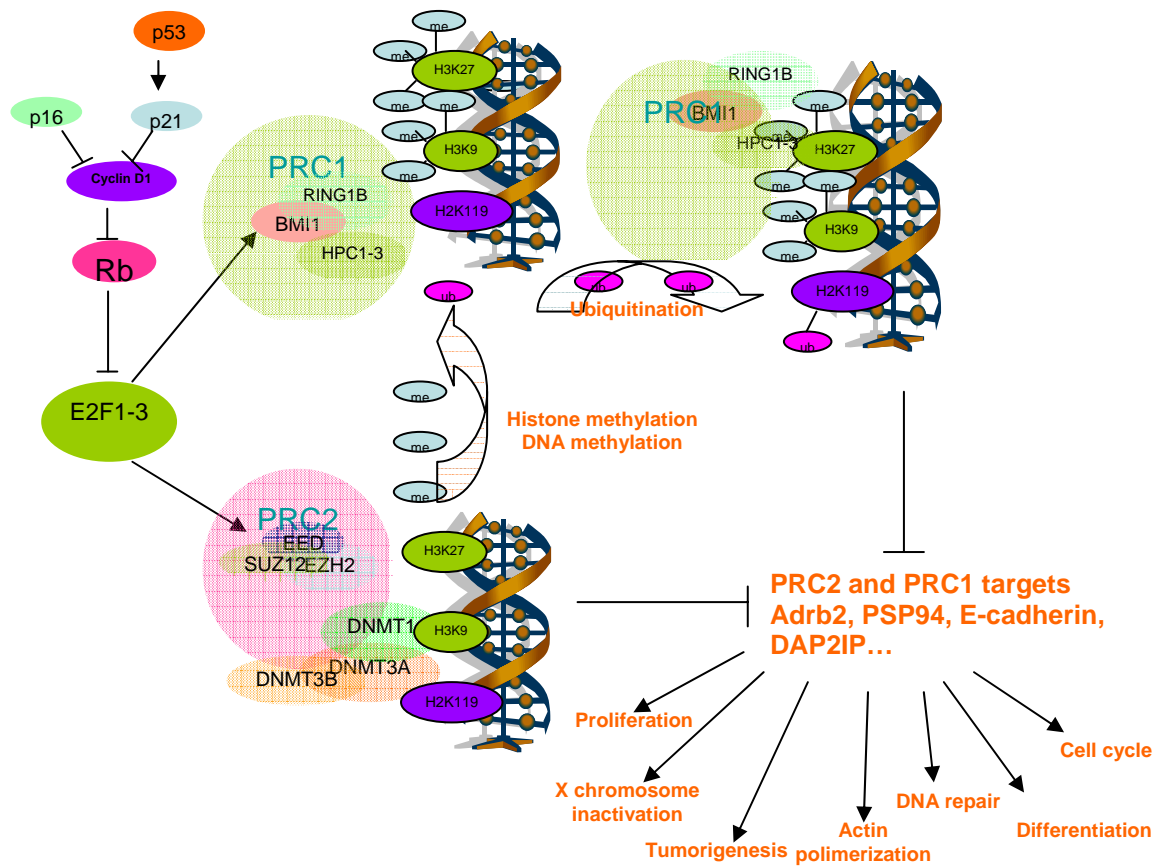


Figure 1.2 Model for PcG regulation and function.

REFERENCES

1. Jacobs, J. J. & van Lohuizen, M. (1999) *Semin Cell Dev Biol* **10**, 227-235.
2. Francis, N. J., Saurin, A. J., Shao, Z., & Kingston, R. E. (2001) *Molecular cell* **8**, 545-556.
3. Bantignies, F. & Cavalli, G. (2006) *Current opinion in cell biology* **18**, 275-283.
4. Vire, E., Brenner, C., Deplus, R., Blanchon, L., Fraga, M., Didelot, C., Morey, L., Van Eynde, A., Bernard, D., Vanderwinden, J. M., *et al.* (2006) *Nature* **439**, 871-874.
5. Negishi, M., Saraya, A., Miyagi, S., Nagao, K., Inagaki, Y., Nishikawa, M., Tajima, S., Koseki, H., Tsuda, H., Takasaki, Y., *et al.* (2007) *Biochemical and biophysical research communications* **353**, 992-998.
6. Kuzmichev, A., Jenuwein, T., Tempst, P., & Reinberg, D. (2004) *Molecular cell* **14**, 183-193.
7. Cao, R., Tsukada, Y., & Zhang, Y. (2005) *Molecular cell* **20**, 845-854.
8. Cao, R., Wang, L., Wang, H., Xia, L., Erdjument-Bromage, H., Tempst, P., Jones, R. S., & Zhang, Y. (2002) *Science (New York, N.Y)* **298**, 1039-1043.
9. Cao, R. & Zhang, Y. (2004) *Molecular cell* **15**, 57-67.
10. Cao, R. & Zhang, Y. (2004) *Current opinion in genetics & development* **14**, 155-164.
11. Simon, J., Peifer, M., Bender, W., & O'Connor, M. (1990) *The EMBO journal* **9**, 3945-3956.
12. Simon, J., Chiang, A., Bender, W., Shimell, M. J., & O'Connor, M. (1993) *Developmental biology* **158**, 131-144.
13. Beuchle, D., Struhl, G., & Muller, J. (2001) *Development (Cambridge, England)* **128**, 993-1004.
14. Ringrose, L. & Paro, R. (2004) *Annual review of genetics* **38**, 413-443.
15. Schuettengruber, B., Chourrout, D., Vervoort, M., Leblanc, B., & Cavalli, G. (2007) *Cell* **128**, 735-745.
16. Wang, J., Mager, J., Schnedier, E., & Magnuson, T. (2002) *Mamm Genome* **13**, 493-503.
17. Sparmann, A. & van Lohuizen, M. (2006) *Nature reviews* **6**, 846-856.
18. Satijn, D. P., Hamer, K. M., den Blaauwen, J., & Otte, A. P. (2001) *Molecular and cellular biology* **21**, 1360-1369.
19. van der Vlag, J. & Otte, A. P. (1999) *Nature genetics* **23**, 474-478.
20. Kim, S. Y., Levenson, J. M., Korsmeyer, S., Sweatt, J. D., & Schumacher, A. (2007) *J Biol Chem* **282**, 9962-9972.
21. Wang, H., Wang, L., Erdjument-Bromage, H., Vidal, M., Tempst, P., Jones, R. S., & Zhang, Y. (2004) *Nature* **431**, 873-878.
22. Wang, L., Brown, J. L., Cao, R., Zhang, Y., Kassis, J. A., & Jones, R. S. (2004) *Molecular cell* **14**, 637-646.

23. Cardoso, C., Mignon, C., Hetet, G., Grandchamps, B., Fontes, M., & Colleaux, L. (2000) *Eur J Hum Genet* **8**, 174-180.
24. Denisenko, O., Shnyreva, M., Suzuki, H., & Bomsztyk, K. (1998) *Molecular and cellular biology* **18**, 5634-5642.
25. Han, Z., Xing, X., Hu, M., Zhang, Y., Liu, P., & Chai, J. (2007) *Structure* **15**, 1306-1315.
26. Sewalt, R. G., van der Vlag, J., Gunster, M. J., Hamer, K. M., den Blaauwen, J. L., Satijn, D. P., Hendrix, T., van Driel, R., & Otte, A. P. (1998) *Molecular and cellular biology* **18**, 3586-3595.
27. Kuzmichev, A., Nishioka, K., Erdjument-Bromage, H., Tempst, P., & Reinberg, D. (2002) *Genes Dev* **16**, 2893-2905.
28. Kuzmichev, A., Margueron, R., Vaquero, A., Preissner, T. S., Scher, M., Kirmizis, A., Ouyang, X., Brockdorff, N., Abate-Shen, C., Farnham, P., *et al.* (2005) *Proc Natl Acad Sci U S A* **102**, 1859-1864.
29. Nekrasov, M., Klymenko, T., Fraterman, S., Papp, B., Oktaba, K., Kocher, T., Cohen, A., Stunnenberg, H. G., Wilm, M., & Muller, J. (2007) *The EMBO journal* **26**, 4078-4088.
30. Sarma, K., Margueron, R., Ivanov, A., Pirrotta, V., & Reinberg, D. (2008) *Molecular and cellular biology*.
31. Kagey, M. H., Melhuish, T. A., & Wotton, D. (2003) *Cell* **113**, 127-137.
32. Schlesinger, Y., Straussman, R., Keshet, I., Farkash, S., Hecht, M., Zimmerman, J., Eden, E., Yakhini, Z., Ben-Shushan, E., Reubinoff, B. E., *et al.* (2007) *Nature genetics* **39**, 232-236.
33. McGarvey, K. M., Greene, E., Fahrner, J. A., Jenuwein, T., & Baylin, S. B. (2007) *Cancer Res* **67**, 5097-5102.
34. O'Carroll, D., Erhardt, S., Pagani, M., Barton, S. C., Surani, M. A., & Jenuwein, T. (2001) *Molecular and cellular biology* **21**, 4330-4336.
35. Erhardt, S., Su, I. H., Schneider, R., Barton, S., Bannister, A. J., Perez-Burgos, L., Jenuwein, T., Kouzarides, T., Tarakhovsky, A., & Surani, M. A. (2003) *Development (Cambridge, England)* **130**, 4235-4248.
36. Schoeftner, S., Sengupta, A. K., Kubicek, S., Mechtler, K., Spahn, L., Koseki, H., Jenuwein, T., & Wutz, A. (2006) *The EMBO journal* **25**, 3110-3122.
37. Ohhata, T., Tachibana, M., Tada, M., Tada, T., Sasaki, H., Shinkai, Y., & Sado, T. (2004) *Genesis* **40**, 151-156.
38. Plath, K., Fang, J., Mlynarczyk-Evans, S. K., Cao, R., Worringer, K. A., Wang, H., de la Cruz, C. C., Otte, A. P., Panning, B., & Zhang, Y. (2003) *Science* **300**, 131-135.
39. Hernandez-Munoz, I., Lund, A. H., van der Stoop, P., Boutsma, E., Muijters, I., Verhoeven, E., Nusinow, D. A., Panning, B., Marahrens, Y., & van Lohuizen, M. (2005) *Proc Natl Acad Sci U S A* **102**, 7635-7640.
40. Heard, E. (2004) *Current opinion in cell biology* **16**, 247-255.
41. Pasini, D., Bracken, A. P., Hansen, J. B., Capillo, M., & Helin, K. (2007) *Molecular and cellular biology* **27**, 3769-3779.
42. Gil, J., Bernard, D., & Peters, G. (2005) *DNA Cell Biol* **24**, 117-125.
43. Kamminga, L. M., Bystrykh, L. V., de Boer, A., Houwer, S., Douma, J., Weersing, E., Dontje, B., & de Haan, G. (2006) *Blood* **107**, 2170-2179.

44. Bracken, A. P., Dietrich, N., Pasini, D., Hansen, K. H., & Helin, K. (2006) *Genes Dev* **20**, 1123-1136.
45. Tolhuis, B., de Wit, E., Muijters, I., Teunissen, H., Talhout, W., van Steensel, B., & van Lohuizen, M. (2006) *Nature genetics* **38**, 694-699.
46. Boyer, L. A., Plath, K., Zeitlinger, J., Brambrink, T., Medeiros, L. A., Lee, T. I., Levine, S. S., Wernig, M., Tajonar, A., Ray, M. K., *et al.* (2006) *Nature* **441**, 349-353.
47. Negre, N., Hennetin, J., Sun, L. V., Lavrov, S., Bellis, M., White, K. P., & Cavalli, G. (2006) *PLoS Biol* **4**, e170.
48. Lee, T. I., Jenner, R. G., Boyer, L. A., Guenther, M. G., Levine, S. S., Kumar, R. M., Chevalier, B., Johnstone, S. E., Cole, M. F., Isono, K., *et al.* (2006) *Cell* **125**, 301-313.
49. Jacobs, J. J., Kieboom, K., Marino, S., DePinho, R. A., & van Lohuizen, M. (1999) *Nature* **397**, 164-168.
50. Jacobs, J. J., Scheijen, B., Voncken, J. W., Kieboom, K., Berns, A., & van Lohuizen, M. (1999) *Genes Dev* **13**, 2678-2690.
51. Cui, H., Hu, B., Li, T., Ma, J., Alam, G., Gunning, W. T., & Ding, H. F. (2007) *The American journal of pathology* **170**, 1370-1378.
52. Voncken, J. W., Roelen, B. A., Roefs, M., de Vries, S., Verhoeven, E., Marino, S., Deschamps, J., & van Lohuizen, M. (2003) *Proc Natl Acad Sci U S A* **100**, 2468-2473.
53. Leeb, M. & Wutz, A. (2007) *J Cell Biol* **178**, 219-229.
54. Ben-Saadon, R., Zaaroor, D., Ziv, T., & Ciechanover, A. (2006) *Molecular cell* **24**, 701-711.
55. Dhanasekaran, S. M., Barrette, T. R., Ghosh, D., Shah, R., Varambally, S., Kurachi, K., Pienta, K. J., Rubin, M. A., & Chinnaiyan, A. M. (2001) *Nature* **412**, 822-826.
56. Sellers, W. R. & Loda, M. (2002) *Cancer cell* **2**, 349-350.
57. Varambally, S., Dhanasekaran, S. M., Zhou, M., Barrette, T. R., Kumar-Sinha, C., Sanda, M. G., Ghosh, D., Pienta, K. J., Sewalt, R. G., Otte, A. P., *et al.* (2002) *Nature* **419**, 624-629.
58. Bachmann, I. M., Halvorsen, O. J., Collett, K., Stefansson, I. M., Straume, O., Haukaas, S. A., Salvesen, H. B., Otte, A. P., & Akslen, L. A. (2006) *J Clin Oncol* **24**, 268-273.
59. Laitinen, S., Martikainen, P. M., Tolonen, T., Isola, J., Tammela, T. L., & Visakorpi, T. (2008) *Int J Cancer* **122**, 595-602.
60. van Leenders, G. J., Dukers, D., Hessels, D., van den Kieboom, S. W., Hulsbergen, C. A., Witjes, J. A., Otte, A. P., Meijer, C. J., & Raaphorst, F. M. (2007) *Eur Urol* **52**, 455-463.
61. Saramaki, O. R., Tammela, T. L., Martikainen, P. M., Vessella, R. L., & Visakorpi, T. (2006) *Genes Chromosomes Cancer* **45**, 639-645.
62. Bachmann, N., Hoegel, J., Haeusler, J., Kuefer, R., Herkommer, K., Paiss, T., Vogel, W., & Maier, C. (2005) *Prostate* **65**, 252-259.
63. Bracken, A. P., Pasini, D., Capra, M., Prosperini, E., Colli, E., & Helin, K. (2003) *The EMBO journal* **22**, 5323-5335.

64. Berezovska, O. P., Glinskii, A. B., Yang, Z., Li, X. M., Hoffman, R. M., & Glinsky, G. V. (2006) *Cell Cycle* **5**, 1886-1901.
65. Yu, J., Yu, J., Rhodes, D. R., Tomlins, S. A., Cao, X., Chen, G., Mehra, R., Wang, X., Ghosh, D., Shah, R. B., *et al.* (2007) *Cancer Res* **67**, 10657-10663.
66. Yu, J., Cao, Q., Mehra, R., Laxman, B., Yu, J., Tomlins, S. A., Creighton, C. J., Dhanasekaran, S. M., Shen, R., Chen, G., *et al.* (2007) *Cancer cell* **12**, 419-431.
67. Tan, J., Yang, X., Zhuang, L., Jiang, X., Chen, W., Lee, P. L., Karuturi, R. K., Tan, P. B., Liu, E. T., & Yu, Q. (2007) *Genes Dev* **21**, 1050-1063.
68. Beke, L., Nuytten, M., Van Eynde, A., Beullens, M., & Bollen, M. (2007) *Oncogene* **26**, 4590-4595.
69. Chen, H., Tu, S. W., & Hsieh, J. T. (2005) *J Biol Chem* **280**, 22437-22444.
70. Nolz, J. C., Gomez, T. S., & Billadeau, D. D. (2005) *Trends Cell Biol* **15**, 514-517.
71. Su, I. H., Dobenecker, M. W., Dickinson, E., Oser, M., Basavaraj, A., Marqueron, R., Viale, A., Reinberg, D., Wulfig, C., & Tarakhovsky, A. (2005) *Cell* **121**, 425-436.
72. Bryant, R. J., Winder, S. J., Cross, S. S., Hamdy, F. C., & Cunliffe, V. T. (2008) *Prostate* **68**, 255-263.
73. Jemal, A., Murray, T., Samuels, A., Ghafoor, A., Ward, E., & Thun, M. J. (2003) *CA: a cancer journal for clinicians* **53**, 5-26.
74. Hayes, D. F. (2000) *Eur J Cancer* **36**, 302-306.
75. Kleer, C. G., Cao, Q., Varambally, S., Shen, R., Ota, I., Tomlins, S. A., Ghosh, D., Sewalt, R. G., Otte, A. P., Hayes, D. F., *et al.* (2003) *Proc Natl Acad Sci U S A* **100**, 11606-11611.
76. Rhodes, D. R., Sanda, M. G., Otte, A. P., Chinnaiyan, A. M., & Rubin, M. A. (2003) *J Natl Cancer Inst* **95**, 661-668.
77. Zeidler, M. & Kleer, C. G. (2006) *J Mol Histol* **37**, 219-223.
78. Zeidler, M., Varambally, S., Cao, Q., Chinnaiyan, A. M., Ferguson, D. O., Merajver, S. D., & Kleer, C. G. (2005) *Neoplasia* **7**, 1011-1019.
79. Shi, B., Liang, J., Yang, X., Wang, Y., Zhao, Y., Wu, H., Sun, L., Zhang, Y., Chen, Y., Li, R., *et al.* (2007) *Molecular and cellular biology* **27**, 5105-5119.
80. Tonini, T., Bagella, L., D'Andrilli, G., Claudio, P. P., & Giordano, A. (2004) *Oncogene* **23**, 4930-4937.
81. Hinz, S., Kempkensteffen, C., Christoph, F., Hoffmann, M., Krause, H., Schrader, M., Schostak, M., Miller, K., & Weikert, S. (2008) *J Cancer Res Clin Oncol* **134**, 331-336.
82. Hinz, S., Kempkensteffen, C., Weikert, S., Schostak, M., Schrader, M., Miller, K., & Christoph, F. (2007) *Tumour Biol* **28**, 151-157.
83. Raman, J. D., Mongan, N. P., Tickoo, S. K., Boorjian, S. A., Scherr, D. S., & Gudas, L. J. (2005) *Clin Cancer Res* **11**, 8570-8576.
84. Arisan, S., Buyuktuncer, E. D., Palavan-Unsal, N., Caskurlu, T., Cakir, O. O., & Ergenekon, E. (2005) *Urol Int* **75**, 252-257.
85. Weikert, S., Christoph, F., Kollermann, J., Muller, M., Schrader, M., Miller, K., & Krause, H. (2005) *Int J Mol Med* **16**, 349-353.
86. Matsukawa, Y., Semba, S., Kato, H., Ito, A., Yanagihara, K., & Yokozaki, H. (2006) *Cancer Sci* **97**, 484-491.

87. Breuer, R. H., Snijders, P. J., Smit, E. F., Sutedja, T. G., Sewalt, R. G., Otte, A. P., van Kemenade, F. J., Postmus, P. E., Meijer, C. J., & Raaphorst, F. M. (2004) *Neoplasia* **6**, 736-743.
88. Sudo, T., Utsunomiya, T., Mimori, K., Nagahara, H., Ogawa, K., Inoue, H., Wakiyama, S., Fujita, H., Shirouzu, K., & Mori, M. (2005) *Br J Cancer* **92**, 1754-1758.
89. Croonquist, P. A. & Van Ness, B. (2005) *Oncogene* **24**, 6269-6280.
90. Tang, X., Milyavsky, M., Shats, I., Erez, N., Goldfinger, N., & Rotter, V. (2004) *Oncogene* **23**, 5759-5769.
91. Nowak, K., Kerl, K., Fehr, D., Kramps, C., Gessner, C., Killmer, K., Samans, B., Berwanger, B., Christiansen, H., & Lutz, W. (2006) *Nucleic Acids Res* **34**, 1745-1754.
92. Cha, T. L., Zhou, B. P., Xia, W., Wu, Y., Yang, C. C., Chen, C. T., Ping, B., Otte, A. P., & Hung, M. C. (2005) *Science* **310**, 306-310.
93. Li, H., Ma, X., Wang, J., Koontz, J., Nucci, M., & Sklar, J. (2007) *Proc Natl Acad Sci U S A* **104**, 20001-20006.
94. Chen, Y., Lin, M. C., Yao, H., Wang, H., Zhang, A. Q., Yu, J., Hui, C. K., Lau, G. K., He, M. L., Sung, J., *et al.* (2007) *Hepatology* **46**, 200-208.
95. Komohara, Y., Harada, M., Arima, Y., Suekane, S., Noguchi, M., Yamada, A., Itoh, K., & Matsuoka, K. (2006) *International journal of oncology* **29**, 1555-1560.

CHAPTER 2

EZH2 IS A MARKER OF AGGRESSIVE BREAST CANCER AND PROMOTES NEOPLASTIC TRANSFORMATION OF BREAST EPITHELIAL CELLS

Breast cancer is a leading cause of cancer-related death in women, accounting for about 40,000 deaths per year in the United States (1). Despite advances in the early detection and treatment of breast cancer, mortality for those 20% of patients with recurrences and or metastases is about 100% (2). Currently, the most important prognostic markers for patients with breast cancer that are used in the clinical setting are components of the staging system, such as primary tumor size and the presence of lymph node metastasis (3). However, the accuracy of these conventional indicators is not as precise as desired, leading to inefficient application of systemic therapy (4). Thus, there is a need for novel molecular predictors of tumor behavior at the time of diagnosis that will help guide clinical therapy decisions.

Few biomarkers of breast cancer progression have been proven to be clinically useful (4). Estrogen receptor (ER) and progesterone receptor (PR) are highly predictive of breast cancer patients that will benefit from endocrine therapy (5) but are weak prognostic factors (6). Other tumor markers that have been considered for prognostication in breast cancer include erbB2 amplification/overexpression, cathepsin D, and uPAR (4). The consensus, however, remains that new prognostic factors that are more precise and reliable are needed (7).

Through our gene expression profiling studies, we identified EZH2 as being overexpressed in metastatic prostate cancer (8). In clinically localized prostate cancer, EZH2 was found to be predictive of poor outcome postprostatectomy (i.e., biochemical recurrence or metastasis). EZH2 is a Polycomb Group (PcG) protein homologous to *Drosophila* Enhancer of Zeste and involved in gene silencing (9, 10). PcG proteins are presumed to function in controlling the transcriptional memory of a cell (9). Dysregulation of this gene silencing machinery can lead to cancer (9, 11, 12). In the context of prostate cancer, we provided evidence that EZH2 functions as a transcriptional repressor, and inhibition of EZH2 blocks prostate cell growth (8). Interestingly, several recent studies demonstrated that EZH2 has enzymatic activity and functions as a histone H3 methyltransferase (13–15).

Biochemical analysis indicates that PcG proteins belong to at least two multimeric complexes, PRC1 (16) and EED-EZH2 (Enx1) (17). These complexes are thought to heritably silence genes by acting at the level of chromatin structure. The EED protein interacts directly with type 1 histone deacetylases (HDACs) in mammalian cells (18), and in *Drosophila* (19), and this has been suggested to be part of the silencing mechanism. Furthermore, recent studies have demonstrated that EED/EZH2 complexes methylate H3-K9 and K27 *in vitro*, with a strong preference for K27 (13–15). Methylation of both H3-K9 (20) and H3-K27 is thought to be involved in targeting the PRC1 complex to specific genetic target loci.

By interrogating publicly available gene expression data sets, we identified EZH2 as being dysregulated in breast cancer. In the present study, we examined EZH2

mRNA transcript and protein level in normal breast and in breast cancer progression. Immunohistochemical analyses performed on a spectrum of breast cancer specimens demonstrated that high EZH2 levels were strongly associated with poor clinical outcome in breast cancer patients. EZH2 was an independent predictor of breast cancer recurrence and death and provided prognostic information above and beyond known clinical, pathologic, and biomarkers studied. Overexpression of EZH2 in normal breast epithelial cell lines produced a neoplastic phenotype characterized by anchorage-independent growth and cell invasion. Neoplastic transformation mediated by EZH2 depended on both the SET domain as well as HDAC activity. Importantly, we propose a biologic basis for the association of EZH2 and tumor aggressiveness in that high levels of EZH2 promote the invasive potential of carcinomas.

EZH2 Transcript and Protein Expression Are Elevated in Breast Cancer.

On the basis of our previous work characterizing EZH2 in prostate cancer (8), we were interested in determining whether EZH2 is dysregulated in breast cancer, which, similar to prostate cancer, is steroid hormone regulated. This was facilitated by our group's ongoing efforts to create a cancer microarray metaanalysis database (see www.ONCOMINE.org) stemming from our initial work in prostate (27). Of the five publicly available breast cancer gene expression datasets (28–32), only the Perou *et al.* (28) study had neoplastic and normal breast tissues to make comparisons between benign and cancer. Interestingly, in this dataset, we found that the EZH2 transcript was overexpressed significantly in invasive breast cancer and metastatic breast cancer relative to normal ($P = 0.002$, *t* test) (28).

To validate these DNA microarray results, we carried out SYBR green quantitative real-time PCR on 19 laser-capture microdissected normal and invasive breast cancers. As predicted, levels of EZH2 mRNA were increased an average of 7.5-fold in invasive carcinomas compared with normal breast epithelial cells (t test, $P = 0.0085$) (**Fig. 2.1A**). To confirm that EZH2 is elevated at the protein level in invasive breast cancer, we analyzed normal breast and breast cancer tissue extracts by immunoblot analysis. Consistent with the transcript data, invasive breast cancer expressed high levels of EZH2 protein relative to normal (**Fig. 2.1B**). Importantly, EED, a PcG protein that forms a complex with EZH2, did not exhibit similar protein dysregulation.

Using high-density tissue microarrays, we next evaluated the expression of EZH2 protein in a wide range of breast tissues (280 patients, $n = 917$ samples) to characterize its expression *in situ* by immunohistochemistry. EZH2 protein expression was observed primarily in the nucleus (**Fig. 2.1C**), as reported previously (33). Invasive breast cancer that expressed high levels of EZH2 (scores 3–4, EZH2+) and those that expressed low levels of EZH2 (scores 1–2, EZH2–) were readily apparent (**Fig. 2.1C Center and Right**). There was a remarkable staining difference between tumor cells that form intravascular emboli and adjacent normal breast epithelia (**Fig. 2.1C Left**). Consistent with our mRNA transcript data, EZH2 protein levels were elevated in invasive carcinoma relative to normal or atypical hyperplasia (Wilcoxon test, $P < 0.0001$, **Fig. 2.1D**). As in the case of metastatic prostate cancer (8), breast cancer metastases expressed high levels of EZH2 (**Fig. 2.1D**). Median EZH2 staining intensities of normal, atypical hyperplasia, ductal carcinoma *in situ* (DCIS), invasive carcinoma, and metastases were 1.47 (SE 0.61), 2 (SE 0), 2.38 (SE 0.52), 2.74 (SE 0.99), and 3.09 (SE 1.04), respectively

(**Fig. 2.1D**). Interestingly, increased EZH2 protein and transcript were already present in DCIS, a precursor of invasive carcinoma (**Fig. 2.1D**).

Prognostic Value of EZH2 in Breast Cancer. To investigate whether EZH2 mRNA expression levels are associated with outcome, we analyzed the published van't Veer *et al.* (30) breast cancer gene expression dataset, which contains outcome information on 78 sporadic invasive carcinomas <5 cm with negative lymph nodes. We found that the levels of EZH2 transcript expression were significantly higher in invasive carcinomas that metastasized within 5 years of primary diagnosis when compared with invasive carcinomas that did not metastasize (Wilcoxon rank test $P = 0.01$, **Fig. 2.2A**). By Kaplan–Meier analysis, high EZH2 expression [>1.26 (\log_{10} ratio >0.1)] was associated significantly with the development of metastasis within 5 years of primary diagnosis (log rank $P < 0.0001$). Multivariable Cox hazards regression analysis showed that EZH2 mRNA expression was an independent predictor of the development of metastases with a hazard ratio of 2.02 (95% confidence interval 1.08–3.76, $P = 0.03$).

By using our breast cancer tissue microarray data, we were in the position to evaluate clinical and pathology associations of EZH2 protein levels in breast cancer. In our cohort of 236 consecutive breast cancer patients ($n = 712$ samples), 194 had complete follow-up information. Clinicopathologic characteristics of the patients can be found in **Table 2.1**. The median age of the study population was 56 years (ranging from 26 to 89 years). After a median follow-up of 3.2 years (range 17 days to 15.8 years), 42 of the 194 patients (21.6%) died of breast cancer. The 5- and 10-year disease-specific survival rates for the entire cohort of patients were 60.28% and 38.66%, respectively. The association

between EZH2 protein levels and clinical characteristics is shown in Table 2.3, which is published as supporting information on the PNAS web site. EZH2 expression was strongly associated with standard pathology predictors of clinical outcome, including tumor diameter ($P = 0.002$) and stage of disease ($P < 0.0001$). Higher EZH2 levels were also significantly associated with decreasing age ($P = 0.0003$), negative ER status ($P = 0.0001$), negative PR status ($P < 0.0001$), and lymph node status ($P = 0.001$), but not HER2/neu overexpression. Hazard ratios of recurrence or metastasis according to EZH2 status were 2.92 ($P < 0.0001$).

The results of the univariate analysis are shown in **Table 2.4**, which is published as supporting information on the PNAS web site. As expected, at the univariate level, lymph node status, tumor diameter, and stage of disease were associated with disease-specific and overall survival. Hormone receptor status was inversely associated with outcome. We found a strong association between EZH2 protein levels and patient outcome. Higher EZH2 protein levels were associated with a shorter disease-free interval after initial surgical treatment, lower overall survival, and a high probability of disease-specific death (or death due to breast cancer) (**Fig. 2.2 B and C**). The 10-year disease-free survival for patients with tumors expressing high EZH2 levels was 24.76% and, by contrast, 58.92% for low levels of EZH2 (log rank $P < 0.0001$, **Fig. 2.2B**). High EZH2 expression was associated with disease-specific survival in patients with lymph node-negative disease (log rank $P = 0.007$). EZH2 expression was associated with disease-specific survival in patients with stage I and II disease (log rank, $P = 0.037$ and $P = 0.048$, respectively), but not in patients with advanced stage (stages III and IV). EZH2 was not associated with survival in patients with positive lymph nodes. The strong inverse

association between high EZH2 protein expression and negative ER status (Kruskal–Wallis test, $P = 0.001$, **Table 2.3**) prompted us to investigate whether the prognostic utility of EZH2 depends on ER status. Kaplan–Meier analysis showed that EZH2 levels were strongly associated with outcome in both ER-positive and -negative invasive carcinomas. Thus, our data suggest that EZH2 has prognostic utility independently of ER status.

The best multivariable model predictive of disease-specific survival included positive lymph nodes, high EZH2 expression, and negative PR status (**Table 2.2**). High EZH2 expression was a strong independent predictor of outcome providing survival information above other independent prognostic features, with a hazard ratio of 2.04 and a 95% confidence interval of 1.17–3.57, $P = 0.01$. Tumor size, angiolymphatic invasion, and ER status, identified as having strong associations with EZH2 at the univariate level, were not independently associated with outcome at the multivariable level.

EZH2 Overexpression Promotes Anchorage-Independent Growth and HDAC Activity in Normal Breast Epithelial Cells. To study the function of dysregulated EZH2 expression in breast epithelial cells, we generated adenovirus constructs expressing EZH2. We also generated an adenovirus expressing a mutant version of EZH2 in which the C-terminal SET domain is truncated (EZH2 Δ SET). Normal immortalized breast epithelial cells (H16N2) (34) were infected with EZH2 and EZH2 Δ SET expressing viruses and protein expression demonstrated in **Fig. 2.3A**. Overexpression of EZH2 in breast epithelial cells did not significantly enhance cell proliferation in tissue culture (**Fig. 2.3B**). Interestingly, EZH2 overexpression markedly

promoted colony formation in soft agar relative to EZH2 Δ SET and vector controls (**Fig. 2.3 C and D**). In fact, colonies were present only in EZH2-infected H16N2 cells, supporting the notion that EZH2 can facilitate anchorage-independent growth. As in our previous study with prostate cells (8), overexpression of EZH2 in breast carcinoma cells induced transcriptional repression of a cohort of target genes (data not shown). Previous studies have demonstrated that the EED–EZH2 complex recruits type I HDACs (18). To determine whether overexpression of EZH2 modulates HDACs, we measured HDAC enzymatic activity in breast epithelial cell lysates. Overexpression of EZH2 but not the EZH2 Δ SET mutant increased total HDAC activity in breast epithelial cells. This activity was completely abrogated in the presence the HDAC inhibitor TSA.

Dysregulated EZH2 Orchestrates the Invasive Potential of Breast Epithelial Cells. We next assessed the biological function of EZH2 in the context of cancer cell invasion. We observed that overexpression of EZH2 in breast epithelial cells promotes invasion in a reconstituted basement membrane invasion chamber assay (**Fig. 2.4 A and B**). The control experiments that included EZH2 Δ SET mutant and vector did not exhibit similar proinvasive properties. Importantly, EZH2-mediated invasion was attenuated with inclusion of the HDAC inhibitors TSA and SAHA. Cell invasion was quantitated by both cell counting and colorimetry (**Fig. 2.4B**). Next, we used SU-ECM (25, 35) as invasion substrates to examine the invasive properties of EZH2 expressing breast epithelial cells. The SU-ECM assay has advantages over the reconstituted basement membrane assay in that it is a uniform, biological, serum-free basement membrane that closely mimics the type of extracellular matrix that cells encounter *in vivo*. As with the reconstituted basement membrane assay, EZH2 overexpression in the SU-ECM assay supported similar

findings regarding the invasive potential of EZH2 and its requirement for HDAC activity (**Fig. 2.4C**).

To examine the role of EZH2-mediated invasion in an *in vivo* setting, we used a CAM assay. In this model, EZH2 overexpressing breast epithelial cells are labeled with fluorescent beads, seeded in duplicate on CAMs, of 10-day-old chicken embryos and incubated. At time of harvest, frozen sections were made from the CAM tissues and examined by fluorescent and light microscopy after hematoxylin/eosin staining. EZH2 overexpressing breast epithelial cells consistently promoted invasion of the CAM (a representative experiment is shown in **Fig. 2.4D**).

In the present study, we characterized the expression pattern of EZH2 transcript and protein in a wide spectrum of breast disease and assessed the utility of EZH2 as a prognostic marker in patients with breast cancer. EZH2 is significantly increased in invasive carcinoma and breast cancer metastases at both the transcript and protein levels when compared with normal breast tissues. Cells forming intravascular tumor emboli had strikingly increased EZH2 expression (**Fig. 2.1C Left**), suggesting that EZH2 may play a role in vascular invasion and breast cancer metastasis. *In vitro* and *in vivo* experiments in which EZH2 was ectopically overexpressed in normal mammary epithelial cell lines provide biological evidence that EZH2 can mediate anchorage-independent growth and cell membrane invasion, hallmarks of cancer (36). This is especially intriguing in that EZH2, which targets transcriptional repression of target genes, presumably mediates an invasive cancer phenotype.

To test the clinical utility of EZH2 protein expression as a prognostic biomarker of breast cancer progression, we evaluated the associations between EZH2 and survival after treatment. At the univariate level, EZH2, tumor stage, tumor size, the presence of axillary lymph node metastases, and hormone receptor status were all significantly associated with survival. In a multivariable Cox regression analysis, high EZH2 expression and lymph node metastasis were independent predictors of outcome. The single best multivariable model included high EZH2 levels, positive lymph nodes, and negative PR status. *In silico* analysis of the cDNA expression profiling of breast cancer performed by van't Veer *et al.* (30) showed that high EZH2 levels were associated with the development of metastasis within 5 years of primary diagnosis in patients with sporadic invasive carcinomas. These findings support the potential clinical utility of incorporating EZH2 into clinical nomograms to help determine the risk of cancer progression.

A major limitation of our analysis is its retrospective nature, which precludes an accurate analysis of survival in the context of hormonal or adjuvant treatment. In our patient cohort, 88% ER-positive tumors received hormonal treatment. Thus, we critically evaluated the prognostic significance of EZH2, taking into account tumor ER status. EZH2 was strongly associated with clinical outcome in hormone-dependent and -independent breast cancer patients, indicating that the prognostic power of EZH2 is independent of ER status. Future studies will test the model developed in this study on a validation cohort to confirm these initial observations.

The prognostic significance of EZH2 as biomarker for aggressive breast cancer is likely linked to its biological functions. EZH2 is a member of a group of polycomb proteins that are involved in maintaining heritable gene expression profiles and thus regulate cell type identity. Thus, dysregulation of the transcriptional machinery of a cell may result in loss of cell type identity and neoplastic transformation. Here we provide biological evidence that dysregulated EZH2 promotes oncogenic transformation. Overexpression of EZH2 in breast epithelial cells induced anchorage-independent growth and cell invasion. Invasive properties of EZH2 overexpressing cells were demonstrated in both *in vitro* assays (i.e., basement membrane invasion chamber and SU-ECM assays) as well as in an *in vivo* assay (i.e., CAM). EZH2 overexpression induced HDAC enzymatic activity in breast epithelial cells. Interestingly, EZH2-mediated cell invasion are abrogated by the HDAC inhibitors TSA and SAHA, implying that EZH2-mediated invasion requires HDAC activity. Previous reports have shown that type I HDACs are recruited to the EZH2-EED PcG complex (18). Our group and other groups have found that EZH2-mediated gene silencing requires an intact SET domain and recruitment of HDAC activity (8), and that inhibition of HDAC activity blocked the transcriptional repressor functions of EZH2. Several HDAC inhibitors, including SAHA, have been shown to have promise clinically as antitumorigenic agents (37). Thus, we suggest that inhibitors of HDAC may be useful therapeutic compounds in EZH2 overexpressing tumors. In addition, the HDAC activity induced by EZH2 may explain the intriguing strong association between EZH2 protein expression and negative ER, and one might speculate that EZH2 may transcriptionally repress ER. Further investigation in this area may be warranted.

Several recent studies provide strong evidence that EZH2 has inherent activity as a histone H3 methyltransferase, which may represent the mechanism of PcG silencing (10, 13–15). Cao *et al.* (13) present evidence that the specific target of EZH2 is lysine 27 on the histone H3 N-terminal tail (13). If EZH2 plays a role in breast cancer progression, its inherent methyltransferase activity may serve as an attractive therapeutic target. Together, these studies suggest that the transcriptional memory machinery of a cell may have a role in cancer progression.

In summary, we discovered that EZH2 is a promising biomarker of aggressive breast cancer, not only extending our initial observations in prostate cancer but also suggesting that EZH2 (and thus the cell memory machinery) may have a role in carcinoma progression in malignancies from hormonally regulated tissues. Clinically, our retrospective studies suggest that EZH2 levels can be used to identify patients with breast cancer of a more aggressive phenotype, thereby enhancing our prognostic knowledge. Although our results are promising, EZH2 expression needs to be validated in relationship to outcome in the context of carefully controlled clinical trials. If confirmed, application of EZH2 immunohistochemical analysis should be technically straightforward and feasible. In addition to the potential prognostic utility of EZH2, we also provide a biologic mechanism for its association with aggressive cancers, by mediating anchorage-independent growth and cell invasion.

Materials and Methods

Selection of Patients and Tissue Microarray Development. Breast tissues for tissue microarray construction were obtained from the Surgical Pathology files at the University of Michigan with Institutional Review Board approval. A total of 280 cases ($n = 917$ tissue microarray samples) were reviewed by the study pathologist and arrayed in three high-density tissue microarrays, as described (21, 22). At least three tissue cores (0.6-mm diameter) were sampled from each block to account for tissue and tumor heterogeneity. The TMAs contained the whole spectrum of breast pathology, with samples of normal breast, atypical hyperplasia, ductal carcinoma *in situ*, invasive carcinoma, and breast cancer metastases. The invasive carcinomas were obtained from 194 consecutive patients ($n = 621$ tissue microarray elements) with follow-up information at the University of Michigan between 1987 and 1991. Clinical and treatment information was extracted by chart review, performed by the surgeon on the study (M.S.S.), with IRB approval. Of the 385 cases of invasive carcinoma of the breast treated at our institution from 1987 to 1991, 236 were available for study. The reasons for exclusion of cases were: (i) unavailability of tissue slides or blocks, and (ii) primary resection performed at a referring institution. In our cohort of 236 consecutive breast cancer patients ($n = 712$ specimens), 194 had complete follow-up information. The median duration of follow-up was 3.2 years (range 17 days to 15.8 years). Clinical and pathological variables were determined following well-established criteria. The histological grade was assessed according to the method described by Elston and Ellis (3); angiolymphatic invasion was classified as either present or absent.

Immunohistochemical Studies. Immunohistochemistry was performed on the tissue microarrays (TMAs) by using standard biotin–avidin complex technique and a polyclonal antibody against EZH2 that was previously validated by immunoblot analysis (8). EZH2 expression was evaluated at least three times for every tissue microarray element and at least nine times for each tumor by using a previously validated Web-based tool (TMA Profiler, University of Michigan, Ann Arbor, MI). Using this method, the pathologist is blinded to tumor stage and clinical information. The highest value of all measurements from a single individual was used for subsequent analysis. Nuclear EZH2 expression was scored by using a validated system as negative (score = 1, no staining); weak (score = 2, < 25% of nuclei staining, any intensity); moderate (score = 3, 25--75% of nuclei staining, any intensity); and strong (score = 4, >75% of nuclei staining, any intensity). High EZH2 was defined as scores 3 and 4; low EZH2 was defined as scores 1 and 2. The TMAs were immunostained for ER and PR and for HER-2/neu by using well described and validated procedures (23). For estrogen receptor (ER) staining, we used ER antibody clone 6F11 (Ventana Medical Systems, Tucson, AZ), prediluted with antigen retrieval by using a microwave in 10 mM citrate buffer. For progesterone receptor (PR), we used antibody clone 636 (DAKO) at 1:400 dilution, subjected to 95°C water bath for 40 min; and for HER2/neu immunostaining, we used CB11 antibody (NovoCastra, Burlingame, CA) at 1:40 dilution, with microwave antigen retrieval with 10 mM citrate buffer. Hormone receptor status was reported as positive or negative when >10% of the neoplastic cells exhibited nuclear staining. HER-2/neu status was reported as 0-3+. As previously reported, we found almost perfect correlation between the hormonal status, as determined in the TMAs and in standard whole-tissue sections.

Statistical Analysis. Comparison of the intensity of EZH2 staining between normal breast, hyperplasia, ductal carcinoma *in situ*, invasive carcinoma, and metastases was carried out by calculating the median staining intensity for each case and applying the Wilcoxon rank test. A *P* value of <0.05 was considered significant. Overall survival was calculated from the date of surgical excision of the primary tumor to the date of death. Patients who died of or with the disease were included in the analysis. For disease-specific survival, data for patients who died from other causes were censored at the time of death. Overall survival and disease-specific survival curves were constructed by the Kaplan–Meier method. Clinical criteria for treatment failure were local recurrence and/or the development of metastases.

Univariate analyses of disease-specific survival were performed by using a two-sided log-rank test to evaluate EZH2 protein expression, age, tumor size, nodal status, stage, angiolymphatic invasion, ER status, PR status, and HER-2/neu status. To assess the influence of several variables simultaneously, a multivariable Cox proportional hazards model of statistically significant covariates was developed by removing nonsignificant parameters in a step-wise manner. Statistical significance in the Cox models was determined by Wald's test.

SYBR Green Quantitative Real-Time PCR. We performed SYBR green real-time quantitative PCR analysis on 19 laser-microdissected frozen breast tissues obtained from the frozen breast tissue bank in our institution with IRB approval. Briefly, 4- μ m-thick frozen sections of six normal breast tissues, obtained from patients that underwent reduction mammoplasties and 13 patients with invasive carcinomas, were cut and stained

with hematoxylin/eosin (H&E) and subsequently subjected to laser capture microdissection (μ Cut, SL-Microtest, Glattsbrugg, Switzerland). Total RNA was isolated from each sample by using the Absolutely RNA Microprep Kit (Stratagene), according to the manufacturer's instructions. Each sample was then vacuum concentrated and reverse transcribed into first-strand cDNA by using Superscript II Reverse Transcriptase (Invitrogen) in the presence of GeneFilter Primer PolydT and random hexamer primers (Invitrogen) and resuspended in 20 μ l of DNase/RNase free water (GIBCO/BRL). For each QRT-PCR amplification, 4 μ l of the cDNA product, 12.5 μ l of 2' SYBR green PCR Master Mix (Applied Biosystems), 1 μ l containing 25 ng of both the forward and reverse EZH2 primers [or 50 ng of both the forward and reverse hydroxymethylbilane synthase (HMBS) primers], and 7.5 μ l of DNase/RNase free water was added for a final volume of 25 μ l. Thermocycling conditions were as suggested by the manufacturer: 95° for 10 min to activate the polymerase followed by 40 cycles of 95° for 15 sec and 60° for 1 min. To confirm the absence of nonspecific amplification and primer dimer binding, a no-template control well was included, and amplified products were separated on a 1.5% agarose gel to confirm the expected product size. Threshold levels were set by using SDS Ver. 1.7 software (Applied Biosystems), and the quantity of DNA in each sample was calculated by interpolating its C_t value from a standard curve of C_t values obtained from serially diluted breast cancer cDNA with Microsoft EXCEL. All standard curves had R^2 values ≥ 0.99 over three orders of magnitude. The calculated quantity of EZH2 from each sample was then divided by the average calculated quantity of the housekeeping gene HMBS corresponding to each sample to give a relative expression of EZH2 for each sample. QRT-PCR was performed in duplicate for EZH2

and HMBS expression in each sample, and mean EZH2/HMBS is reported. The EZH2 oligonucleotide primers were designed by using Primer Select (DNASTAR, Madison, WI) to minimize primer--dimer formation and amplify cDNA products spanning an intron--exon junction to eliminate amplification of genomic DNA. The oligonucleotide sequences are as follows: EZH2-F (5' -3') GCG CGG GAC GAA GAA TAA TCA T, EZH2-R (5' -3') TAC ACG CTT CCG CCA ACA AAC T.

Immunoblot Analysis. Protein extracts were prepared from normal and cancerous breast tissues by using NP-40 lysis buffer containing 50 mM Tris, pH 7.4; 1% Nonidet P-40; and a cocktail of protease inhibitors. Fifteen micrograms of proteins was boiled in sample buffer, separated by SDS/PAGE, and transferred onto nitrocellulose membrane. The membrane was incubated for 1 hr in blocking buffer [Tris-buffered saline with 0.1% Tween (TBS-T) and 5% nonfat dry milk] and incubated overnight at 4°C with anti-EZH2 rabbit polyclonal antibody at a dilution of 1:1,000 in blocking buffer. After washing in TBS-T, the blot was incubated with horseradish peroxidase-conjugated secondary antibody, and the signals were visualized by the enhanced chemiluminescence system as described by the manufacturer (Amersham Pharmacia). The blot was reprobed with β -tubulin to confirm equal loading of the different tissue samples

Adenovirus Constructs. Adenoviral constructs were generated by *in vitro* recombination. In brief, the full-length EZH2 or SET domain deleted EZH2 (EZH2 Δ SET) were inserted in an adenoviral shuttle plasmid [pACCMVpLpA(-)loxP-SSP]. Viruses were generated by transfection into the 293-complementation cell line. Virus was propagated in 911 cells and purified on a CsCl gradient. Multiplicities of infection were

calculated, and purified viruses were stored in 10 mM Tris·HCl (pH 7.4)/137 mM NaCl/5 mM KCl/1 mM MgCl₂ in 10% glycerol (by volume).

Cell Count. H16N2 were infected with EZH2 adenovirus. Cell counts were estimated by trypsinizing cells and analysis by Coulter counter at the indicated time points in triplicate.

Soft Agar Assay. A 0.6% (wt/vol) bottom layer of low melting point agarose in normal medium was prepared in six-well culture plates. On top, a layer of 0.6% agarose containing 1×10^5 stable transfected cells was placed (24). After 25 days, foci were stained with P-Iodonitrotetrazolium violet and counted.

HDAC Assay. HDAC activity assays were performed according to the manufacturer instructions (Biomol, Plymouth Meeting, PA). Briefly, cell lysates were prepared by using lysis buffer (Biomol) from the H16N2 cells that were infected with EZH2, EZH2 SET, and vector virus, and substrate was added and incubated for 30 min at room temperature. For HDAC inhibitor treatment, TSA were added to the lysate and incubated at room temperature for 30 min. The reaction was stopped, and fluorescence was measured at excitation range of 340-380 nm and emission range of 440-460 nm (Packard Fluorocount).

Basement Membrane Matrix Invasion Assay. Cells were infected with vector, EZH2, and EZH2 Δ SET adenovirus. Forty-eight hours after infection, the cells were trypsinized and seeded at equal numbers onto the basement membrane matrix 24-well culture plates [extracellular membrane (ECM); Chemicon] in the presence or absence of

HDAC inhibitors suberoylanilide hydroxamic acid (SAHA) (7.5 μ M) and trichostatin A (TSA) (0.5 μ M). FBS was added to the lower chamber to act as a chemoattractant. After 48-h incubation, the noninvading cells and ECM were removed gently by cotton swab. The cells that are invaded that are present on the lower side of the chamber were stained, air dried, and photographed. The invaded cells were counted under the microscope. For colorimetric assay, the inserts were treated with 150 μ l of 10% acetic acid, and absorbance was measured at 560 nm.

Sea Urchin (SU) Embryo Basement Membrane Invasion Assay. H16N2 cells were infected with vector, EZH2, and EZH2 SET adenovirus and trypsinized after 48 hr. The infected cells alone or treated with HDAC inhibitors SAHA (7.5 μ M) and TSA (0.5 μ M) and analyzed for invasiveness by using the SU embryo basement membrane invasion assay (25). The trypsinized cells were then resuspended to a concentration of 20,000 cells/ml in the appropriate media. The cells were layered on top of the embryo basement membrane invasion substrates and incubated for 4 hr at 37°C. Relative invasion was scored by phase-contrast microscopic examination. For each sample, 50-100 SU extracellular matrix (ECM) were examined, and the ratio of cells located inside vs. adhering to the outside of the SU-ECMs was calculated.

Chick Chorioallantoic Membrane (CAM) Invasion Assay. EZH2 and control virus-infected H16N2 cells were labeled with Fluoresbrite carboxylated polystyrene nanospheres (26) of 48 nm diameter (Polysciences) as described forty-eight hours after infection. The cells were detached from the culture dish with 2 mM EDTA in PBS, counted, and resuspended in 50 μ l of PBS with Ca^{2+} and Mg^{2+} . To apply cells onto the

CAM of 10-day chick embryos, in which an artificial air sac was created, a 1-cm-diameter-wide window was opened aseptically in the flat pole of the eggshell with an electric drill (Dremel moto-tool, Emerson, Racine, WI). The resuspended labeled cells (10^6 cells/CAM) were then applied onto the small patch of the CAM. The embryo was returned to the incubator in an upright position after inoculation and remained there for additional 48 hr. At time of harvest, frozen sections were made from the CAM tissues after immersion in 10% formaldehyde. The frozen sections were mounted with Vectashield mounting media with 4',6-diamidino-2-phenylindole (Vector Laboratories), monitored under a fluorescent microscope (Leica DMLB, Leica, Wetzlar, Germany) and photographed with the SPOT cooled color digital camera (Diagnostic Instruments, Sterling Heights, MI). The serial sections were also prepared and stained with H&E as histological sections.

Table 2.1 Demographics of patients with clinical follow-up used in this study

<i>Parameter</i>	<i>value</i>
No. of patients	194
Median age, years (range)	56 (26-89)
Follow-up/years, median (range)	3.2 years (17 d-16 years)
Pathologic stage, no. (%)	
I	78 (40)
II	66 (34)
III	32 (16)
IV	18 (10)
Tumor size, cm (range)	2 (0.3-6.7)
Lymph node status, no. (%)	67 (36)
Negative	78 (44)
Positive	
ER status, no. (%)	
Negative	67 (36)

Positive	120 (64)
PR status, no. (%)	
Negative	86 (45)
Positive	107 (55)
HER-2/neu status, no. (%)	
Negative	163 (85)
Positive	28 (15)

Table 2.2 Independent factors predictive of death from breast cancer

Parameter	<i>p</i> value	Hazard ratio	95% confidence interval for hazard ratio	
EZH2 positive	0.01	2.04	1.17	3.57
Positive lymph nodes (≥ 4, 1-3, 0)	<0.0001	1.9	1.4	2.57
PR positive (vs. negative)	0.02	0.54	0.32	0.91

Multivariate Cox Model with backward selection, $n = 161$, $P < 0.0001$ disease-free survival.

Table 2.3 Association between EZH2 and clinical characteristics

Variable	N	Wilcoxon P value
Age (≤ 50, >50)	194	0.0003
Positive lymph node (0, 1-3, ≥ 4)	177	0.001
Size (≤ 2, >2)	182	0.002
TNM Stage (1, 2, 3, 4)	176	<0.0001
ER status (positive, negative)	187	0.0001
PR status (positive, negative)	193	<0.0001
HER2NEU (positive, negative)	191	0.8

Table 2.4 Univariate Cox model

Variable	<i>N</i>	<i>P</i> value	Hazard ratio	95% confidence interval for hazard ratio	
EZH2	194	<0.0001	2.65	1.64	4.29
Lymph node status	177	<0.0001	1.97	1.51	2.59
Age	194	0.05	0.64	0.42	0.99
Tumor size	182	0.004	1.94	1.23	3.06
Stage	176	<0.0001	2.37	1.72	3.25
ER	187	0.002	0.50	0.32	0.78
PR	193	0.0006	0.47	0.30	0.72
HER2NEU	191	0.81	0.93	0.49	1.75

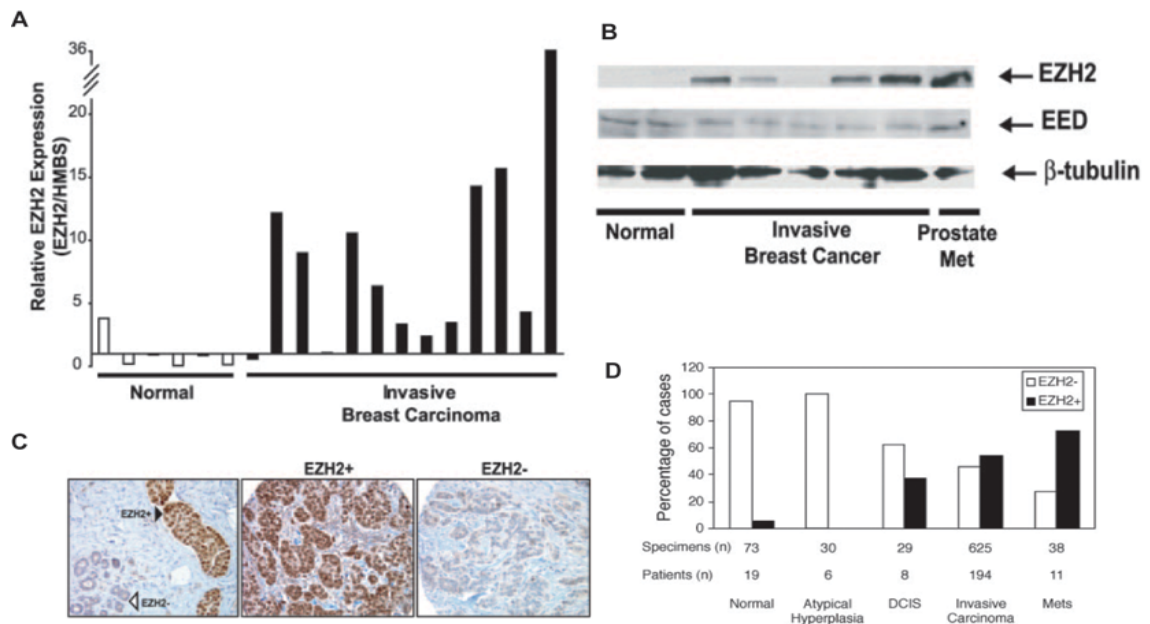


Fig. 2.1 EZH2 mRNA transcript and protein levels are elevated in breast cancer. (A) Quantitative SYBR green RT-PCR of EZH2 transcript in laser-capture microdissected normal and breast cancer epithelia. Each sample was performed in duplicate, and a ratio was calculated relative to the housekeeping gene hydroxymethylbilane synthase (HMBS). (B) Immunoblot analysis of EZH2 and EED in breast tissue extracts. Metastatic (Met) prostate cancer was used as a positive control. β-Tubulin was included as a loading control. (C) Representative breast tissue sections stained with an antibody to EZH2. (Left) Normal breast epithelia (open triangle) and adjacent intravascular breast cancer emboli (filled triangle). (Center) An invasive breast cancer expressing high levels of EZH2. (Right) An invasive breast cancer expressing low levels of EZH2. (D) Tissue microarray analysis of EZH2 expression in breast cancer progression. Tumor specimens were stratified into high EZH2 expressors (filled bars, scored 3 or 4) and low EZH2 expressors (open bars, scored 1 or 2). The y axis represents the percentage of patients in each category.

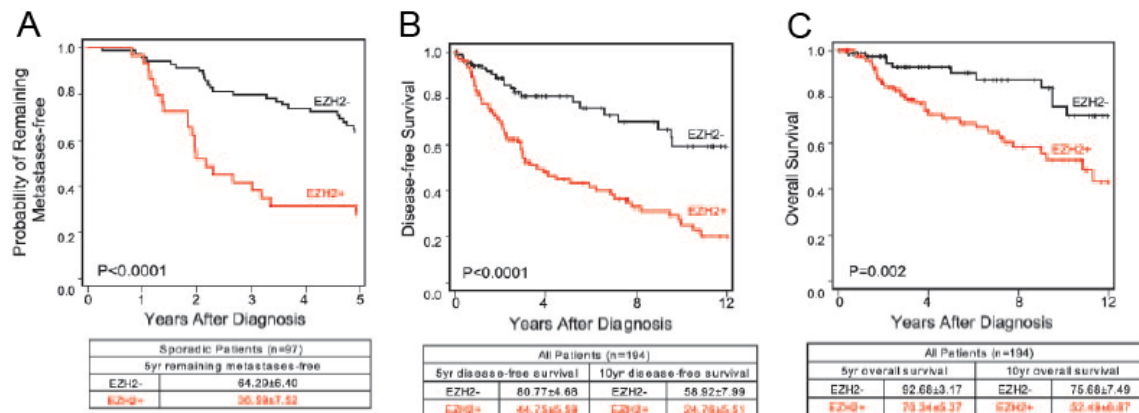


Fig. 2.2 High EZH2 levels are associated with aggressive breast cancer. (A) Kaplan–Meier analysis of metastasis-free survival according to EZH2 mRNA transcript levels as measured using DNA microarrays by van't Veer *et al.* (30). Kaplan–Meier analysis of disease-specific (B) and overall (C) survival according to EZH2 protein levels as assessed by immunohistochemical analysis. Patients grouped on the basis of high (+) or low (–) EZH2 expression levels. *P* values were calculated by using the log-rank test.

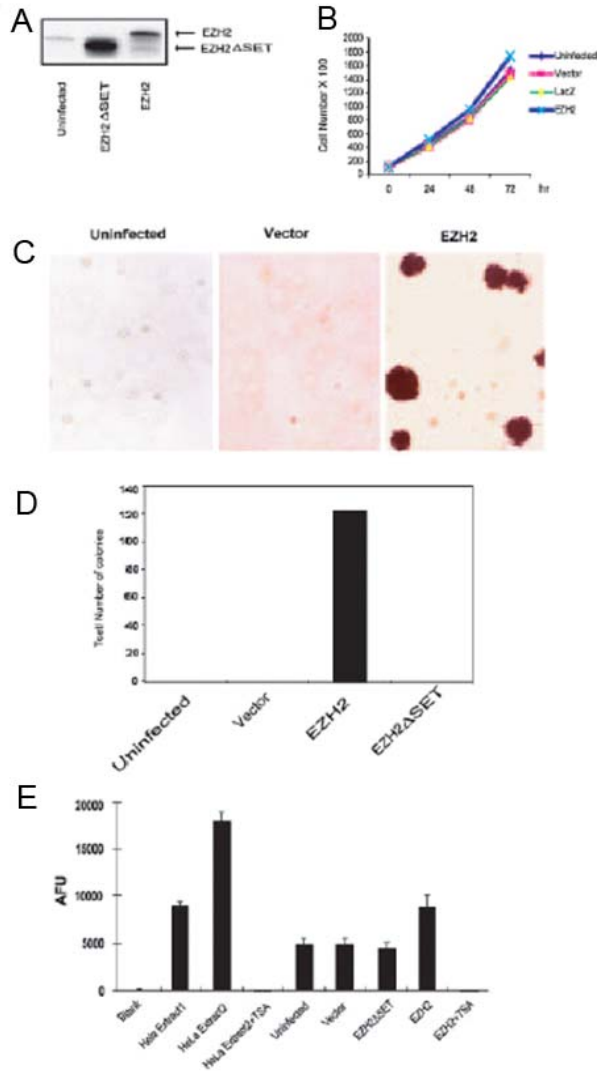


Fig. 2.3. Anchorage-independent growth mediated by EZH2. (A) Immunoblot analysis of breast cell line H16N2 infected with adenovirus encoding EZH2 or EZH2ΔSET mutant. (B) Ectopic overexpression of EZH2 does not significantly enhance growth of breast epithelial cells in culture. H16N2 cells were infected with EZH2 adenovirus and controls, and cells were counted at indicated time points. LacZ adenovirus and vector adenovirus were used as controls. (C) EZH2 expression enhances anchorage-independent growth *in vitro*. H16N2 cells were infected with EZH2, EZH2ΔSET, or vector adenoviruses. Anchorage-independent growth was determined by assaying colony formation in soft agar. After 25 days, the plates were stained and photographed. (D) Quantitation of soft agar colonies from experiments described in C. Colonies from three wells were quantitated for each condition. (E) EZH2 induces HDAC activity in breast epithelial cells. HDAC activity was measured in extracts from H16N2 cells infected with indicated viruses ± treatment with TSA (1.0 μM). As indicated by the manufacturer (Biomol), nuclear extracts from HeLa cells were used as positive controls. Extract 2 had 2-fold more HDAC activity than Extract 1. AFU, arbitrary fluorescence units.

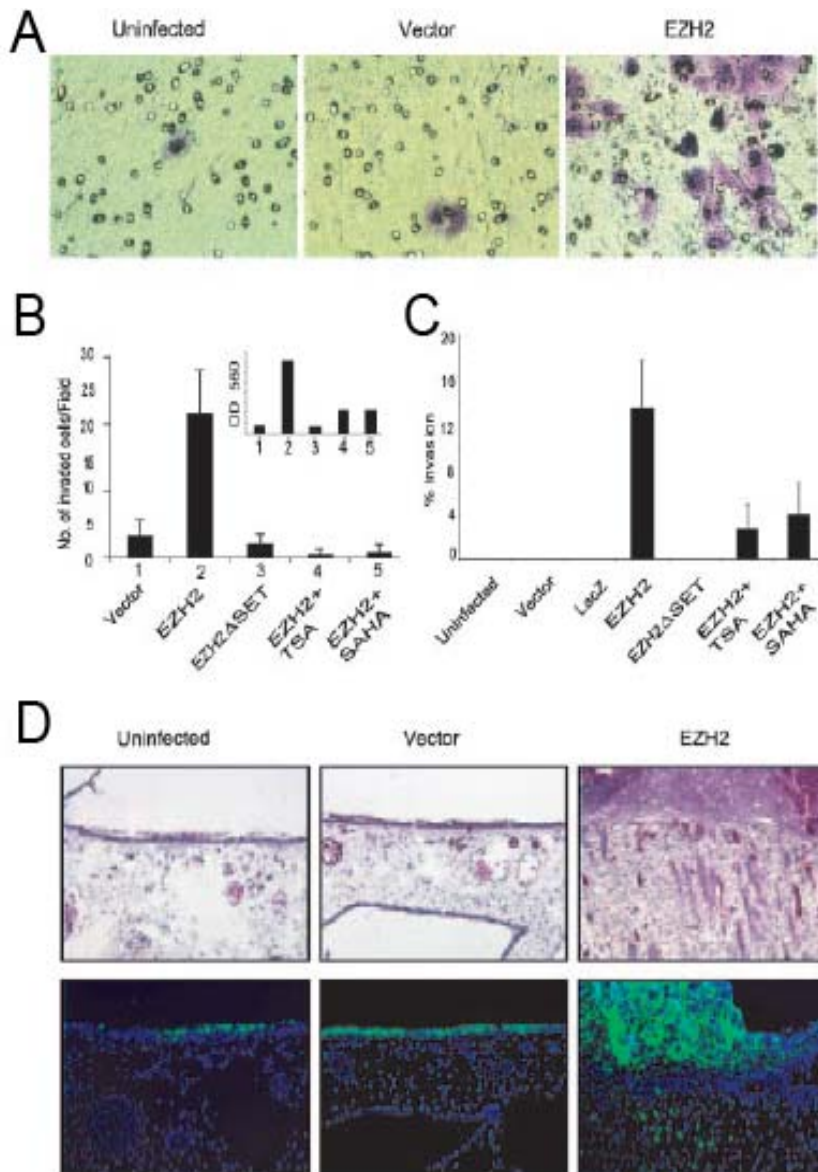


Fig. 2.4. EZH2 orchestrates cell invasion both *in vitro* and *in vivo*. (A) A reconstituted basement membrane invasion chamber assay (Chemicon) was used to assess breast epithelial cell lines infected with EZH2 and control adenoviruses. Representative fields of invaded and stained cells are shown. (B) The numbers of invaded cells were counted in six fields, and the mean values were determined. Quantitation by colorimetry (absorbance at 560 nm) is shown in *Inset*. (C) EZH2-mediated invasion of SU-ECM. H16N2 cells were infected with EZH2, EZH2ΔSET, or control adenoviruses. (D) EZH2 overexpression mediates invasion of breast epithelial cells in a CAM assay. (*Upper*) CAM tissues stained with hematoxylin/eosin. Arrows indicate the cells that have invaded the CAM. Because cells were labeled with Fluoresbrite carboxylated polystyrene nanospheres, they could also be visualized by fluorescence (*Lower*).

REFERENCES

1. Jemal, A., Murray, T., Samuels, A., Ghafoor, A., Ward, E. & Thun, M. J. Cancer Statistics, 2003. *CA Cancer J. Clin.* 2003;**53**: 5–26.
2. Ellis, M., Hayes, D. & Lippman, M. (2000) in *Diseases of the Breast*, eds. Harris, J., Lippman, M. E. & Morrow, M. (Lippincott–Raven, Philadelphia), pp. 749–798.
3. Hayes, D. F., Isaacs, C. & Stearns, V. Prognostic factors in breast cancer: current and new predictors of metastasis (2001) *J. Mammary Gland Biol. Neoplasia* 2001;**6**:375–392.
4. Hayes, D. F., Trock, B. & Harris, A. L. (1998) *Breast Cancer Res. Treat.* **52**, 305–319.
5. Honig, S. (1996) in *Diseases of the Breast*, eds. Harris, J. L. M., Morrow, M. & Hellman, S. (Lippincott–Raven, Philadelphia), pp. 461–485.
6. Clark, G. M. (1996) in *Diseases of the Breast*, eds. Harris, J. L. M., Morrow, M. & Hellman, S. (Lippincott–Raven, Philadelphia), pp. 461–485.
7. Hayes, D. F. (2000) *Eur. J. Cancer* **36**, 302–306.
8. Varambally, S., Dhanasekaran, S. M., Zhou, M., Barrette, T. R., Kumar-Sinha, C., Sanda, M. G., Ghosh, D., Pienta, K. J., Sewalt, R. G., Otte, A. P., *et al.* (2002) *Nature* **419**, 624–629.
9. Laible, G., Wolf, A., Dorn, R., Reuter, G., Nislow, C., Lebersorger, A., Popkin, D., Pillus, L. & Jenuwein, T. (1997) *EMBO J.* **16**, 3219–3232.
10. Satijn, D. P. & Otte, A. P. (1999) *Biochim. Biophys. Acta* **1447**, 1–16.
11. Jacobs, J. J., Kieboom, K., Marino, S., DePinho, R. A. & van Lohuizen, M. (1999) *Nature* **397**, 164–168.
12. Jacobs, J. J., Scheijen, B., Voncken, J. W., Kieboom, K., Berns, A. & van Lohuizen, M. (1999) *Genes Dev.* **13**, 2678–2690.
13. Cao, R., Wang, L., Wang, H., Xia, L., Erdjument-Bromage, H., Tempst, P., Jones, R. S. & Zhang, Y. (2002) *Science* **298**, 1039–1043.
14. Czermin, B., Melfi, R., McCabe, D., Seitz, V., Imhof, A. & Pirrotta, V. (2002) *Cell* **111**, 185–196.
15. Muller, J., Hart, C. M., Francis, N. J., Vargas, M. L., Sengupta, A., Wild, B., Miller, E. L., O'Connor, M. B., Kingston, R. E. & Simon, J. A. (2002) *Cell* **111**, 197–208.
16. Shao, Z., Raible, F., Mollaaghababa, R., Guyon, J. R., Wu, C. T., Bender, W. & Kingston, R. E. (1999) *Cell* **98**, 37–46.
17. Sewalt, R. G., van der Vlag, J., Gunster, M. J., Hamer, K. M., den Blaauwen, J. L., Satijn, D. P., Hendrix, T., van Driel, R. & Otte, A. P. (1998) *Mol. Cell. Biol.* **18**, 3586–3595.
18. van der Vlag, J. & Otte, A. P. (1999) *Nat. Genet.* **23**, 474–478.
19. Tie, F., Furuyama, T., Prasad-Sinha, J., Jane, E. & Harte, P. J. (2001) *Development (Cambridge, U.K.)* **128**, 275–286.
20. Sewalt, R. G., Lachner, M., Vargas, M., Hamer, K. M., den Blaauwen, J. L., Hendrix, T., Melcher, M., Schweizer, D., Jenuwein, T. & Otte, A. P. (2002) *Mol. Cell. Biol.* **22**, 5539–5553.

21. Dhanasekaran, S. M., Barrette, T. R., Ghosh, D., Shah, R., Varambally, S., Kurachi, K., Pienta, K. J., Rubin, M. A. & Chinnaiyan, A. M. (2001) *Nature* **412**, 822–826.
22. Perrone, E. E., Theoharis, C., Mucci, N. R., Hayasaka, S., Taylor, J. M., Cooney, K. A. & Rubin, M. A. (2000) *J. Natl. Cancer Inst.* **92**, 937–939.
23. Camp, R. L., Charette, L. A. & Rimm, D. L. (2000) *Lab. Invest.* **80**, 1943–1949.
24. Zhou, M., Chinnaiyan, A. M., Kleer, C. G., Lucas, P. C. & Rubin, M. A. (2002) *Am. J. Surg. Pathol.* **26**, 926–931.
25. Livant, D. L., Linn, S., Markwart, S. & Shuster, J. (1995) *Cancer Res.* **55**, 085–5093.
26. Morris, V. L., Koop, S., MacDonald, I. C., Schmidt, E. E., Grattan, M., Percy, D., Chambers, A. F. & Groom, A. C. (1994) *Clin. Exp. Metastasis* **12**, 357–367.
27. Rhodes, D. R., Barrette, T. R., Rubin, M. A., Ghosh, D. & Chinnaiyan, A. M. (2002) *Cancer Res.* **62**, 4427–4433.
28. Perou, C. M., Sorlie, T., Eisen, M. B., van de Rijn, M., Jeffrey, S. S., Rees, C. A., Pollack, J. R., Ross, D. T., Johnsen, H., Akslen, L. A., *et al.* (2000) *Nature* **406**, 747–752.
29. Hedenfalk, I., Duggan, D. D., Chen, Y., Radmacher, M., Bittner, M., Simon, R., Meltzer, P., Gusterson, B. A., Esteller, M., Kallioniemi, O. P., *et al.* (2001) *New Engl. J. Med.* **344**, 539–548.
30. van't Veer, L. J., Dai, H., van de Vijver, M. J., He, Y. D., Hart, A. A., Mao, M., Peterse, H. L., van der Kooy, K., Marton, M. J., Witteveen, A. T., *et al.* (2002) *Nature* **415**, 530–536.
31. Gruvberger, S., Ringner, M., Chen, Y., Panavally, S., Saal, L. H., Borg, A., Ferno, M., Peterson, C. & Meltzer, P. S. (2001) *Cancer Res.* **61**, 5979–5984.
32. Sorlie, T., Perou, C. M., Tibshirani, R., Aas, T., Geisler, S., Johnsen, H., Hastie, T., Eisen, M. B., van de Rijn, M., Jeffrey, S. S., *et al.* (2001) *Proc. Natl. Acad. Sci. USA* **98**, 10869–10874.
33. Raaphorst, F. M., van Kemenade, F. J., Blokzijl, T., Fieret, E., Hamer, K. M., Satijn, D. P., Otte, A. P. & Meijer, C. J. (2000) *Am. J. Pathol.* **157**, 709–715.
34. Ignatoski, K. M., Lapointe, A. J., Radany, E. H. & Ethier, S. P. (1999) *Endocrinology* **140**, 3615–3622.
35. Livant, D. L., Brabec, R. K., Pienta, K. J., Allen, D. L., Kurachi, K., Markwart, S. & Upadhyaya, A. (2000) *Cancer Res.* **60**, 309–320.
36. Hanahan, D. & Weinberg, R. A. (2000) *Cell* **100**, 57–70.
37. Huang, L. & Pardee, A. B. (2000) *Mol. Med.* **6**, 849–866.

CHAPTER 3

REPRESSION OF E-CADHERIN BY THE POLYCOMB GROUP PROTEIN EZH2 IN CANCER

Tumor invasion and metastasis are the major catalysts of morbidity and mortality in cancer patients (1, 2). The initial stages of tumor invasion are characterized by the disruption of cell-cell adhesion, and decreased E-cadherin expression characterizes the invasive phenotype. E-cadherin is a Ca^{2+} -dependent, transmembrane receptor that mediates cell-cell adhesion at adherent junctions via homophilic binding, thus maintaining epithelial cellular adhesion and integrity. (3). There is compelling evidence that E-cadherin expression is repressed in cancer, which suggests that it may play a critical role in the malignant progression of epithelial tumors (4-6). It has been implicated as a tumor suppressor via negative regulation during the course of invasion (7, 8). While many epithelial cancer cell lines that lack E-cadherin expression were invasive, administrative of exogenous E-cadherin to these cells prevented invasion, suggesting a critical role for this receptor in invasive process (7) . E-cadherin forms dimers, and the cytoplasmic domain of E-cadherin is complexed with catenins that are linked to the actin cytoskeleton network of the cells (9). The interaction between these molecules regulate the cell-cell adhesion(10).

Reduced E-cadherin expression has been linked to metastasis. Numerous studies have demonstrated that aberrant expression of E-cadherin is associated with the

development of metastases in breast cancer (11, 12) and gastric cancer (13) among others. A number of mechanisms have been suggested for the repression of E-cadherin function during cancer progression including promoter methylation, mutations, transcriptional repression by snail and slug, ubiquitination and degradation of the E-cadherin, and lysosomal targeting of the E-cadherin for degradation (14-20) .

Recent studies have shown that histone H3 lysine 27 trimethylation, which is mediated by EZH2 at the promoters of the gene, leads to silencing of gene expression (21-23). As part of a multi-protein complex with the other members of PRC2 (24), EZH2 trimethylates histone H3 tails at lysine 27 (25, 26). This epigenetic modification is also known to be responsible for X-inactivation (27). Previously, we demonstrated that EZH2 is upregulated in aggressive prostate and breast tumors (28, 29). Several reports have also shown that EZH2 is over-expressed in other aggressive tumors including bronchial cancer (30) melanoma (31), bladder cancer (32) liver cancer (33), as well as *in vitro* cancer cell lines such as SKBR3, MDA-MB-231, T47D breast cell lines (34), and the prostate cell lines DU145 and LNCaP (35) .

EZH2 is a transcriptional repressor that plays a crucial role in maintaining the delicate homeostatic balance between gene expression and repression, the disruption of which may lead to oncogenesis (36-38). Recent studies revealed that EZH2 can physically recruit DNA methyltransferases (DNMTs) to certain target genes and silence them, suggesting cross-talk between the two distinct epigenetic silencing mechanisms (39, 40). Cancer cells that contain DNA-methylated genes are specifically packaged in nucleosomes with the histone H3K27 trimethylation (41). Reports also suggest that stem cell polycomb group targets are more likely to exhibit cancer-specific promoter DNA

hypermethylation and histone H3 trimethylation of Lys27 relative to non-targets (42, 43). In human and mouse embryonic stem cells, as well as in *Drosophila*, Polycomb Group (PcG) proteins contribute to pluripotency and plasticity via repression of developmental transcriptional factors that normally promote differentiation (44-47).

In this study, we explored the role of histone methylation mediated by PRC2 in the silencing of E-cadherin during cancer progression and provide evidence of a functional link between dysregulation of EZH2 and repression of E-cadherin during cancer development.

Materials and Methods

Basement Membrane Matrix Invasion Assay

For invasion assays, the breast cell lines H16N2, HME, and MCF10A (ATCC, Manassas, VA), as well as normal prostate epithelial cells (PrEC, Cambrex, East Rutherford, NJ), were infected with vector, EZH2 and EZH2 Δ SET adenovirus. Forty-eight hours post-infection, cells were seeded onto the basement membrane matrix (EC matrix, Chemicon, Temecula, CA) present in the insert of a 24 well culture plate. Fetal bovine serum was added to the lower chamber as a chemoattractant with or without HDAC inhibitor suberoylanilide hydroxamic acid (SAHA) (Biovision Inc., Mountain View, CA). After 48 hours, the non-invading cells and EC matrix were gently removed with a cotton swab. Invasive cells located on the lower side of the chamber were stained with crystal violet, air dried and photographed. They were then enumerated microscopically using multiple representative areas. For colorimetric assays, the inserts were treated with 150 μ l of 10% acetic acid and the absorbance measured at 560nm using a spectrophotometer (GE Healthcare Bio-Sciences Corp, Piscataway, NJ).

RNA interference

The knockdown of EZH2 was accomplished with either siRNA duplex (Dharmacon, Lafayette, CO) as previously described (28) or shRNA expression vectors (Open Biosystems, Huntsville, AL). E-cadherin knockdown was performed using siRNA duplex. (Dharmacon)

Immunoblot Analyses

The breast cell lines H16N2, HME, and MCF10A, as well as normal prostate epithelial cells, were grown to 60% confluency and infected with either EZH2 adenovirus, vector control, or Delta SET virus for 48 hours. Cells were homogenized in NP40 lysis buffer (50 mM Tris-HCl, 1% NP40, pH 7.4, Sigma, St. Louis, MO), and complete proteinase inhibitor mixture (Roche, Indianapolis, IN). Ten micrograms of each protein extract were boiled in sample buffer, separated by SDS-PAGE, and transferred onto Polyvinylidene Difluoride membrane (GE Healthcare). The membrane was incubated for one hour in blocking buffer [Tris-buffered saline, 0.1% Tween (TBS-T), 5% nonfat dry milk] and incubated overnight at 4°C with the following: anti-EZH2 mouse monoclonal (1:1000, 1:5000 in dilution buffer, BD Biosciences, San Jose, CA), anti-E-CAD mouse monoclonal antibodies (1:1000, 1:5000 in dilution buffer, BD Biosciences), anti-EED rabbit polyclonal antibody (1:1000 in dilution buffer, Upstate, Charlottesville, VA), and anti-SUZ12 rabbit polyclonal antibodies (1:1000 in dilution buffer, kind gift from Prof. Otte). Following a wash with TBS-T, the blot was incubated with horseradish peroxidase-conjugated secondary antibody and the signals visualized by enhanced

chemiluminescence system as described by the manufacturer (GE Healthcare). The blot was re-probed with β -tubulin for confirmation of equal loading.

Northern blot analyses

Total RNA was isolated from H16N2 cells that were infected with either vector, EZH2, or EZH2 Δ SET adenovirus. An additional set of cells were infected with EZH2 adenovirus and were treated with HDAC inhibitor SAHA (Biovision, Mountain View, CA). Twenty micrograms of total RNA from each condition were resolved on a denaturing-formaldehyde agarose gel and subsequently transferred onto a Hybond-NX membrane (Amersham Biosciences, Piscataway, NJ). EZH2, E-cadherin, and GAPDH probes were labeled with p32dCTP (GE Healthcare) and hybridized to the blots. The signal was visualized and quantified using a Typhoon Scanner 9000B and Image Quant Software (Amersham Biosciences). E-cadherin and EZH2 signals were normalized to that of GAPDH.

SYBR Green Quantitative Real-Time PCR

Total RNA was isolated from H16N2 cells that were infected either with vector, EZH2, or EZH2 Δ SET adenovirus. Quantitative PCR (QPCR) was performed using SYBR Green dye on an Applied Biosystems 7300 Real Time PCR system (Applied Biosystems, Foster City, CA). Briefly, 1 μ g of total RNA was reverse transcribed into cDNA using SuperScript III (Invitrogen, Carlsbad, CA) in the presence of random hexamers and oligo dT primers (Invitrogen). All reactions were performed in duplicate with SYBR Green Master Mix (Applied Biosystems) plus 25 ng of both the forward and reverse primer according to the manufacturer's recommended thermocycling conditions, then subjected to melt curve analysis. Threshold levels for each experiment were set

during the exponential phase of the QPCR reaction using Sequence Detection Software version 1.2.2 (Applied Biosystems). The DNA in each sample was quantified by interpolation of its threshold cycle (C_t) value from a standard curve of C_t values, which were created from a serially diluted cDNA mixture of all samples. The calculated quantity of the target gene for each sample was divided by the average sample quantity of the housekeeping genes, glyceraldehyde-3-phosphate dehydrogenase (*GAPDH*) and hydroxymethylbilane synthase (*HMBS*) to obtain the relative gene expression. All oligonucleotide primers were synthesized by Integrated DNA Technologies (Coralville, IA). Primers for *HMBS* and *GAPDH* were as described (48). Primers for CDH1 were: CDH1-F, 5'-GGAGGAGAGCGGTGGTCAAA-3'; CDH1-R, 5'-TGTGCAGCTGGCTCAAGTCAA-3'.

Immunofluorescence

H16N2 cells were grown using chamber slides (Nunc, Rochester, NY) and infected with either control or EZH2 virus for cell line co-immunostaining with EZH2 and E-cadherin antibody. Forty-eight hours post-infection, the slides were washed with PBS, and were fixed using ice cold methanol. Following an additional PBS wash, the slides were blocked for two hours using 5% donkey serum in PBS-T (phosphate buffered saline, 0.05% Tween-20). A mixture of rabbit anti-E-cadherin antibody (Labvision, Fremont, CA) and mouse anti-EZH2 antibody (BD Biosciences, San Jose, CA) were added to the slides at 1:250 and 1:100 dilutions, respectively, and incubated overnight at 4° C. Following an additional wash, the slides were incubated with Alexa 555-conjugated goat, anti-rabbit antibody and Alexa 488-conjugated goat, anti-rabbit secondary antibody (Invitrogen) for one hour in the dark at room temperature. After

washing, the slides were mounted using Vectashield mounting medium containing DAPI (Vector Laboratories, Burlingame, CA).

Breast tissues samples were collected with informed consent and prior institutional review board approval. To prepare for tissue section staining, paraffin-embedded breast tissue slides were soaked in xylene for one hour removal of paraffin. Slides were placed in citrate buffer (pH 6.0) and heated under pressure for 15 minutes for antigen retrieval. They were then blocked in PBS-T with 5% normal donkey serum for one hour. A mixture of rabbit anti-E-cadherin antibody (Labvision) and mouse anti-EZH2 antibody (BD Biosciences) was added to the slides at 1:250 and 1:100 dilutions respectively and incubated overnight at 4° C. Slides were then incubated with secondary antibodies for one hour (anti-mouse IgG horse radish peroxidase conjugate and anti-rabbit Alexa 555, both at 1:1000 dilution). Following a wash, fluorescently-labeled tyramide (Aelxa Fluor 488, Invitrogen) was added and the slides incubated for 10 minutes at room temperature. They were washed and then mounted using Vectashield mounting medium. Confocal images were taken with a Ziess LSM510 META imaging system using Argon and Helium Neon 1 and Helium Neon 2 light source (Carl Zeiss, Thornwood, NY). The color images were exported as TIFF images.

Luciferase Assay

E-cadherin regulation by EZH2 was examined using the E-cadherin promoter luciferase reporter gene and transient transfection assays were performed. The breast cell lines H16N2, MCF10A and HME were transfected with wild-type or E-box mutant E-cadherin luciferase construct (kind gift of Dr. Eric Fearon) as well as pRL-TK vector as internal control for luciferase activity, then subsequently infected with either EZH2 or

control viruses. Following two days of incubation, the cells were lysed and luciferase assays conducted using the dual luciferase assay system (Promega, Madison, WI). Each experiment was performed in triplicate. Using siRNA duplex, an EZH2 knockdown was performed in the invasive prostate cell line DU145. Both were simultaneously transfected with E-cadherin promoter-luciferase reporter constructs, and the luciferase activity was measured after two days as previously described.

Chromatin immunoprecipitation (ChIP) Assay

ChIP experiments were carried out as described by Yu, et al.(49). For each ChIP assay, 5ug of antibodies were used; EZH2 (BD Biosciences), SUZ12 (Abcam, Cambridge, MA), EED, trimethyl H3-Lys27 and acetyl H3 (Upstate), Myc (Abcam) or IgG control (Santa Cruz). Approximately 2-5 ul of ChIP-enriched chromatin were subjected to a standard ChIP-PCR reaction, and the enrichment of specific genomic regions was assessed relative to either control IgG or control cells. Each ChIP experiment was repeated at least three times. For ChIP with human tissues, ChIP-enriched DNA and input DNA were amplified through ligation-mediated PCR. Equal amounts (50ng) of amplified ChIP DNA and input DNA were subjected to PCR. Enrichment by ChIP was assessed relative to the input DNA and normalized to the level of GAPDH. The primers used in the ChIP experiments were designed to flank the promoter regions of CDH1 and the WNT1 positive control gene, as well as the intragenic region of the NUP214 negative control. The sequences of the primers were: CDH1-pF, TAGAGGGTCACCGCGTCTAT; CDH1-pR, TCACAGGTGCTTTGCAGTTC; WNT1-pF1, ACCCGTCAGCTCTCGGCTCA; WNT1-pR1, TGCAGTTGCGGCGACTTTGG;

NUP214_pF1, CAGTGAGGTCTCAGCATCAGCA; NUP214_pR1,
CTGGAGGCTATGGGGGTACTTG.

Bisulfite Modification and Methylation-Specific PCR of *CDH1* promoter. H16N2 cells were infected with vector control or EZH2 adenovirus for 48hrs and genomic DNA was isolated (Qiagen). The genomic DNA was modified by sodium bisulfite treatment using the CpGenomeTM DNA Modification Kit (S7820, Chemicon, Temecula, CA). The DNA promoter methylation status of E-cadherin gene was investigated by PCR using primers specific to methylated and unmethylated promoters using the CpG WIZTM E-cadherin Amplification Kit (S7804, Chemicon). The methylated and unmethylated control DNA (provided in the S7804 kit, Chemicon) were also subjected to bisulfite DNA modification and PCR analysis, and serves as positive controls for methylated and unmethylated DNA respectively. H2O was used as negative control for the PCR reaction.

Results and Discussion

Alteration in EZH2 expression changes the invasive phenotype of the cells.

We have reported previously that EZH2 expression is increased in aggressive prostate and breast cancer (28, 29). Herein, we evaluated the effect of EZH2 overexpression in multiple primary and non-invasive prostate and breast cells. A modified Boyden chamber assay was used to determine if primary prostate epithelial cells and immortalized breast cell lines (with very low endogenous EZH2 expression) undergo invasion upon ectopic over-expression of EZH2. Primary cells and immortalized benign epithelial cell lines infected with an EZH2-encoding adenovirus, but not a control adenovirus, induced cell invasion (**Fig. 3.1A**). Importantly, a truncated mutant version

of EZH2 (EZH2 Δ SET, missing the C-terminal SET domain that is required for methyltransferase activity) did not induce invasion. Additionally, EZH2-mediated invasion could be attenuated by incubating cells with the histone deacetylase (HDAC) inhibitor, SAHA, across all of the primary cultures and cell lines tested (**Fig. 3.1A**). This suggests a role for histone deacetylation in EZH2-mediated effects.

To expand our investigations, we explored whether perturbation of endogenous EZH2 would affect the invasiveness of cancer cell lines. For these studies, we employed the highly invasive prostate cancer cell line DU145. Over-expression of EZH2 Δ SET in DU145 cells markedly reduced their invasive potential (**Fig. 3.1B**), suggesting that this mutant version of EZH2 functioned as a dominant negative. Similarly, when EZH2 levels were depleted using siRNA duplexes (**Fig. 3.1C**) or shRNA (**Fig. 3.1D**), there was marked attenuation of DU145 invasive potential.

EZH2 regulates E-cadherin transcript and protein expression. As earlier studies from our group suggested an inverse relationship between EZH2 and E-cadherin expression in prostate cancer (50), we hypothesized that EZH2 might regulate E-cadherin in the neoplastic process. We infected an immortalized benign breast epithelial cell line, H16N2, with EZH2, EZH2 Δ SET, and control adenoviruses to determine whether EZH2 represses expression of the E-cadherin mRNA transcript. As hypothesized, EZH2 overexpression resulted in abrogation of E-cadherin transcripts as confirmed by two independent methods; Northern blot analysis (**Fig. 3.2A**) and quantitative PCR (**Fig. 3.2B**). Mutant EZH2 (EZH2 Δ SET) or EZH2-infected cells treated with SAHA did not show down regulation of E-cadherin, indicating the importance of the SET domain of EZH2 as well as HDAC activity. The effect of EZH2 overexpression on E-cadherin

protein was examined in four cell lines or primary cultures (H16N2, HME, MCF10A, and PrEC). We observed marked attenuation of E-cadherin protein levels by EZH2 overexpression, but not EZH2 Δ SET, nor when EZH2 overexpressing cells were treated with HDAC inhibitor SAHA (**Fig. 3.2C**). Immunoblot analysis also showed that E-cadherin repression is dependent on the expression of EZH2; higher EZH2 expression resulting in increased E-cadherin repression (**Fig. 3S1**). Interestingly, a panel of breast and prostate cell lines showed an inverse correlation of EZH2 and E-cadherin protein expression (**Fig. 3.2D**), suggesting that PRC2 may be regulating E-cadherin levels *in vivo*. Similarly, this inverse association between EZH2 and E-cadherin protein levels was recapitulated *in situ* in both H16N2 breast epithelial cells (**Fig. 3.2E**) as well as in breast tumors (**Fig. 3.2F**).

E-cadherin expression can rescue EZH2 mediated invasion. To determine if E-cadherin loss is a significant factor in the downstream regulation of EZH2-mediated invasion, we re-introduced E-cadherin under the regulation of a CMV promoter. We assessed the possibility that this might counteract the effects of EZH2-mediated silencing of E-cadherin. While H16N2 cells infected with EZH2 adenovirus were highly invasive and exhibited strong repression of E-cadherin (**Fig. 3.1A and 3.2A**), this was attenuated by overexpression of E-cadherin under a non-EZH2 repressible promoter (i.e., CMV) (**Fig. 3.3A**). To confirm that the loss of E-cadherin was a critical step in conferring invasiveness to H16N2 cells, E-cadherin was depleted using siRNA duplexes. H16N2 cells treated with siRNA against E-cadherin acquired invasive potential (**Fig. 3.3B**), while control siRNA did not show this phenotype.

EZH2 regulates the E-cadherin expression by methylating the histone H3 lysine 27 at the promoter region. To determine if EZH2 can repress its activity, we performed a luciferase assay with an E-cadherin promoter-luciferase reporter construct that contained an endogenous regulatory region of E-cadherin 1.4 KB upstream (51). As predicted, EZH2 inhibited the activity of the transfected E-cadherin promoter-reporter across all three cell lines tested (**Fig 3.4A**). EZH2-mediated repression of the E-cadherin promoter was blocked by SAHA, highlighting the role of histone deacetylation during EZH2-mediated E-cadherin regulation. Interestingly, the E-cadherin-luciferase reporter was slightly induced by expression of EZH2 Δ SET (**Fig. 3.4A**), which suggested a dominant, negative effect. Knockdown of EZH2 in DU145 cells led to increased activity of the transfected E-cadherin promoter-reporter construct (**Fig. 3.4B**).

In order to determine the minimal region of the E-cadherin promoter required for EZH2-mediated repression, we tested mutant E-cadherin promoter-luciferase reporters (19) including Ecad-EboxA.MUT-luc (mutated Ebox A), Ecad-EboxC.MUT-luc (mutated Ebox C), Ecad-EboxABC.MUT-luc (all the three E-boxes, A, B and C are mutated) as well as wild-type E-cadherin promoter-luciferase reporter. While EZH2 repressed the wild-type E-cadherin promoter activity, none of the E-boxes mutants tested were inhibited, indicating that the wild type E-cadherin promoter is required for EZH2 mediated E-cadherin repression (**Fig. 3S2**).

Ectopically overexpressed, myc-tagged EZH2 assembles endogenous PRC2 components including SUZ12 and EED, as demonstrated by their presence in anti-myc immunoprecipitates (**Fig. 3.4C**). Addition of SAHA did not inhibit the binding of PRC2

complex members, indicating that the HDAC inhibitors do not inhibit PRC2 protein-protein interactions.

The polycomb group proteins are known to bind to a selected group of target genes and inhibit transcription (44, 45). To determine whether the endogenous PRC2 complex binds to the E-cadherin gene promoter, we carried out chromatin immunoprecipitation (ChIP) assay using antibodies specific to the PRC2 components and to the histone modifications. The invasive prostate cancer cell line DU145, which expresses high level of EZH2 (**Fig. 3.2D**), was used to test complex formation by endogenous EZH2 and other PRC2 complex members. These investigations indicated binding of EZH2, SUZ12, and EED to the E-cadherin promoter (**Fig. 3.4D**). Additionally, histone H3 was found to be trimethylated at lysine 27 on the E-cadherin promoter. Of particular importance was the finding that the HDAC inhibitor SAHA, while increasing histone acetylation as expected, markedly reduced PRC2 occupancy and H3K27 trimethylation on the E-cadherin promoter.

As ectopic EZH2 assembles the PRC2 complex (**Fig. 3.4C**), we explored the possibility that it might recruit the PRC2 complex proteins to the E-cadherin promoter. The H16N2 immortalized breast epithelial cell line, which has low level of endogenous EZH2, was infected with either vector control or EZH2 adenovirus and examined for PRC2 occupancy on the E-cadherin promoter. Using an antibody against Myc epitope, tagged at both EZH2 and mutant EZH2 constructs, we confirmed that ectopically expressed EZH2 binds to the E-cadherin promoter by ChIP (**Fig. 3.4E**).

Interestingly, ectopic over-expression of EZH2 recruited other PRC2 components to the E-cadherin promoter and markedly increased H3K27 trimethylation

(**Fig. 3.4E**). The histone H3K27 trimethylation mark was used to assess PRC2 occupancy at the E-cadherin promoter by a ChIP analysis in one localized prostate tumor and three metastatic prostate cancer tissues. Results indicated that the E-cadherin promoter contained high levels of H3K27 trimethylation in the three metastatic tumor specimens tested as compared to the localized prostate cancer tissue specimen (**Fig. 3.4F**). Recently, it has been shown that DNA methyltransferases (DNMTs) and EZH2 cooperate in silencing genes such as *MYT1*, *WNT1*, *KCNA1* and *CNR1* (39). Additional H3K9 methylation may lead to promoter CpG island DNA methylation (43). However, E-cadherin promoter methylation analyses of EZH2 over-expressing cells did not exhibit E-cadherin promoter DNA methylation. This indicated that histone trimethylation-mediated by EZH2 plays a major role in the silencing of E-cadherin.

Thus, our data suggests a novel mechanism by which E-cadherin is down-regulated in EZH2-overexpressing cells through histone H3K27 trimethylation at the E-cadherin promoter. While EZH2 expression was low in benign epithelial tissues, the expression of EZH2 destabilized with tumor progression. EZH2 expression became dysregulated concurrently with increased HDAC activity, which resulted in trimethylation of histone H3 lysine 27 at the E-cadherin promoter with subsequent repression of expression (**Fig. 3.4G**). This enzymatic activity was inhibited, however, when the cells were treated with HDAC inhibitor despite overexpression of EZH2.

A large body of evidence suggests that loss of E-cadherin expression is associated with the acquisition of invasiveness and advanced tumor stage for cancers of epithelial origin including prostate (52, 53), gastric (54), colon (55), and breast cancer (11, 56, 57). While several mechanisms have been proposed for the downregulation of

E-cadherin, our data suggest a novel mechanism whereby increased levels of EZH2 in aggressive tumors silence E-cadherin expression through histone H3K27 trimethylation. EZH2 regulates E-cadherin transcription by physically binding to its promoter. The expression of EZH2 recruits HDAC activity with removal of the acetyl group from the histone H3K27 at the promoter region of E-cadherin. This enables EZH2 to exert its histone methyltransferase enzymatic activity. Tri-methylation of histone H3 on lysine 27 leads to compaction of chromatin and blocks transcription factors from binding and initiating transcription. EZH2 may mediate increased invasiveness and metastasis by silencing a number of downstream targets in addition to E-cadherin.

Interestingly, we demonstrated that HDAC inhibitors inhibited the function of EZH2 and prevented the EZH2 mediated downregulation of E-cadherin and reduced the invasion, thus suggesting a mechanism for these anti-cancer drugs. Our findings suggest that EZH2 may be a viable target for therapeutic inhibition in aggressive tumors of epithelial origin.

Acknowledgments

We thank Professor Eric Fearon for providing the E-cadherin promoter-reporter constructs. We thank Jill Granger for critically reading the manuscript and thoughtful suggestions. We thank R. Kunkel for help in figure preparation and the staff of the Microscopy and Image Analyses laboratory at the University of Michigan for their assistance in the microscopic analyses employed in this study. We thank the University of Michigan Vector Core for virus generation.

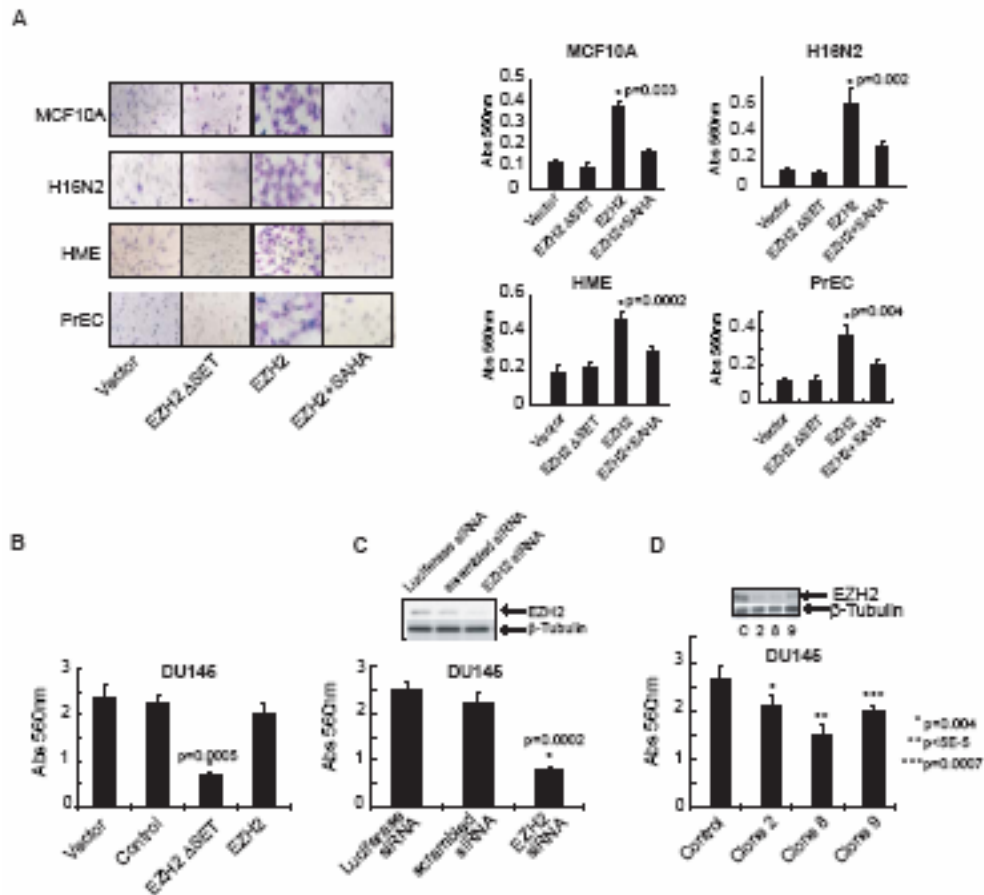
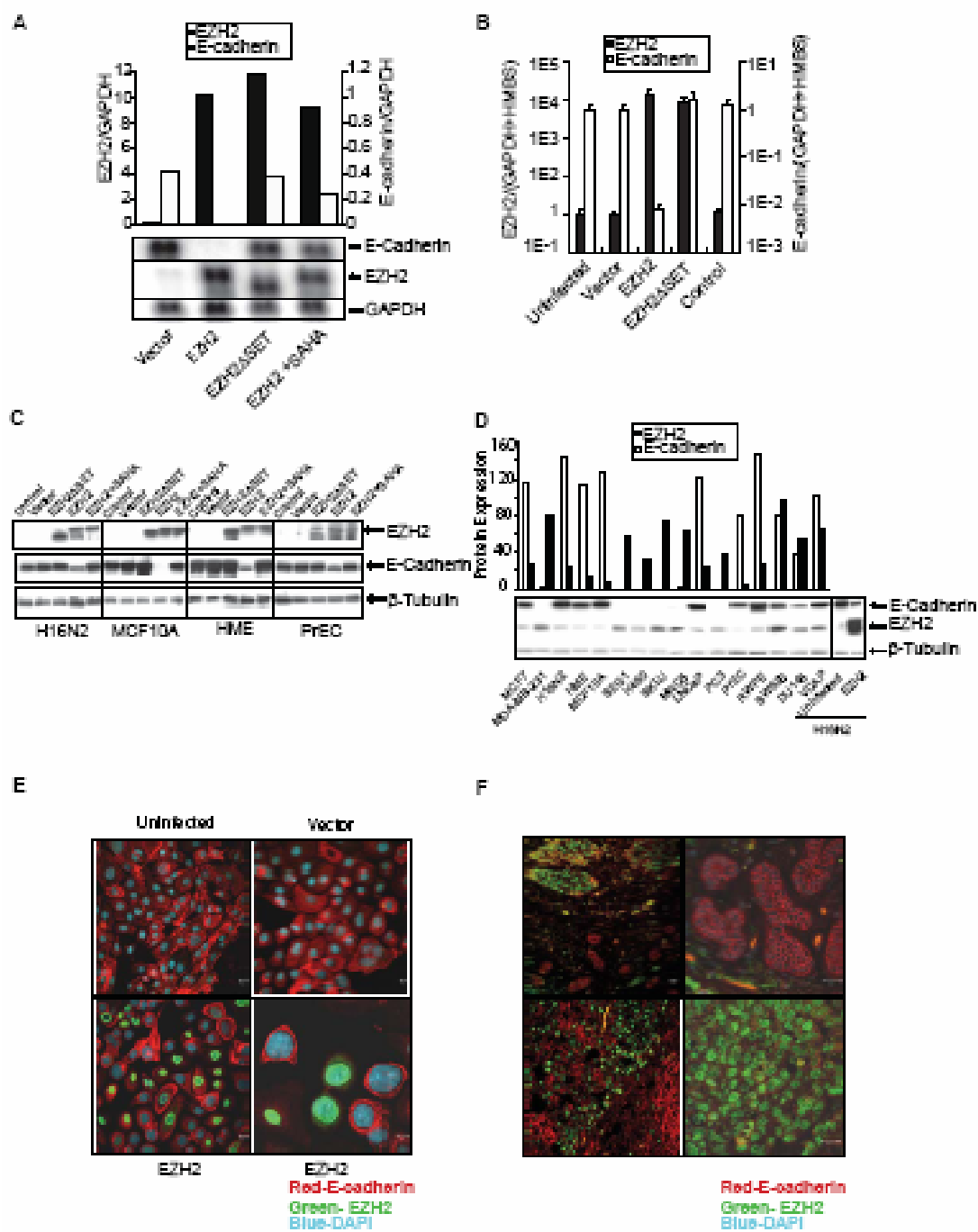


Figure 3.1. Over expression of EZH2 enhances invasion. **A**, Ectopic expression of EZH2 induces invasion of primary prostate epithelial cells and benign immortalized breast cell lines. A reconstituted basement membrane invasion chamber assay (Boyden chamber assay) was used to assess the invasive potential of primary prostate and benign breast epithelial cell lines infected with EZH2, EZH2ΔSET or control adenovirus. EZH2 infected cells were also treated with the histone deacetylase inhibitor SAHA. Representative fields of invaded and stained cells are shown (left). Invasion was quantitated using colorimetry (absorbance at 560 nm, right). All p values were calculated between EZH2 and vector treated samples. **B**, The SET domain mutant of EZH2 inhibits cancer cell invasion. DU145 cells, which express high levels of endogenous EZH2, were infected with EZH2, EZH2ΔSET, and control adenoviruses. Invasion was quantitated using colorimetry. The p value was calculated between EZH2ΔSET and vectors. **C**, Cell invasion is attenuated by EZH2 knockdown. Boyden chamber invasion assay using DU145 cells treated with siRNA duplexes targeting EZH2. Inset demonstrates knockdown of EZH2 protein by RNA interference. All p values were calculated between control and EZH2 knockdown clones. **D**, Stable knockdown of EZH2 decreases invasiveness of DU145 cells. DU145 cells were stably transfected with EZH2 shRNA and assessed by invasion assay. Three stable clones exhibiting knockdown of EZH2 are shown. Inset demonstrates knockdown of EZH2 protein by RNA interference.

Figure 3.2. EZH2 mediates repression of E-cadherin transcript and protein. A, Northern blot analyses of the E-cadherin gene in EZH2 over expressing cells. Northern blot analysis was carried out using the RNA from H16N2 cells infected with EZH2 and control adenovirus. EZH2, E-cadherin and GAPDH probes were labeled with p32dCTP and hybridized to the blots. Note that uninfected H16N2 cells do not express EZH2, while E-cadherin is expressed at high levels in these cells. **B,** Quantitative SYBR green RT-PCR of EZH2 transcript in cell lines infected with EZH2 and control adenoviruses. RT-PCR on each sample was performed in duplicate, and a ratio was calculated relative to the housekeeping genes GAPDH and hydroxymethylbilane synthase (HMBS). **C,** Immunoblot analysis of EZH2 and E-cadherin in breast cell lines H16N2, MCF10A, HME and primary prostate cell PrEC infected with EZH2, EZH2 Δ SET mutant, and control adenovirus infected cells as well as EZH2 infected cells treated with SAHA. β -tubulin was included as a loading control. Experiments were performed multiple times and a representative immunoblot is shown. **D,** Immunoblot analysis of EZH2 and E-cadherin in a panel of breast and prostate cell lines. The cultured lines include both invasive and non-invasive cells. β -tubulin was included as a loading control. Semi-quantitation of EZH2 and E-cadherin in multiple cell lines is represented in a graphical format (top panel). **E,** Immunostaining of the breast cell line H16N2 infected with EZH2 and control adenovirus. Green staining represents EZH2 protein, red staining represents E-cadherin, and blue represents nuclear staining with DAPI. Lower right panel shows a higher magnification image. **F,** Association between EZH2 and E-cadherin protein levels in human breast tumors by immunofluorescence. Upper left panel shows invasive carcinoma of the breast with high EZH2 protein expression in the nuclei (green) and low E-cadherin expression (red), evidenced by a decrease in the membrane staining. A normal lobule is present in the lower part of the figure. Top right panel shows the higher magnification of the normal lobule shown with crisp membrane staining for E-cadherin. EZH2 staining is absent in this region. The lower left panel shows invasive carcinoma with foci of high EZH2 expression. The lower right panel shows higher magnification of a focus of invasive carcinoma with high EZH2 expression and nearly absent E-cadherin staining.



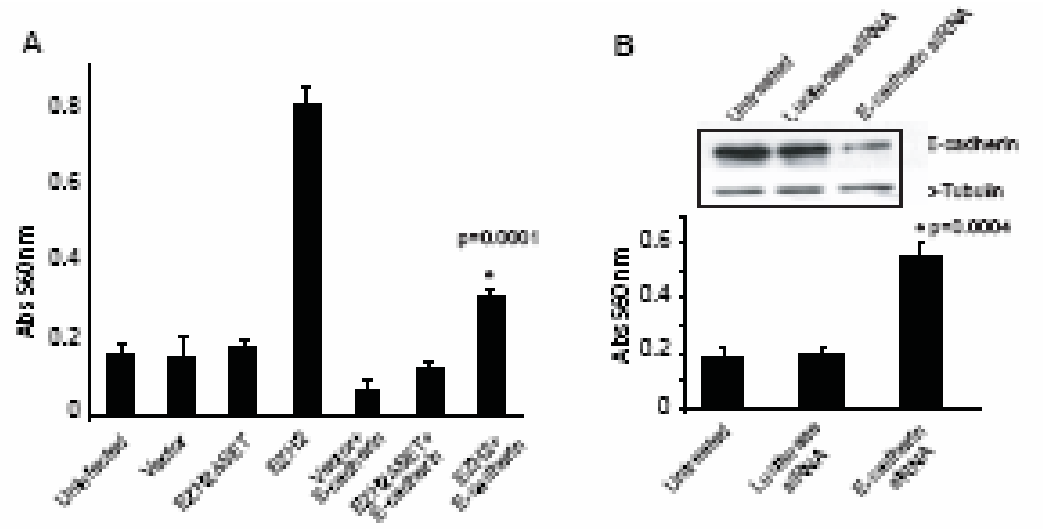


Figure 3.3. E-cadherin over-expression attenuates EZH2-mediated cell invasion. **A**, H16N2 cells were transfected with E-cadherin or vector alone. Transfected cells were infected with EZH2, EZH2ΔSET, and control adenovirus. Cell invasion was assessed by Boyden chamber assay, and p values were calculated between EZH2 and EZH2+E-cadherin samples. **B**, E-cadherin knockdown in H16N2 cells was carried out using siRNA duplex. siRNA targeting luciferase served as a control. The p values were calculated between Luciferase RNAi and EZH2 RNAi samples. The inset demonstrates knockdown of E-cadherin protein by RNA interference.

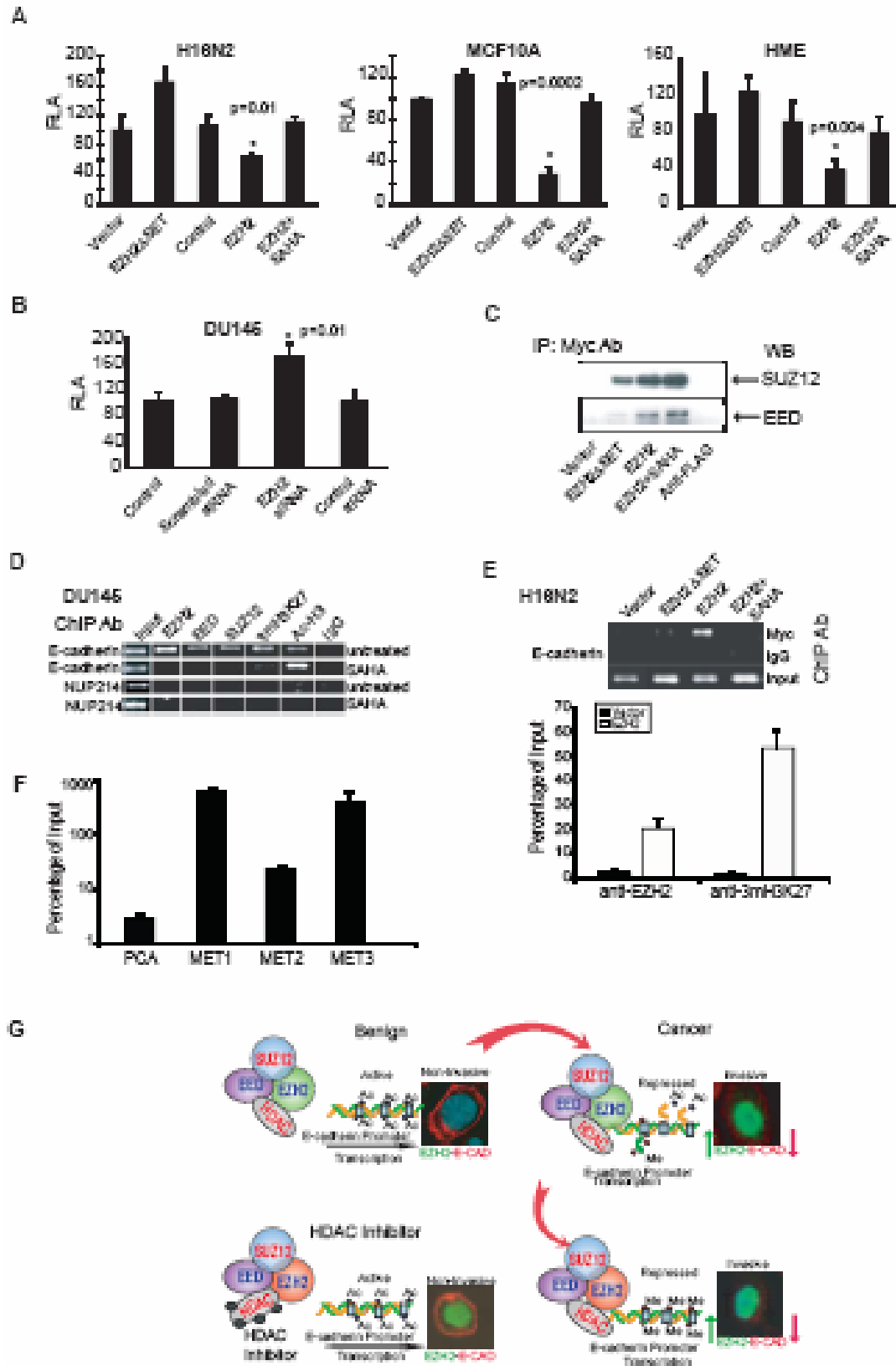


Figure 3.4. Regulation of the E-cadherin promoter by EZH2. A, Benign breast cell lines H16N2, MCF10A and HME were transfected with an E-cadherin-luciferase

promoter construct and infected with either EZH2, EZH2 Δ SET or control adenovirus. EZH2 infected cells were also incubated with SAHA. Relative luciferase activity (RLA) was assessed. **B**, Knockdown of EZH2 in DU145 cells induces E-cadherin promoter activity. EZH2 expression was inhibited by RNA interference in DU145 cells that were transfected with the E-cadherin promoter-luciferase construct. The p value was calculated between EZH2 RNAi and scrambled RNAi samples. **C**, Ectopically expressed EZH2 functions in a complex with endogenous PRC2 components SUZ12 and EED. H16N2 cells were infected with myc-tagged EZH2 adenovirus. Immunoprecipitation was carried out using anti-myc antibody, and subsequent Western blotting performed with either SUZ12 or EED antibody. **D**, The endogenous PRC2 complex is recruited to the E-cadherin promoter. ChIP was carried out using antibodies against EZH2, EED, SUZ12, trimethyl-histone H3-Lys27 (3mH3K27), acetyl histone H3 (Ac-H3) and IgG control. Addition of SAHA curtails the recruitment of these complexes to the E-cadherin promoter, while acetylated histone levels increase at the E-cadherin promoter. Each ChIP experiment was repeated at least three times and a representative experiment is shown. **E**, Ectopically expressed EZH2 binds the E-cadherin promoter and leads to H3K27 trimethylation. ChIP was carried out in H16N2 cells infected with EZH2 or control adenovirus and assayed by PCR analysis. The upper panel shows that using Myc antibody, which is the epitope tag in the EZH2 constructs, myc-EZH2 is found to bind the E-cadherin promoter. The lower panel showed by qPCR that EZH2 and 3mH3K27 co-occupy the E-cadherin promoter in the EZH2-overexpressing H16N2 cells. Error bar: n = 3, mean \pm SEM. **F**, The E-cadherin promoter is trimethylated at histone H3K27 in metastatic prostate cancer tissues. ChIP experiments were performed using anti-3mH3K27 antibody in one localized prostate tumor and three independent metastatic prostate tumors. ChIP-enriched DNA and the input DNA were first amplified through ligation-mediated PCR. Equal amounts (50ng) of amplified ChIP DNA and the input DNA were then subjected to PCR, and enrichment by ChIP was assessed relative to the input DNA, then normalized to the level of GAPDH. Error bar: n = 3, mean \pm SEM. **G**, A model depicting the mechanism of EZH2 mediated E-cadherin repression. In benign cells the E-cadherin promoter is not occupied by PRC2 complex. In cancer, the increased expression of PRC2 leads to tight binding to the promoter of E-cadherin, followed by deacetylation of histone H3 and subsequent trimethylation of lysine 27. This leads to repression of E-cadherin expression. Addition of HDAC inhibitors prevents the first step of histone deacetylation, and hence the EZH2 complex cannot methylate histone H3.

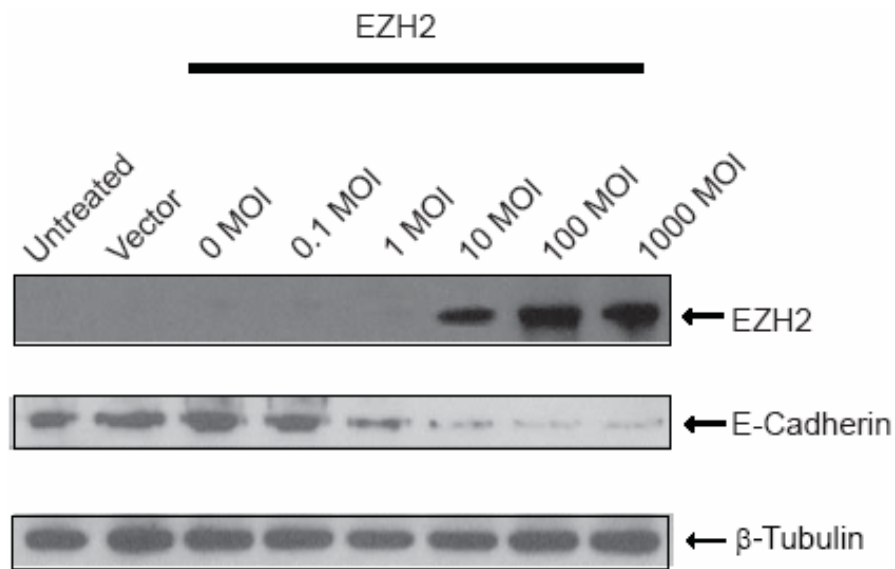


Figure 3S1. The repression of E-cadherin increases with EZH2 increases. Benign breast cell line H16N2 was infected with EZH2 by 0 MOI, 0.1 MOI, 1 MOI, 10 MOI, 100MOI or 1000MOI. EZH2 and E-cadherin level were examined by immunoblot. β -tubulin was included as a loading control.

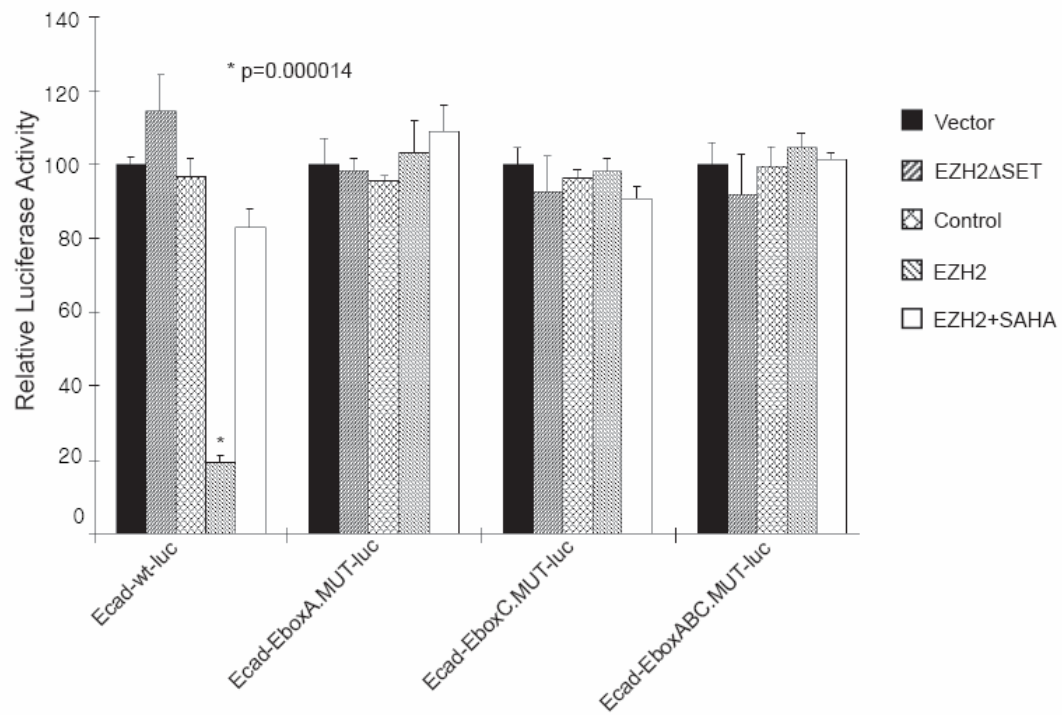


Figure 3S2. E-boxes of E-cadherin are necessary for EZH2 to repress E-cadherin promoter activity. Benign breast cell line HME was transfected with E-cadherin promoter luciferase construct wild-type or mutants and infected with either EZH2, EZH2ΔSET or control adenovirus. EZH2 infected cells were also incubated with SAHA. Relative luciferase activity (RLA) was assessed.

REFERENCES

1. Haybittle JL, Blamey RW, Elston CW, *et al.* A prognostic index in primary breast cancer. *British journal of cancer* 1982;45(3):361-6.
2. Rosen PP, Groshen S. Factors influencing survival and prognosis in early breast carcinoma (T1N0M0-T1N1M0). Assessment of 644 patients with median follow-up of 18 years. *Surg Clin North Am* 1990;70(4):937-62.
3. Damsky CH, Richa J, Solter D, Knudsen K, Buck CA. Identification and purification of a cell surface glycoprotein mediating intercellular adhesion in embryonic and adult tissue. *Cell* 1983;34(2):455-66.
4. Day ML, Zhao X, Vallorosi CJ, *et al.* E-cadherin mediates aggregation-dependent survival of prostate and mammary epithelial cells through the retinoblastoma cell cycle control pathway. *The Journal of biological chemistry* 1999;274(14):9656-64.
5. Pierceall WE, Woodard AS, Morrow JS, Rimm D, Fearon ER. Frequent alterations in E-cadherin and alpha- and beta-catenin expression in human breast cancer cell lines. *Oncogene* 1995;11(7):1319-26.
6. Frixen UH, Nagamine Y. Stimulation of urokinase-type plasminogen activator expression by blockage of E-cadherin-dependent cell-cell adhesion. *Cancer research* 1993;53(15):3618-23.
7. Frixen UH, Behrens J, Sachs M, *et al.* E-cadherin-mediated cell-cell adhesion prevents invasiveness of human carcinoma cells. *The Journal of cell biology* 1991;113(1):173-85.
8. Hirohashi S, Kanai Y. Cell adhesion system and human cancer morphogenesis. *Cancer Sci* 2003;94(7):575-81.
9. Wijnhoven BP, Dinjens WN, Pignatelli M. E-cadherin-catenin cell-cell adhesion complex and human cancer. *The British journal of surgery* 2000;87(8):992-1005.
10. Halbleib JM, Nelson WJ. Cadherins in development: cell adhesion, sorting, and tissue morphogenesis. *Genes & development* 2006;20(23):3199-214.
11. Oka H, Shiozaki H, Kobayashi K, *et al.* Expression of E-cadherin cell adhesion molecules in human breast cancer tissues and its relationship to metastasis. *Cancer research* 1993;53(7):1696-701.
12. Moll R, Mitze M, Frixen UH, Birchmeier W. Differential loss of E-cadherin expression in infiltrating ductal and lobular breast carcinomas. *The American journal of pathology* 1993;143(6):1731-42.
13. Wu ZY, Zhan WH, Li JH, *et al.* Expression of E-cadherin in gastric carcinoma and its correlation with lymph node micrometastasis. *World J Gastroenterol* 2005;11(20):3139-43.
14. Takeno S, Noguchi T, Fumoto S, Kimura Y, Shibata T, Kawahara K. E-cadherin expression in patients with esophageal squamous cell carcinoma: promoter hypermethylation, Snail overexpression, and clinicopathologic implications. *Am J Clin Pathol* 2004;122(1):78-84.
15. Saito T, Oda Y, Kawaguchi K, *et al.* E-cadherin mutation and Snail overexpression as alternative mechanisms of E-cadherin inactivation in synovial sarcoma. *Oncogene* 2004;23(53):8629-38.
16. Fujita Y, Krause G, Scheffner M, *et al.* Hakai, a c-Cbl-like protein, ubiquitinates and induces endocytosis of the E-cadherin complex. *Nat Cell Biol* 2002;4(3):222-31.

17. Batlle E, Sancho E, Franci C, *et al.* The transcription factor snail is a repressor of E-cadherin gene expression in epithelial tumour cells. *Nat Cell Biol* 2000;2(2):84-9.
18. Peinado H, Ballestar E, Esteller M, Cano A. Snail mediates E-cadherin repression by the recruitment of the Sin3A/histone deacetylase 1 (HDAC1)/HDAC2 complex. *Mol Cell Biol* 2004;24(1):306-19.
19. Hajra KM, Chen DY, Fearon ER. The SLUG zinc-finger protein represses E-cadherin in breast cancer. *Cancer research* 2002;62(6):1613-8.
20. Palacios F, Tushir JS, Fujita Y, D'Souza-Schorey C. Lysosomal targeting of E-cadherin: a unique mechanism for the down-regulation of cell-cell adhesion during epithelial to mesenchymal transitions. *Mol Cell Biol* 2005;25(1):389-402.
21. Koyanagi M, Baguet A, Martens J, Margueron R, Jenuwein T, Bix M. EZH2 and histone 3 trimethyl lysine 27 associated with Il4 and Il13 gene silencing in Th1 cells. *The Journal of biological chemistry* 2005;280(36):31470-7.
22. Chen H, Tu SW, Hsieh JT. Down-regulation of human DAB2IP gene expression mediated by polycomb Ezh2 complex and histone deacetylase in prostate cancer. *The Journal of biological chemistry* 2005;280(23):22437-44.
23. Yu J, Yu J, Rhodes DR, *et al.* A polycomb repression signature in metastatic prostate cancer predicts cancer outcome. *Cancer research* 2007;67(22):10657-63.
24. Satijn DP, Otte AP. Polycomb group protein complexes: do different complexes regulate distinct target genes? *Biochim Biophys Acta* 1999;1447(1):1-16.
25. Kirmizis A, Bartley SM, Kuzmichev A, *et al.* Silencing of human polycomb target genes is associated with methylation of histone H3 Lys 27. *Genes & development* 2004;18(13):1592-605.
26. Cao R, Wang L, Wang H, *et al.* Role of histone H3 lysine 27 methylation in Polycomb-group silencing. *Science (New York, NY)* 2002;298(5595):1039-43.
27. Plath K, Fang J, Mlynarczyk-Evans SK, *et al.* Role of histone H3 lysine 27 methylation in X inactivation. *Science (New York, NY)* 2003;300(5616):131-5.
28. Varambally S, Dhanasekaran SM, Zhou M, *et al.* The polycomb group protein EZH2 is involved in progression of prostate cancer. *Nature* 2002;419(6907):624-9.
29. Kleer CG, Cao Q, Varambally S, *et al.* EZH2 is a marker of aggressive breast cancer and promotes neoplastic transformation of breast epithelial cells. *Proceedings of the National Academy of Sciences of the United States of America* 2003;100(20):11606-11.
30. Breuer RH, Snijders PJ, Smit EF, *et al.* Increased expression of the EZH2 polycomb group gene in BMI-1-positive neoplastic cells during bronchial carcinogenesis. *Neoplasia (New York, NY)* 2004;6(6):736-43.
31. Bachmann IM, Halvorsen OJ, Collett K, *et al.* EZH2 expression is associated with high proliferation rate and aggressive tumor subgroups in cutaneous melanoma and cancers of the endometrium, prostate, and breast. *J Clin Oncol* 2006;24(2):268-73.
32. Weikert S, Christoph F, Kollermann J, *et al.* Expression levels of the EZH2 polycomb transcriptional repressor correlate with aggressiveness and invasive potential of bladder carcinomas. *International journal of molecular medicine* 2005;16(2):349-53.
33. Sudo T, Utsunomiya T, Mimori K, *et al.* Clinicopathological significance of EZH2 mRNA expression in patients with hepatocellular carcinoma. *British journal of cancer* 2005;92(9):1754-8.

34. Tan J, Yang X, Zhuang L, *et al.* Pharmacologic disruption of Polycomb-repressive complex 2-mediated gene repression selectively induces apoptosis in cancer cells. *Genes & development* 2007;21(9):1050-63.
35. Beke L, Nuytten M, Van Eynde A, Beullens M, Bollen M. The gene encoding the prostatic tumor suppressor PSP94 is a target for repression by the Polycomb group protein EZH2. *Oncogene* 2007;26(31):4590-5.
36. Jacobs JJ, van Lohuizen M. Polycomb repression: from cellular memory to cellular proliferation and cancer. *Biochim Biophys Acta* 2002;1602(2):151-61.
37. Jacobs JJ, van Lohuizen M. Cellular memory of transcriptional states by Polycomb-group proteins. *Semin Cell Dev Biol* 1999;10(2):227-35.
38. Sparmann A, van Lohuizen M. Polycomb silencers control cell fate, development and cancer. *Nat Rev Cancer* 2006;6(11):846-56.
39. Vire E, Brenner C, Deplus R, *et al.* The Polycomb group protein EZH2 directly controls DNA methylation. *Nature* 2006;439(7078):871-4.
40. Taghavi P, van Lohuizen M. Developmental biology: two paths to silence merge. *Nature* 2006;439(7078):794-5.
41. Schlesinger Y, Straussman R, Keshet I, *et al.* Polycomb-mediated methylation on Lys27 of histone H3 pre-marks genes for de novo methylation in cancer. *Nat Genet* 2007;39(2):232-6.
42. Widschwendter M, Fiegl H, Egle D, *et al.* Epigenetic stem cell signature in cancer. *Nat Genet* 2007;39(2):157-8.
43. Ohm JE, McGarvey KM, Yu X, *et al.* A stem cell-like chromatin pattern may predispose tumor suppressor genes to DNA hypermethylation and heritable silencing. *Nat Genet* 2007;39(2):237-42.
44. Boyer LA, Plath K, Zeitlinger J, *et al.* Polycomb complexes repress developmental regulators in murine embryonic stem cells. *Nature* 2006;441(7091):349-53.
45. Lee TI, Jenner RG, Boyer LA, *et al.* Control of developmental regulators by Polycomb in human embryonic stem cells. *Cell* 2006;125(2):301-13.
46. Bracken AP, Dietrich N, Pasini D, Hansen KH, Helin K. Genome-wide mapping of Polycomb target genes unravels their roles in cell fate transitions. *Genes & development* 2006;20(9):1123-36.
47. Tolhuis B, de Wit E, Muijters I, *et al.* Genome-wide profiling of PRC1 and PRC2 Polycomb chromatin binding in *Drosophila melanogaster*. *Nat Genet* 2006;38(6):694-9.
48. Vandesompele J, De Preter K, Pattyn F, *et al.* Accurate normalization of real-time quantitative RT-PCR data by geometric averaging of multiple internal control genes. *Genome Biol* 2002;3(7):RESEARCH0034.
49. Yu J, Cao Q, Mehra R, *et al.* Integrative genomics analysis reveals silencing of beta-adrenergic signaling by polycomb in prostate cancer. *Cancer cell* 2007;12(5):419-31.
50. Rhodes DR, Sanda MG, Otte AP, Chinnaiyan AM, Rubin MA. Multiplex biomarker approach for determining risk of prostate-specific antigen-defined recurrence of prostate cancer. *J Natl Cancer Inst* 2003;95(9):661-8.
51. Hajra KM, Ji X, Fearon ER. Extinction of E-cadherin expression in breast cancer via a dominant repression pathway acting on proximal promoter elements. *Oncogene* 1999;18(51):7274-9.

52. Umbas R, Isaacs WB, Bringuier PP, *et al.* Decreased E-cadherin expression is associated with poor prognosis in patients with prostate cancer. *Cancer research* 1994;54(14):3929-33.
53. Umbas R, Isaacs WB, Bringuier PP, Xue Y, Debruyne FM, Schalken JA. Relation between aberrant alpha-catenin expression and loss of E-cadherin function in prostate cancer. *International journal of cancer* 1997;74(4):374-7.
54. Mayer B, Johnson JP, Leitzl F, *et al.* E-cadherin expression in primary and metastatic gastric cancer: down-regulation correlates with cellular dedifferentiation and glandular disintegration. *Cancer research* 1993;53(7):1690-5.
55. Dorudi S, Hanby AM, Poulson R, Northover J, Hart IR. Level of expression of E-cadherin mRNA in colorectal cancer correlates with clinical outcome. *British journal of cancer* 1995;71(3):614-6.
56. Rasbridge SA, Gillett CE, Sampson SA, Walsh FS, Millis RR. Epithelial (E-) and placental (P-) cadherin cell adhesion molecule expression in breast carcinoma. *J Pathol* 1993;169(2):245-50.
57. Palacios J, Benito N, Pizarro A, *et al.* Relationship between ERBB2 and E-cadherin expression in human breast cancer. *Virchows Arch* 1995;427(3):259-63.

CHAPTER 4

A CAUSAL ROLE FOR MICRORNA-101 IN UPREGULATING EZH2 IN AGGRESSIVE TUMORS

Recent studies have shown that histone H3 lysine 27 trimethylation, which is mediated by EZH2 on the promoters of the EZH2 target genes, leads to silencing of gene expression(1). Our previously studies demonstrated that EZH2 is upregulated in aggressive prostate and breast tumors(2,3). Also multiple studies showed that EZH2 is overexpressed in other aggressive tumors, including bronchial cancer(4), melanoma(5), bladder cancer(6), liver cancer(7), as well as *in vitro* cancer cell lines(8) .

Functional studies have demonstrated that EZH2 is a bona fide oncogene. Knock-down of EZH2 protein by RNA interference results in growth arrest in prostate cancer cells (2), myeloma cells (9) as well as TIG3 fibroblasts(10). By contrast, ectopic overexpression of EZH2 promotes cell proliferation and invasion *in vitro* (3,10,11), and induces xenograft tumor growth *in vivo*(10). A wide varsity of studies revealed that the C-terminal SET domain which possesses the histone methyltransferase activity, is essential for EZH2 to perform its oncogenic functions, indicating that histone modification and epigenetic silencing play an important role during cancer progression. A recent study demonstrated that E2F6 complex contains EZH2 in proliferating cells, suggesting that this complex may be involved in regulating genes required for cell cycle

control(12). Several mechanisms have been proposed to illuminate the regulation of EZH2, including the pRB-E2F pathway and amplification(13), as well as repression by tumor suppressor p53(14). However there is no clear cut mechanism that has been implicated in overexpression of EZH2 in tumors. We here investigated the possibility of EZH2 regulation by microRNAs.

MicroRNAs are a type of regulatory, non-coding, endogenous RNAs that have recently gained considerable attention and have been implicated in regulating diverse cellular processes. MicroRNAs are 18-24 nucleotides in length and are proposed to regulate gene expression through translational repression by binding to the 3'-UTR (untranslated region) of target mRNAs(15). They are also proposed to regulate gene expression by mRNA cleavage, and mRNA decay initiated by miRNA-guided rapid deadenylation (16). miRNAs are abundant, highly conserved molecules and predicted to regulate a large number of transcripts. To date the international miRNA Registry database (<http://microrna.sanger.ac.uk>) has more than 800 human identified microRNAs(17) and their total number in humans has been predicted to be as high as 1,000(18). A large number of microRNAs exhibit tissue-specific expression(19) and defined to be either tumor suppressors or oncogenes (20,21), playing a crucial role in variety of cellular processes such as cell cycle control, apoptosis, haematopoiesis as well as the dysregulation of several miRNAs are demonstrated to play a significant role in human disease processes including tumorigenesis(22). Several microRNAs are located in the region of hot spots for chromosomal abnormalities^{23,24}. This results in abnormal expression of miRNAs which affect cellular functions.

Recent studies indicate that multiple miRNAs may play a role in human cancer pathogenesis. For example, deletions or mutations in genes that encode miRNA tumor suppressors might lead to loss of a miRNA or miRNA cluster, and thereby contribute to oncogene deregulation (21,25). Large-scale miRNA profilings of normal and cancer tissues suggest that a number of microRNAs are either overexpressed or downregulated in tumors (26,27). It has been shown that miRNA genes are frequently located in cancer-associated genomic regions or fragile sites(24). The genes encoding mir-15 and mir-16 are located at chromosome 13q14, a region that is deleted in the majority of B-cell chronic lymphocytic leukemias (B-CLL) suggesting that mir-15 and mir-16 may possibly function as tumor suppressors. let-7 miRNA family members are known to down regulate the oncogene RAS(28). Its expression is reduced in tumors which in turn contributes to the elevated activity of the RAS pathway(27). Expression levels of miR-143 and miR-145 were decreased in colon cancer tissues as well as in cancer cell lines(29). In contrast, several microRNAs are upregulated in cancer which may function as oncogenes. Members of the miR-17 cluster provide an oncogenic function via their upregulated expression by c-Myc leading to effects on downstream genes which are mediators of cell cycle and apoptosis events(30). Many microRNAs play a role during development and tissue differentiation(31). miR-181, a microRNA that is strongly upregulated during differentiation, participates in establishing the muscle phenotype. Recent studies demonstrated that miR-181 down regulates the homeobox protein Hox-A11(32). Similarly miR-196 is involved in regulating HOXB8(33), confirming the significant roles played by microRNA during developmental processes. Furthermore, it has been shown recently that microRNA 10b is involved in breast cancer

metastasis(34) . Huang et al by using genetic screen using a nonmetastatic, human breast tumour cell line that was transduced with a miRNA-expression library found that miR-373 and miR-520c promote tumor invasion and metastasis(35).

Interestingly a recent study from Lim et al., (36) showed that a few microRNAs can regulate large number of target mRNA and their studies also indicated that the miRNA can downregulate not only the proteins, but the transcript level of the target mRNA. In this present study we explored the possible by which microRNAs dysregulate EZH2 expression. Here we identified a role of miR101 in regulating EZH2 expression in tumors as well as implicate a deletion or loss of heterozygosity in miR101 genomic localization as the cause for EZH2 upregulation.

Results and Discussion

microRNA 101 targets EZH2. Our previous studies demonstrated that EZH2 expression is increased in aggressive prostate and breast cancer. Several other studies later reported overexpression of EZH2 in several aggressive cancers. However the mechanism by which EZH2 is dysregulated during cancer progression is not clearly understood. In order to search for possible microRNAs that targets EZH2, we utilized four target prediction databases- PicTar, Microinspector, miRanda and TargetScan (**Fig 4.1a**). Mir101 and miR217 were recognized as top two which target to EZH2 in all the target prediction sites (**Fig 4.1b**). Bioinformatical analysis indicated that hsa-miR101 has two binding sites on EZH2 3'UTR region of EZH2 (**Fig 4.1c**). To examine whether hsa-miR101 could interact with the 3'UTR of EZH2, we generated luciferase reporters with 3'UTR or complementary 3'UTR of EZH2. We observed that overexpression of hsa-

miR-101 but not the control microRNA (hsa-miR-16) decreased activity of luciferase with 3'UTR of EZH2 (**Fig. 4.1d**), while the activity of luciferase with complementary 3'UTR of EZH2 was not altered by hsa-miR-101. This indicates that hsa-miR-101 indeed binds to 3'UTR of EZH2 and represses EZH2 expression.

microRNA101 downregulates both EZH2 transcript and protein. Since hsa-miR-101 could interact with 3'UTR of EZH2, we examined if the EZH2 transcript and protein levels can be repressed by miR101 overexpression. As shown in **figure 4.2a**, precursor of miR101 but not control microRNAs reduces the EZH2 transcripts. Similarly, immunoblot analysis using EZH2 specific antibody demonstrated that miR101 downregulates EZH2 protein expression in prostate cell line DU145 as well as breast cell line SKBr3 which have high endogenous EZH2 expression (**Fig 4.2b**). Interestingly, another predicted target of hsa-miR-101, N-Myc was not repressed by hsa-miR-101 overexpression (**Fig 4.2c**), indicating that miR101 might specifically downregulates EZH2. Importantly, similar to the effect of siRNA against EZH2, the other polycomb group members EED and SUZ12 expression were significantly decreased because of hsa-miR-101 overexpression in SKBr3 and DU145 (**Fig 4.2d**), suggesting hsa-miR-101 downregulates not only EZH2 but also the other members of PRC2. Furthermore, when low endogenous EZH2 expression breast cell line HME was treated with anti-miR-101, EZH2 expression was upregulated, confirming that hsa-miR-101 indeed regulates EZH2 expression(**Fig 4.2e**). Additionally, when the non-invasive HME cells were treated with anti-miR-101, the cells become invasive (**Fig 4.2f**) suggesting the activity of EZH2 is increased.

microRNA101 reduces cell growth, invasion and tumor formation. Our earlier studies have shown that down regulating the EZH2 expression by RNA interference results in reduced cell growth as well decreases invasion, we hypothesized that hsa-miR-101 will induce similar phenotype. In hsa-miR-101 overexpressed SKBr3 cells, E-cadherin (and other EZH2 targets) expression is increased (**Fig 4.3a**). Similar to the effect of siRNA against EZH2, overexpression of hsa-miR-101 reduced the cell growth (**Fig 4.3b**) to an extent similar to siRNA against EZH2. Furthermore, overexpression of hsa-miR-101 or siRNA against EZH2 in highly invasive cell line SKBr3 significantly decreased the invasive potential of cells, suggesting function of EZH2 is inhibited by hsa-miR-101 (**Fig 4.3c**).

To address the role of hsa-miR-101 in tumor formation, we generated DU145 cells which stably express hsa-miR-101, and injected it or control cells into nude mice. The vector control stable DU145 formed tumors whose size increased dramatically (**Fig 4.3d**). However, DU145 stably expressing hsa-miR-101 formed the tumors slowly and the size of tumors was much smaller compared to vector control. This finding suggests that hsa-miR-101 plays an important role in tumor formation through the regulation of EZH2. In order to test if hsa-miR-101 could de-repress the targets of EZH2, we performed chromatin immunoprecipitation analysis. When hsa-miR-101 was overexpressed, the binding of EZH2 to the promoters of WNT1 and CNR1, which are known as the targets of EZH2, was reduced significantly compared to the binding to a non specific control, Actin (**Fig 4.3e**). Since EZH2 knockdown by siRNA and hsa-miR-101 have similar functional and phenotypic effects, we hypothesized that the global gene

expression regulation by both treatment will have significant overlap. In order to test this, we performed gene expression analysis by cDNA microarray from the cell lines treated with siRNA against EZH2 or hsa-miR-101. As shown in **Fig 4.3f**, there was a significant overlap between the genes dysregulated by hsa-miR-101 and siRNA against EZH2.

miR101 has the opposite expression pattern to that of EZH2 in tumors and show deletion or loss of heterozygosity. In order to test the expression of hsa-miR-101 in tumors, we utilized total RNA from the normal, prostate tumor and metastatic prostate tissues to perform qRT-PCR. EZH2 and hsa-miR-217 expression in corresponding tissues were also examined. While hsa-miR-101 expression is decreased from normal to tumor tissue with lowest expression in metastatic tissue, the EZH2 expression showed opposite pattern (**Fig 4.4a**) indicating supporting our hypothesis that miR101 indeed regulates the EZH2 expression in tissues. However, hsa-miR-217 did not show significant alteration in expression between normal and cancer tissue. Furthermore, to test the mechanism by which hsa-miR-101 expression is dysregulated and consequently leads to upregulation of EZH2, we performed genomic DNA relative quantitation of miR101 locus. The result indicates that most of tissues with high EZH2 overexpression show a deletion or copy loss of hsa-miR-101 chromosome location (**Fig 4.4b**), suggesting a novel mechanism by which EZH2 is dysregulated in metastatic cancers.

Thus, our data suggests a novel mechanism by which hsa-miR-101 represses the expression of histone methyltransferase EZH2. In normal tissues, hsa-miR-101 chromosome location is intact, and EZH2 expression is too low to detect. However, once the chromosome location of hsa-miR-101 is mutated or deleted, the decrease of

hsa-miR-101 expression will result in upregulating EZH2 expression and promote cell invasion and tumorigenesis.

Materials and method

Luciferase Assay. The 3'-UTR or complementary sequence of 3'-UTR of EZH2 were cloned into pMIR-REPORT™ miRNA Expression Reporter Vector (Ambion).

SKBr3 cells were pre-transfected with pre-hsa-miR-101 or controls and then co-transfected with 3'-UTR-luc or complementary 3'-UTR-luc, as well as pRL-TK vector as internal control for luciferase activity. Post 48 hours of incubation, the cells were lysed and luciferase assays conducted using the dual luciferase assay system (Promega, Madison, WI). Each experiment was performed in triplicate.

Small RNA interference and microRNA transfection. The knockdown of EZH2 was accomplished with siRNA duplex (Dharmacon, Lafayette, CO) as previously described (2). Precursors of microRNA and negative control were purchased from Ambion (Austin, TX). Antagomir-101 and negative control were purchased from Dharmacon. Transfection were performed with oligofectamine (Invitrogen, Carlsbad, CA) or lipofectamine (Invitrogen).

SYBR Green Quantitative Real-Time PCR. Total RNA was isolated from SKBr3 and DU145 cells that were transfected either with pre-hsa-miR-101, or control precursors (Qiagen). Quantitative PCR (QPCR) was performed using SYBR Green dye on an Applied Biosystems 7300 Real Time PCR system (Applied Biosystems, Foster City, CA). Briefly, 1 µg of total RNA was reverse transcribed into cDNA using SuperScript III (Invitrogen, Carlsbad, CA) in the presence of random hexamers and oligo

dT primers (Invitrogen). All reactions were performed in duplicate with SYBR Green Master Mix (Applied Biosystems) plus 25 ng of both the forward and reverse primer according to the manufacturer's recommended thermocycling conditions, then subjected to melt curve analysis. Threshold levels for each experiment were set during the exponential phase of the QPCR reaction using Sequence Detection Software version 1.2.2 (Applied Biosystems). The DNA in each sample was quantified by interpolation of its threshold cycle (C_t) value from a standard curve of C_t values, which were created from a serially diluted cDNA mixture of all samples. The calculated quantity of the target gene for each sample was divided by the average sample quantity of the housekeeping genes, glyceraldehyde-3-phosphate dehydrogenase (*GAPDH*) to obtain the relative gene expression. All oligonucleotide primers were synthesized by Integrated DNA Technologies (Coralville, IA).

Immunoblot Analyses. The breast cancer cell lines SKBr3 and prostate cancer cell DU145 were transfected with pre-hsa-miR-101 or controls. The breast cell lines H16N2 and HME, as well as normal prostate epithelial cells PrEC were transfected with antagomiR-101 or negative controls. Post 72 hours transfection, cells were homogenized in NP40 lysis buffer (50 mM Tris-HCl, 1% NP40, pH 7.4, Sigma, St. Louis, MO), and complete proteinase inhibitor mixture (Roche, Indianapolis, IN). Ten micrograms of each protein extract were boiled in sample buffer, separated by SDS-PAGE, and transferred onto Polyvinylidene Difluoride membrane (GE Healthcare). The membrane was incubated for one hour in blocking buffer [Tris-buffered saline, 0.1% Tween (TBS-T), 5% nonfat dry milk] and incubated overnight at 4°C with the following: anti-EZH2 mouse monoclonal (1:1000, 1:5000 in dilution buffer, BD Biosciences, San

Jose, CA), anti-EED rabbit polyclonal (1:1000 in dilution buffer, Upstate, Charlottesville, VA), anti-SUZ12 rabbit polyclonal (1:1000 in dilution buffer, Upstate, Charlottesville, VA), and anti-N-myc rabbit polyclonal antibodies (1:1000 in dilution buffer, Santa Cruz). Following a wash with TBS-T, the blot was incubated with horseradish peroxidase-conjugated secondary antibody and the signals visualized by enhanced chemiluminescence system as described by the manufacturer (GE Healthcare). The blot was re-probed with β -tubulin for confirmation of equal loading.

Basement Membrane Matrix Invasion Assay. For invasion assays, the breast cell lines H16N2 and HME, as well as normal prostate epithelial cells (PrEC, Cambrex, East Rutherford, NJ), were transfected with antagomiR-101 or negative controls. Invasive breast cancer cell SKBr3 and prostate cancer cell DU145 were transfected with pre-hsa-miR-101 or controls. Forty-eight hours post-transfection, cells were seeded onto the basement membrane matrix (EC matrix, Chemicon, Temecula, CA) present in the insert of a 24 well culture plate. Fetal bovine serum was added to the lower chamber as a chemoattractant. After 48 hours, the non-invading cells and EC matrix were gently removed with a cotton swab. Invasive cells located on the lower side of the chamber were stained with crystal violet, air dried and photographed. They were then enumerated microscopically using multiple representative areas. For colorimetric assays, the inserts were treated with 150 μ l of 10% acetic acid and the absorbance measured at 560nm using a spectrophotometer (GE Healthcare Bio-Sciences Corp, Piscataway, NJ).

Cell Counting. Cells were plated to 24-well plates at desire cell concentration. After cells attach to the bottom, transfect cells with precursor microRNA or controls. At the measure time, wash the cells with PBS once and add 400ul 1X 0.05%Trypsin-EDTA,

incubate then aspirate to single cells. Add 200ul to 9.8ml Isotone, use the Z2 coulter counter to count cells. The final reading 1000 means 100,000 cells

Chromatin immunoprecipitation (ChIP) Assay. ChIP experiments were carried out as described by Yu, et al.(49). For each ChIP assay, 5ug of antibodies were used; EZH2 (BD Biosciences), trimethyl H3-Lys27 (Upstate), or IgG control (Santa Cruz). Approximately 2-5 ul of ChIP-enriched chromatin were subjected to a standard ChIP-PCR reaction, and the enrichment of specific genomic regions was assessed relative to either control IgG or control cells. Each ChIP experiment was repeated at least three times. For ChIP with human tissues, ChIP-enriched DNA and input DNA were amplified through ligation-mediated PCR. Equal amounts (50ng) of amplified ChIP DNA and input DNA were subjected to PCR. Enrichment by ChIP was assessed relative to the input DNA and normalized to the level of Actin.

Expression Profiling. Expression profiling was performed using the Agilent Whole Human Genome Oligo Microarray (Santa Clara, CA) according to the manufacturer's protocol. SKBr3 and DU145 cells were transfected with pre-hsa-miR-101 or negative control for precursor microRNA. Over- and under-expressed signatures were generated by filtering to include only features with significant differential expression (Log ratio, $P < .01$) in all hybridizations and two-fold average over- or under-expression (Log ratio) after correction for the dye flip.

Murine Prostate Tumor Xenograft Model. All procedures involving mice were approved by the University Committee on Use and Care of Animals (UCUCA) at the University of Michigan and conform to their relevant regulatory standards. Five-week-old male nude athymic BALB/c nu/nu mice (Charles River Laboratory,

Wilmington, MA) were used for examining the tumorigenicity. To evaluate the role of miR-101 overexpression in tumor formation, the stable miR-101 overexpression DU145 cells or the vector control cells were propagated and inoculated by subcutaneous injection into the dorsal flank of ten mice (n = 5 per group). Tumor size was measured every week, and tumor volumes were estimated using the formula $(\pi/6) (L \times W^2)$, where L = length of tumor and W = width.

qRT-PCR for miRNA for cell lines and tissue samples. Total RNA with small RNA was isolated from SKBr3 and DU145 cells that were transfected either with pre-hsa-miR-101, or control precursors. Dilute total RNA at 10ng/ul. For RT, make master mix of 0.15ul 100mM dNTPs, 1.00ul MultiScribe Reverse Transcriptase (50U/ul), 1.50 10X Reverse Transcription Buffer, 0.188ul RNase Inhibitor (20U/ul) and 4.192ul Nuclease-free water. For each 15ul RT reaction, add 7ul of master mix, 5ul of RNA samples (10ng/ul) and 3ul 5X specific RT primer. Leaving the thermal cycler in the 9600 Emulation mode, program the thermal cycler as follows: 16°C for 30 minutes, 42°C for 30 minutes and 85°C for 5 minutes. For each 20ul PCR reaction, mix Taqman 10ul 2X Universal PCR Master Mix (No AmpErase UNG), 6.67ul Nuclease-free water, 1ul 20X specific PCR primer and 1.33ul RT product. Leaving the thermal cycler in the 9600 Emulation mode, program the thermal cycler as follows: 95°C for 10 minutes, 40 cycles of 95°C for 15seconds and 60°C for 60seconds. Using the comparative CT method, we use endogenous control (RNU6B) to normalize the expression levels of target micro-RNA by correcting differences in the amount of RNA loaded into qPCR reactions.

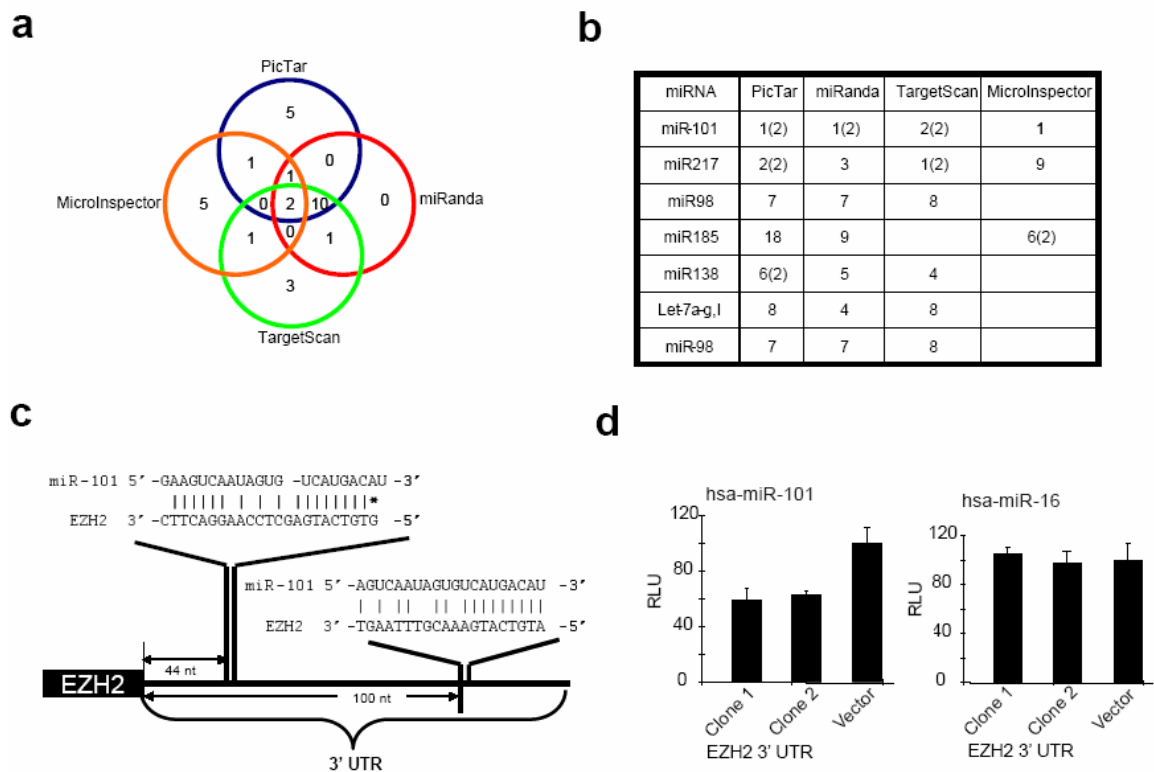


Figure 4.1. EZH2 is a target of hsa-miR-101. **a.** 4-way Venn diagram displaying miRNAs computationally predicted to target EZH2 by PicTar (blue), miRanda (red), TargetScan (green), and MicroInspector (orange). **b.** Ranking of binding sites that were predicted by three or more programs displayed relative to the score calculated by each respective program. The number in parenthesis represents miRNAs with multiple binding sites. **c.** Schematic of two predicted hsa-miR-101 binding sites in the EZH2 3' UTR. **d.** Luciferase activity assay of EZH2 3' UTR-luc constructs in the presence of hsa-miR-101 and hsa-miR-16 relative to a control vector.

Figure 4.2. hsa-miR-101 regulates EZH2 transcript and protein expression. **a.** hsa-miR-101 overexpression represses EZH2 mRNA expression in SKBr3 cells, while negative controls and unrelated microRNAs (hsa-miR-26a, hsa-miR-128a, and hsa-miR-16) did not inhibit EZH2 expression. **b.** Immunoblot analysis reveals downregulation of EZH2 protein in DU145 and SKBr3 cell lines by overexpression of hsa-miR-101, but not in hsa-miR-217 treated cells and negative controls. **c.** hsa-miR-101 downregulates specifically EZH2 but not the other predicted target N-myc in SKBr3 cells. Several other unrelated precursor miRNAs (hsa-miR-26a, hsa-miR-128a, hsa-miR-16 and hsa-miR-495) do not repress EZH2. **d.** Both EZH2 RNAi and hsa-miR-101 down regulate the PRC2 complex members EZH2, EED and SUZ12 in comparison hsa-miR-217, a control siRNA, and negative pre-miRNA control. **e.** HME cells with low EZH2 expression are treated with antagomir-101 or negative control. Antagomir-101 treated cells show clear up regulation of EZH2 protein. **f.** Antagomir-101 increases cell invasion. Non-invasive HME cells treated with antagomir-101 attain invasive property. The negative control did not alter the non-invasive cell phenotype.

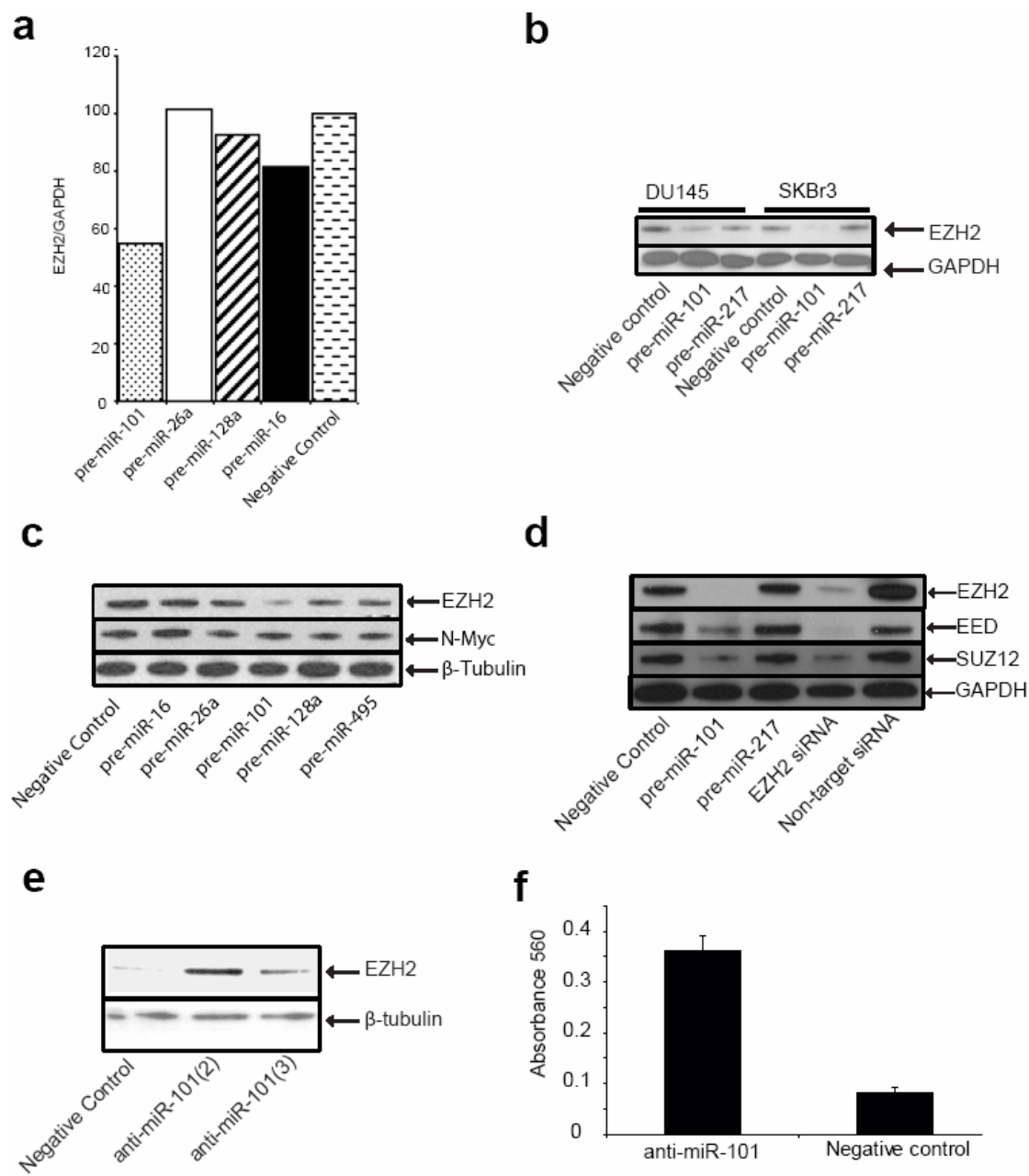
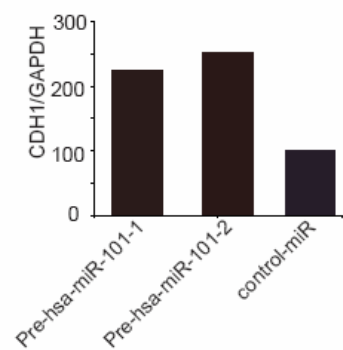
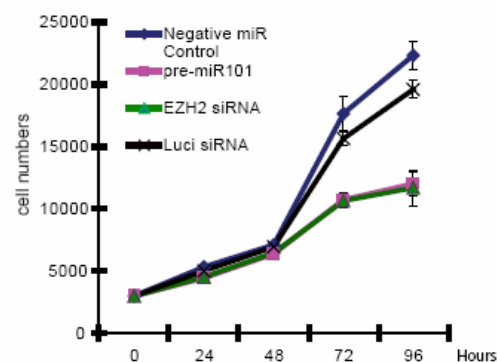
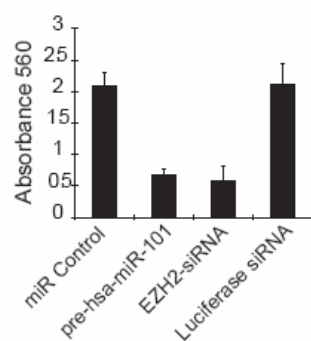
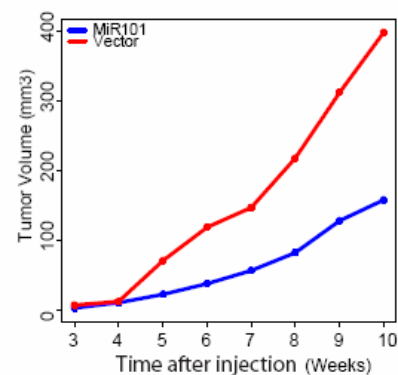
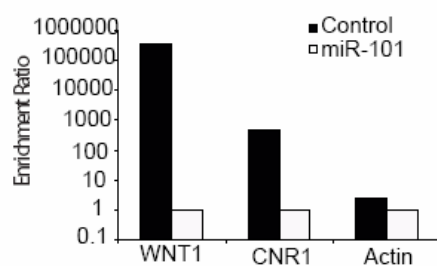
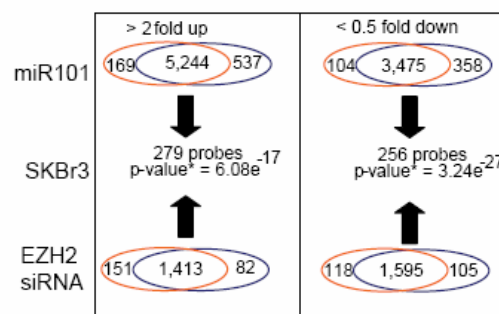


Figure 4.3. hsa-miR-101 inhibits cell growth, and invasion and tumor growth. **a.** Overexpression of hsa-miR-101 results in upregulating genes which is repressed by EZH2. **b.** hsa-miR-101 (purple) or siRNA targeting EZH2 (green) inhibit cell growth relative to the control miRNA (blue) and luciferase siRNA duplex (black). **c.** hsa-miR-101 or EZH2-siRNA inhibits the invasive phenotype of the breast and prostate cell lines SKBr3. Negative control miRNA and luciferase siRNA duplexes were used as controls. **d.** Tumor growth curves of Du145 stably overexpressing hsa-miR-101 or control vector. Data points represent mean tumor volume for five samples infected with vector (red) or miR-101 (blue) at the indicated time points. **e.** Chromatin immunoprecipitation assay by anti-H3K27-me3 demonstrates that hsa-miR-101 decreases the binding between EZH2 and the promoters of its targets, WNT1 and CNR1. Actin is used as a negative control. **f.** Microarray analysis shows that there is a significant overlap, via Fisher's exact test, between SKBr3 cells treated with miR-101 and SKBr3 cells treated with EZH2 siRNA regulated genes. The Venn diagram represents the level of overlap for up- and down-regulated probes in each biological replicates for each experiment. Only those probes that demonstrated altered expression in both biological replicates were compared across experiments.

a**b****c****d****e****f**

*Using Fisher's exact test, which assumes a hypergeometric distribution under H₀

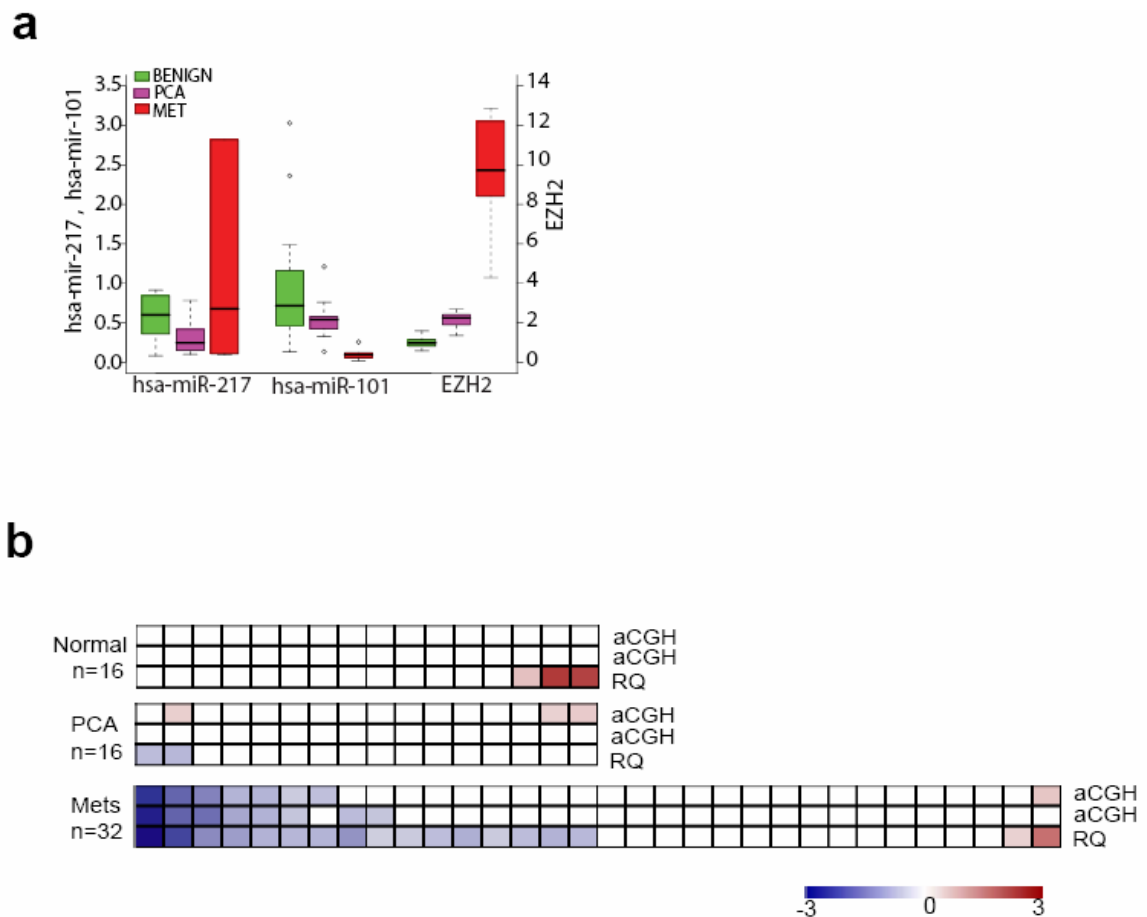


Figure 4.4. Genomic aberration in cancer leads to the down regulation of miR-101.
a. Box plot showing qPCR data for hsa-miR-101, hsa-miR-217 and EZH2 expression in benign, prostate cancer (PCA), and metastatic (MET) tumor tissue RNA. **b.** Heatmap of amplification or deletion of mir-101 from aCGH and genomic DNA qPCR. For normal, prostate cancer, and metastatic cohorts, there are two rows for the upstream and downstream aCGH probe and one row representing the relative quantity (RQ) from genomic DNA qPCR. Each column is a different patient sample. A value greater than 0.5 represents and amplification (red) whereas a value < -0.5 represents a deletion (blue). Both platforms are congruent in detecting a copy number change in advanced stages of prostate cancer.

REFERENCES

- 1 M. Koyanagi, A. Baguet, J. Martens et al., *The Journal of biological chemistry* 280 (36), 31470 (2005);
- 2 S. Varambally, S. M. Dhanasekaran, M. Zhou et al., *Nature* 419 (6907), 624 (2002).
- 3 C. G. Kleer, Q. Cao, S. Varambally et al., *Proc Natl Acad Sci U S A* 100 (20), 11606 (2003).
- 4 R. H. Breuer, P. J. Snijders, E. F. Smit et al., *Neoplasia* 6 (6), 736 (2004).
- 5 I. M. Bachmann, O. J. Halvorsen, K. Collett et al., *J Clin Oncol* 24 (2), 268 (2006).
- 6 S. Weikert, F. Christoph, J. Kollermann et al., *International journal of molecular medicine* 16 (2), 349 (2005).
- 7 T. Sudo, T. Utsunomiya, K. Mimori et al., *Br J Cancer* 92 (9), 1754 (2005).
- 8 L. Beke, M. Nuytten, A. Van Eynde et al., *Oncogene* 26 (31), 4590 (2007).
- 9 P. A. Croonquist and B. Van Ness, *Oncogene* 24 (41), 6269 (2005).
- 10 A. P. Bracken, D. Pasini, M. Capra et al., *EMBO J* 22 (20), 5323 (2003).
- 11 S. Varambally, S. M. Dhanasekaran, M. Zhou et al., *Nature* 419 (6907), 624 (2002).
- 12 C. Attwooll, S. Oddi, P. Cartwright et al., *The Journal of biological chemistry* 280 (2), 1199 (2005).
- 13 A. P. Bracken, D. Pasini, M. Capra et al., *The EMBO journal* 22 (20), 5323 (2003).
- 14 X. Tang, M. Milyavsky, I. Shats et al., *Oncogene* 23 (34), 5759 (2004).
- 15 L. P. Lim, M. E. Glasner, S. Yekta et al., *Science* 299 (5612), 1540 (2003);
- 16 L. Wu, J. Fan, and J. G. Belasco, *Proc Natl Acad Sci U S A* 103 (11), 4034 (2006).
- 17 S. Griffiths-Jones, H. K. Saini, S. van Dongen et al., *Nucleic acids research* 36 (Database issue), D154 (2008).
- 18 E. Berezhikov, V. Guryev, J. van de Belt et al., *Cell* 120 (1), 21 (2005).
- 19 P. Sood, A. Krek, M. Zavolan et al., *Proc Natl Acad Sci U S A* 103 (8), 2746 (2006).
- 20 Y. S. Lee and A. Dutta, *Curr Opin Investig Drugs* 7 (6), 560 (2006);
- 21 B. Zhang, X. Pan, G. P. Cobb et al., *Dev Biol* (2006).
- 22 H. W. Hwang and J. T. Mendell, *Br J Cancer* 94 (6), 776 (2006); J. M. Thomson, M. Newman, J. S. Parker et al., *Genes Dev* 20 (16), 2202 (2006).
- 23 G. A. Calin and C. M. Croce, *Oncogene* 25 (46), 6202 (2006).
- 24 G. A. Calin, C. Sevignani, C. D. Dumitru et al., *Proc Natl Acad Sci U S A* 101 (9), 2999 (2004).
- 25 G. A. Calin, C. D. Dumitru, M. Shimizu et al., *Proc Natl Acad Sci U S A* 99 (24), 15524 (2002).
- 26 I. Alvarez-Garcia and E. A. Miska, *Development* 132 (21), 4653 (2005);
- 27 N. Yanaihara, N. Caplen, E. Bowman et al., *Cancer Cell* 9 (3), 189 (2006).

28 S. M. Johnson, H. Grosshans, J. Shingara et al., *Cell* 120 (5), 635 (2005).
 29 M. Z. Michael, O' Connor SM, N. G. van Holst Pellekaan et al., *Mol Cancer Res*
 1 (12), 882 (2003).
 30 K. A. O'Donnell, E. A. Wentzel, K. I. Zeller et al., *Nature* 435 (7043), 839 (2005).
 31 A. E. Pasquinelli, S. Hunter, and J. Bracht, *Curr Opin Genet Dev* 15 (2), 200
 (2005).
 32 I. Naguibneva, M. Ameyar-Zazoua, A. Polesskaya et al., *Nat Cell Biol* 8 (3), 278
 (2006).
 33 S. Yekta, I. H. Shih, and D. P. Bartel, *Science* 304 (5670), 594 (2004).
 34 L. Ma, J. Teruya-Feldstein, and R. A. Weinberg, *Nature* 449 (7163), 682 (2007).
 35 Q. Huang, K. Gumireddy, M. Schrier et al., *Nature cell biology* 10 (2), 202 (2008).
 36 L. P. Lim, N. C. Lau, P. Garrett-Engle et al., *Nature* 433 (7027), 769 (2005).
 37 R. Umbas, W. B. Isaacs, P. P. Bringuier et al., *Cancer Res* 54 (14), 3929 (1994);
 38 B. Mayer, J. P. Johnson, F. Leidl et al., *Cancer Res* 53 (7), 1690 (1993).
 39 S. Dorudi, A. M. Hanby, R. Poulson et al., *Br J Cancer* 71 (3), 614 (1995).
 40 S. A. Rasbridge, C. E. Gillett, S. A. Sampson et al., *J Pathol* 169 (2), 245 (1993);

CHAPTER 5

CONCLUSION

Through cDNA microarray gene expression profiling of prostate cancer specimens, our previous study showed that EZH2 is associated with metastatic prostate cancer. In metastatic prostate cancer, EZH2 is upregulated at both the transcript and protein levels. By cDNA microarray profiling of samples with EZH2 overexpression or knock-down, we demonstrated that EZH2 is a transcriptional repressor which represses expression of many tumor suppressors. HDAC activity is required for EZH2 to perform its function since the HDAC inhibitor TSA could block EZH2 mediated gene repression. Furthermore, we demonstrated that EZH2 is essential for cell proliferation. Another study from our group identified that there is an inverse correlation between EZH2 and a tumor suppressor E-cadherin in prostate cancer. We found that in EZH2 negative prostate samples, E-cadherin expression is high; but in EZH2 positive prostate samples, E-cadherin expression is repressed.

In this study, we extended our previous observation in prostate cancer to breast cancer, because both prostate and breast cancers are hormone regulated. Here we showed for the first time that EZH2 is a biomarker of aggressive breast cancer. By quantitative real time PCR and western, we demonstrated that, similar to prostate cancer, EZH2 is

upregulated in invasive and metastatic breast cancer at both the transcript and protein levels. By tissue microarray (TMA), we showed that EZH2 is mainly expressed in nuclei with invasive and metastatic breast carcinomas staining strongly. High EZH2 levels were strongly associated with poor clinical outcome in breast cancer patients. A shorter disease-free interval after initial surgical treatment, lower overall survival, and a high probability of disease-specific death were overserved. Kaplan–Meier analysis showed that EZH2 levels were strongly associated with outcome in both ER-positive and -negative invasive carcinomas suggesting that EZH2 has prognostic utility independent of ER status.

To study the role of EZH2 in breast cancer, we generated adenovirus expressing wild-type EZH2 or a dominant negative mutant, EZH2 Δ SET. Overexpression of EZH2 promotes anchorage-independent growth in the breast epithelial cell line H16N2 which has low endogenous levels of this protein. Furthermore, by three different *in vitro* or *in vivo* invasion assays, we demonstrated that wild-type EZH2 could increase the invasive potential of breast epithelial cells, while the dominant negative mutant, EZH2 Δ SET could not. Importantly EZH2 overexpression could increase HDAC enzymatic activity, and the HDAC inhibitors TSA or SAHA could attenuate EZH2 mediated cell invasion.

In order to illuminate the mechanism by which EZH2 mediates cell invasion and cancer progression, we performed cDNA microarray profiling and ChIP-on-chip analyses with samples of EZH2 overexpression. Interestingly, among the genes repressed by EZH2, several tumor suppressors, including E-cadherin and ADRB2 showed up as the targets since they are well-known cell adhesion proteins involved in multiple pathways related to cancer progression. In this study, we identified an inverse correlation between

EZH2 and E-cadherin in breast cancer tissues and cell lines similar to our observations in prostate cancer. Also, we demonstrated that overexpression of EZH2 significantly represses E-cadherin expression by qPCR, Northern blot and immunoblot analysis. Co-expression of E-cadherin to some extent inhibits the invasion induced by EZH2. Interestingly, the dominant negative mutant of EZH2, EZH2 Δ SET could inhibit invasion of cancer cell lines. Knock-down of EZH2 by siRNA or shRNA also inhibits invasion of cancer cell lines. Most importantly, the cancer cell lines in which EZH2 is stably knock-down by shRNA were unable to form tumors in nude mice, indicating that EZH2 plays an essential role in tumorigenesis.

Next, in this study we identified dysregulation of microRNAs as a possible mechanism of EZH2 upregulation in aggressive breast and prostate cancers. Among the possible microRNAs which are predicted to regulate EZH2 by bioinformatics analysis, we showed that only hsa-miR-101 can down-regulate EZH2. In cancer cell lines with low endogenous levels of hsa-miR-101 and high EZH2, transfection of the microRNA markedly repressed EZH2 protein and mRNA levels. Notably, by cDNA microarray expression profiling, we showed that there is a significant overlap between genes dysregulated by EZH2 siRNA and genes dysregulated by hsa-miR-101 overexpression, indicating that hsa-miR-101 may perform a function like siRNA against EZH2 *in vivo* to repress EZH2 expression. Furthermore, cancer cell lines stably transfected with pre-hsa-miR-101 or shRNA against EZH2 form smaller tumors or no tumors in mice relative to control cells, suggesting that hsa-miR-101 could be a potentially promising target for cancer therapy.

Most importantly, many microRNA profiling studies demonstrated that hsa-miR-101 is down-regulated in prostate, breast, lung and other cancers. In our prostate cancer samples, we showed that there is an inverse correlation between hsa-miR-101 and EZH2. By array CGH (comprehensive genomic hybridization) and genomic DNA qPCR, we demonstrated that in metastatic prostate and breast cancers, about 30-50% of samples which had high EZH2 expression showed deletion or LOH in the genomic region of hsa-miR-101-1. This finding provides a mechanism for how EZH2 is upregulated during cancer progression.

Taken together, this study showed that EZH2 is a prognostic biomarker of aggressive breast cancer and plays an important role during cancer progression. Also this study illuminated a novel mechanism by which EZH2 represses the tumor suppressor E-cadherin and promotes cell invasion. Importantly, this study provides a mechanism by which EZH2 is dysregulated during cancer progression by demonstrating that EZH2 is promising target for cancer therapy. By repressing EZH2 expression or activity, tumor formation could be inhibited or attenuated.

APPENDIX

Supplementary Information for the individual chapters is available online at the following addresses:

CHAPTER 2

<http://www.pnas.org/cgi/content/full/1933744100/DC1>

Multiple individuals contributed to the work presented in these chapters and resulting manuscripts. Contributions of individuals for each chapter are as follows:

CHAPTER 2

Celina Kleer, Qi Cao, Sooryanarayana Varambally and Arul Chinnaiyan conceived the experiments and wrote the paper represented in this chapter. Celina Kleer performed Tissue microarray. Qi Cao, Ichiro Ota, and Donna Livant performed invasion assays. Qi Cao and Sooryanarayana Varambally performed immuno blots. Scott A. Tomlins performed qPCR. Ronglai Shen and Debashis Ghosh provided biostatistical support.

CHAPTER 3

Qi Cao, Sooryanarayana Varambally and Arul Chinnaiyan conceived the experiments and wrote the paper represented in this chapter. Qi Cao performed

luciferease assays and invasion assays. Qi Cao and Sooryanarayana Varambally performed immuno blots. Jindan Yu performed ChIP and ChIP-on-chip assays. Sooryanarayana Varambally performed immunofluorescence microscopy. Jindan Yu, Saravana Dhanasekaran and Julie Kim performed promoter DNA methylation assays. Jindan Yu and Bharathi Laxman generated the stable cell lines and performed the *in vivo* assay. Saravana Dhanasekaran performed northern blots. Scott A. Tomlins performed qPCR. Jianjun Yu provided biostatistical support. Xuhong Cao performed cDNA microarrays. Rohit Mehra and Celina Kleer provided breast tissue samples. Jill Granger helped revise the manuscript and figures.

CHAPTER 4

Qi Cao, Sooryanarayana Varambally and Arul Chinnaiyan conceived the experiments and wrote the paper represented in this chapter. Qi Cao performed qRT-PCR, luciferease assays, cell proliferation assay, and invasion assays. Qi Cao and Sooryanarayana Varambally performed immuno blots. Jindan Yu performed ChIP and ChIP-on-chip assays. Christopher Maher, Saravana Dhanasekaran and Julie Kim analyzed aCGH data. Xuhong Cao performed aCGH and gene expression profiling. Bharathi Laxman generated the stable cell lines and performed the *in vivo* assay. Saravana Dhanasekaran performed helped Qi Cao generate 3UTR EZH2 luciferase construct. Chandan Kumar and Sunita Shankar Kumar performed genomic DNA PCR